The Metabolic Role of the Hippo Pathway in Liver Development and Cancer

The Metabolic Role of the Hippo Pathway in Liver Development and Cancer

A dissertation presented

by

Katie Lee Hwang

to

The Division of Medical Sciences

in partial fulfillment of the requirements
for the degree of
Doctor of Philosophy
in the subject of

Biological and Biomedical Sciences

Harvard University
Cambridge, Massachusetts

April 2015

The Metabolic Role of the Hippo Pathway in Liver Development and Cancer

Abstract

Hepatocellular carcinoma (HCC) is a global health problem with poor prognosis and limited therapeutic options. While the clinical risk factors for HCC are well described, the precise molecular and metabolic mechanisms contributing to malignant transformation remain largely unknown. Recently, the Hippo signaling pathway has been identified as a key regulator of cellular proliferation, organ size, and tumorigenesis in numerous tissues, including the liver. However, the metabolic impact of the pathway in supporting liver growth and tumorigenesis has not been studied. The zebrafish, *Danio rerio*, has successfully been applied as a model to investigate signaling pathways important in organ development to model liver development and cancer. Here, we utilize the zebrafish to investigate the functional and metabolic roles of the Hippo pathway in liver development and cancer *in vivo*.

Using a transgenic zebrafish model with liver-specific activation of the transcriptional co-activator Yap, the downstream target of the Hippo pathway, we show Yap is functionally conserved in its ability to promote embryonic and adult hepatomegaly. These livers demonstrate signs of dysplasia and increased tumor susceptibility upon chemical carcinogen exposure. Using transcriptomic and metabolomic analysis, we discover that nitrogen metabolism is significantly altered in Yap-transgenic livers. Yap upregulates glutamine synthetase (Glul) expression leading to elevated steady-state levels of glutamine, which significantly contributes to its ability to enhance liver growth and *de novo* purine biosynthesis.

To further probe the functional and metabolic role of Yap prior to liver outgrowth, we utilize *yap* knockout zebrafish and heat-shock inducible transgenic zebrafish that modulate Yap activity to examine early liver development. We show Yap is important for hepatoblast formation and expansion. Further, Yap modulates glucose uptake and glycolytic flux into

de novo nucleotide synthesis. Overall, this dissertation reveals novel roles of Yap in cellular metabolism to support proliferation and growth by directing glucose into the building blocks of DNA in the context of development and cancer.

Contents

List of Figures

List of Tables

List of Abbreviations

APC	Adenomatous polyposis coli
BMP	Bone morphogenetic protein
CC	Cholangiocarcinoma
DMBA	7,12-dimethylbenz[a]anthracene
Dpf	Days post fertilization
ENU	Ethylnitrosurea
ES	Embryonic stem
FGF	Fibroblast growth factor
FOXA	Forkhead box A
GATA	GATA-binding factor
Glul	Glutamine synthetase
HCC	Hepatocellular carcinoma
HHEX	Hematopoietically expressed homeobox
HNF	Hepatocyte nuclear factor
Hpf	Hours post fertilization
Hpo	Hippo
ifabp	Intestinal fatty acid binding protein
iPS	Induced pluripotent stem
Lats	Warts
Mats	Mobs as tumor suppressor
MNNG	N-methyl-nitrosguanadine

MSO	Methionine sulfoximine
OxPhos	Oxidative phosphorylation
PFA	Paraformaldehyde
PPP	Pentospe phosphate pathway
PROX1	Prospero homeobox protein 1
qPCR	Quantitative PCR
Sav	Salvador
Scalloped	Sd
SH3	Src homology
STE20	Sterile 20-like
STM	Septum transversum mesenchyme
TAZ	Transcriptional co-activator with PDZ-binding motif
TEAD	Transcriptional effector activator domain
TGFβ	Transforming growth factor β
Wts	Warts
YAP	Yes-associated protein
Yki	Yorkie

Acknowledgments

I would like to take this opportunity to express my gratitude for all of the important people in my life and those who have shaped me into the person I am today and the physician-scientist that I am becoming.

First and foremost, I would like to express my deepest thanks to my advisor, Dr. Wolfram Goessling, whose journey and path as a physician-scientist, mentor, and cancer-survivor has been inspiring. Thank you for taking me into your lab home even when you yourself were facing great adversity in the face of cancer. Your enthusiasm for science, your commitment to your patients, and your dedication to developing your lab members as young scientists has been a gift to witness and experience.

I would also like to thank the members of my Dissertation Advisory Committee, Dr. David Cohen, Dr. Len Zon, and Dr. Brendan Manning, for their scientific guidance, support, and expertise throughout my research training. Their support of my goals and insights into my project proved invaluable. I also would like to thank my Dissertation Examination Committee, Dr. David Langenau, Dr. Thomas Bernhardt, Dr. Matthew Steinhauser, and Dr. Matthew Vander Heiden for agreeing to serve on my exam and for taking the time to read this dissertation. I would also like to express my appreciation for the Biological and Biomedical Sciences Program and the MD-PhD Program as they have guided me through my training and offered their support through this physician-scientist training path.

I have also had the pleasure of being mentored by great scientists as I pursued research in my training throughout the years. I would like to express my gratitude to Dr. Jeannie Lee for her investment in me as a young graduate student and expanding my ideas of scientific questions and rigorous inquiry. I am especially grateful to her for being supportive as I decided to pursue other scientific paths more directly in line with my clinical interests. I would also like to thank my Oxford research mentor Dr. Paul Fairchild, my SHURP mentor

Dr. Karl Munger, my senior thesis advisor Dr. Susan Murphy, and my very first research mentors Dr. Timothy Behrens and Dr. Keli Hippen for encouraging me to think of science mechanistically, creatively, and with great purpose.

I also would like to acknowledge my deep appreciation for Dr. Jocelyn Spragg, who unfortunately passed away during my time here at Harvard from cancer. Her mentorship, guidance, and wisdom during my young undergraduate summers here at Harvard Medical School that continued through my graduate studies was instrumental to my decision to become a physician-scientist. Her love for her students was felt by all of her "SHURPers," and her individual encouragement, steadfast belief, and leadership provided inspiration to us all. For this, I am so grateful.

Being part of many research labs over the past 12 years has given me the incredible opportunity to work beside extremely talented post-docs, graduate students, technicians, and undergraduates. To all of my current and former lab mates, I would like to say thank you for your patience with my questions, your teaching, your ability to turn the everyday into a memorable one, and for most of all being sources of inspiration and support.

I have had the privilege of working in close collaboration with a very talented and brilliant post-doc in the Goessling lab, Andy Cox. I would like to extend my deep thanks for his taking me under his wing to teach me and for providing a tremendous role model in our scientific endeavors. To the members of "Team Hippo," Allison and Keelin, you have been a tremendous support and we would not have been able to make the rapid progress without your contribution and ideas. More importantly, you have been amazing lab mates and friends. I would also like to thank the graduate students of the Goessling lab: Leah, Gal, and Olivia, your company, support, go-getter attitude, and similar coffee/tea drinking habits have greatly enriched my life, and I feel so incredibly lucky to have you as classmates and friends. To the post-docs of the lab: Kristen, who has also become our lab mom, Sahar, Chad, and Hongchao, thank you for all of your help and guidance. To our lab technicians past and present: Diane, Julia, AJ, John and Steph, a very hearty thank you. You help make

the lab run smoothly and facilitate all of our science. And a special thank you to Diane and Julia: your welcome packet on my first day of lab introduced me to your wonderful kindness. Your creativity, artistic prowess, baking, organization skills, and general enthusiasm enriched the Goessling lab in so many ways, and I am grateful to have you as friends. I would also like to thank the Lee lab graduate students, Johnny, Chen Yiu, Lin, John, David and Nick, for being wonderful friends and classmates as well as sources of support. To the post-docs of the Lee lab (who would take up page if I named you all!), especially Cathy and Montserrat, thank you for teaching me so much in a short period of time and for your support and friendship.

I would also like to take this opportunity to thank my wonderful MD-PhD classmates: Rishi Puram, Alex Bagley, Vineeta Agrawala, Divya Jayaraman, Jon Herman, Justin Lo, Michael Coulter, Wendy Liu, Michael Susman, Aswin Sekar, Derek Peters, Wen Fan, Sylvan Baca and Yamicia Connor. You have been a source of friendship, laughter, and tremendous fun as we go on this marathon journey together. I would also like to thank fellow Lowell-fellowships tutor, Susanna Mieurau, for being one of my dearest friends and supporters. I have so enjoyed our late night teas, passionate discussions about the future of science and medicine, and working together to help students be able to experience the Oxford we love.

I would like to express my deep thanks and gratitude to my in-laws, Yuan-Yuan and Phillip Hwang, who have taken me into their family these past 5 years as a daughter. Thank you for your love and support, the multiple loads of laundry and freshly prepared, delicious dinners, and for your help fixing things around our house. I truly think we would be much unhealthier without all of your love and care.

To my parents, Joe and Patricia Lee, and my brother, Austin Lee, I would like to express my deepest thanks and love for being my longest supporters, biggest cheerleaders, and believers in my dreams. Thank you Mom and Dad for instilling in me a passion for learning, courage to explore, and caring for others. The countless hours you dedicated to teaching me late into the night, the driving to violin lessons, piano lessens, tennis, badminton, night

college math classes (the list could go on and on!) so that I could pursue my passions, and for developing my character into the person I am today. Thank you Austin for being the best brother in the whole world. I am so grateful for the day that I became your older sister. You have brought me so much joy and laughter with your sense of humor, quiet wit, and enthusiasm for life, and you continue to inspire me with your work ethic, intelligence, and drive.

Finally, but most definitely not least, thank you to the most wonderful husband, William Hwang. Little did I know that on my first day in Oxford I would meet you, the love of my life. I feel so very fortunate that I have been able to go through this journey with you, my best friend, every step of the way. Whether we are cooking together, watching silly TV shows, cheering on our favorite football teams, troubleshooting molecular cloning, discussing our latest hypothesis, or aliquoting protein in the cold room until the wee morning hours, I love spending this time together as we talk as if we are still on our first date with the time just flying by. Your unending support and love, through the highs and lows, has been a tremendous gift. I am excited to enter this next step of training together in our shared passion for scientific research and helping patients, and I look forward to our future together as we continue on life's path.

To my dearest husband, Billy, who's love, support, belief, and encouragement made this possible.

To my family, for their love and faith in me and nurturing of my explorative and inquisitive nature.

To Dr. Spragg, in loving memory for her unwavering belief in all of her SHURPers and for her support of me to reach my dreams.

Chapter 1

Introduction

Cancer is a devastating disease with more than 1.6 million people newly diagnosed each year and more than 1,600 people dying each day in the United States alone (Society, 2015). While there have been numerous advances in the fundamental knowledge, detection, and treatment of cancer, the relentless morbidity and mortality of this disease indicates that we still have much to learn about the mechanisms underlying this complex disease in order to develop better therapies. Originating from normal, healthy cells, cancer is in its very nature insidious as it co-opts normal cellular processes to proliferate and transform. This is aptly described by Siddhartha Mukherjee:

> That this seemingly simple mechanism—cell growth without barriers—can lie at the heart of this grotesque and multifaceted illness is a testament to the unfathomable power of cell growth. Cell division allows us as organisms to grow, to adapt, to recover, to repair—to live. And distorted and unleashed, it allows cancer cells to grow, to flourish, to adapt, to recover, and to repair—to live at the cost of our living. Cancer cells can grow faster, adapt better. They are more perfect versions of ourselves (Mukherjee, 2010).

Understanding the mechanisms behind our normal ability to grow, especially in the context of development, will allow us to better understand the basis for how cancer can metamorphose our healthy tissues into unchecked tumors with fatal potential.

One key question in developmental growth that has remained poorly understood is how organs are able to grow to their appropriate sizes and then halt their continued growth. The Hippo signaling pathway has recently been identified as a key regulator of organ size by controlling proliferation, differentiation and apoptosis. When hijacked, these fundamental cellular processes in normal development are at the heart of cancer's ability to proliferate unchecked.

In 2000, Hanahan and Weinberg outlined in a landmark paper the hallmarks of cancer, which they define to be (1) self-sufficiency in growth signals, (2) insensitivity to anti-growth signals, (3) evading apoptosis, (4) limitless replicative potential, (5) sustained angiogenesis, and (6) tissue invasion and metastasis (Hanahan and Weinberg, 2000). Mutations in oncogenic pathways are known to cause misexpression of genes involved in these traditional features. However, more recently, cancer studies have recognized an additional hallmark, the deregulation of metabolism to support the high energy and biosynthesis demands of rapidly proliferating cells (Hanahan and Weinberg, 2011). Interestingly, some of these same known cancer pathways, such as MYC, RAS and p53, can coordinate this reprogramming of cellular metabolism and form central regulators of cancer formation (Cairns et al., 2011).

The Hippo pathway, when deregulated, can cause overgrowth in multiple tissues, and as such it has been postulated to be important for human cancer. Studies in mammalian systems where the Hippo pathway is perturbed have supported this hypothesis, and examination of human carcinomas has revealed Hippo pathway deregulation (Harvey et al., 2013). Greater understanding of how the Hippo pathway can coordinate these cellular processes, especially to meet the metabolic demands to promote proliferation and growth are needed. Towards this end, the study of the Hippo pathway in liver development and cancer is especially useful. As described in the story of Prometheus, the liver has the unique capability to regenerate to its original mass following up to two-thirds resection. Its special plasticity offers unique advantages to the study of the mechanisms behind its development and growth. More importantly, liver cancer is the second leading cause of cancer death in men worldwide,

and sixth most common cause of cancer death in women (Jemal et al., 2011). Investigating how the Hippo pathway can contribute to liver cancer and support uncontrolled cellular proliferation, especially at the metabolic level, can further our understanding of these immortal cells and will ultimately allow us to develop novel therapeutic targets to treat this abominable disease.

1.1 Cellular Metabolism

Metabolism is central to providing the energetics and building blocks necessary for cellular proliferation, whether in the physiological role of development or in the pathogenic case of cancer. The initial discovery that cancer cells have unique metabolic requirements due to their highly proliferative nature was described by Otto Warburg almost a century ago (Warburg et al., 1926; Ferreira et al., 2012; Warburg, 1956). With the advance of genetic understanding of cancers and the boon of oncogenes and tumor suppressors, cancer metabolic studies were relegated to the sidelines for a period of time. However, it soon became clear that many key oncogenic signaling pathways converge to modulate tumor cell metabolism to support their growth and survival, thereby pushing tumor metabolism back to the forefront of cancer research (Cairns et al., 2011). Recent advances in metabolomics and metabolic flux analysis, high-throughput sequencing data, and computational power have advanced the study of these metabolic pathways and their regulation.

In normal, non-proliferating cells, the metabolic program serves to maintain homeostasis; however, self-renewing stem cells and cancer cells must balance the catabolic demands to support proliferation with the anabolic demands of macromolecule synthesis. Glucose is a primary source of energy and carbon for biomolecular synthesis. With one mole of glucose, up to 38 moles of ATP can be generated in normal aerobic conditions through oxidative phosphorylation (OxPhos). Glycolysis breaks down glucose into pyruvate, which is then further oxidized in the mitochondria to fuel the TCA cycle. The TCA cycle produces car-

bon intermediates as well as NADH and $FADH_2$ that then in turn fuel OxPhos for ATP production. In contrast, anaerobic conditions cause glucose metabolism to truncate at the level of glycolysis with reduction of pyruvate to lactate, generating only 2 moles of ATP per mole glucose. In cancer cells and stem cells, a different paradigm has been found in which glucose is primarily processed by glycolysis regardless of the availability of oxygen (aerobic glycolysis, or the Warburg effect), instead of the more energetically favorable OxPhos (Warburg, 1956; Koppenol et al., 2011; Vander Heiden et al., 2009). Alterations to the PI3K pathway, HIF1, MYC, AMPK, p53, and OCT1 have all been shown to promote aerobic glycolysis in cancer cells (Cairns et al., 2011). Moreover, in numerous studies of embryonic stem cells *in vitro*, it has been shown that undifferentiated cells have high rates of glycolysis and lactate production independent of oxygen state (Chung et al., 2007; Kondoh et al., 2007; Prigione et al., 2010; Varum et al., 2011; Zhang et al., 2011b). As they differentiate, glycolytic flux decreases and the more energetically favorable mitochondrial respiration predominates. Conversely, reprogramming of differentiated cells to iPS cells shows a reversal to aerobic glycolysis from OxPhos (Shyh-Chang et al., 2013a). Furthermore, low oxygen conditions promoting glycolysis enhanced the ability to generate iPS cells whereas pharmacological inhibition of glycolysis or stimulation of OxPhos impaired iPS cell reprogramming (Yoshida et al., 2009; Folmes et al., 2011). This increased flux of glucose through glycolysis in undifferentiated cells is thought to promote biosynthetic pathways by providing glycolytic intermediates necessary for amino acid, lipid, and nucleotide synthesis. Supporting this conjecture, mouse ES cells show increased activity in the pentose phosphate pathway (PPP), which generates ribose 5-phosphate for the synthesis of nucleic acids (Filosa et al., 2003; Manganelli et al., 2012).

In the developing embryo, the first cell fate decision to inner cell mass and trophectoderm occurs as proliferation and metabolic activity increases. Glucose transporters GLUT1 and GLUT3 (SLC2A1 and SLC2A3) are upregulated and hexokinase (HK) and phosphofructokinase 1 (PFK1) are activated, increasing glycolytic flux (Pantaleon and Kaye, 1998; Shyh-

Chang et al., 2013a). With this increase in glycolytic flux, lactate synthesis also increases. OxPhos rates in general are increased; however, this is largely due to the trophectoderm. Similar to the ES cell culture, which is derived from the inner cell mass, there is lower OxPhos due to a decreased mitochondrial membrane potential (Shyh-Chang et al., 2013a).

Cancer cells were described over a hundred years ago to have this same increase in glycolysis and lactate production even in the presence of oxygen, which was termed the Warburg effect. While previously postulated to be due to limited energetic resources and the fact that glycolysis has the capacity to generate ATP faster than OxPhos, this hypothesis appears not to be the predominant mechanism given that cells using aerobic glycolysis also demonstrate high ATP/ADP and NADH/NAD^+ ratios (Vander Heiden et al., 2009). Furthermore, cells possess finely tuned sensors to energy status and will activate signaling pathways to reactivate catabolic metabolism when their ability to make ATP from glucose is impaired (Vander Heiden et al., 2009). Instead, cancer cells are likely utilizing aerobic glycolysis for biomass production to meet the high biosynthetic demands of rapid cellular proliferation. Further evidence supporting this concept came from studies of pyruvate kinase isoenzymes, which are responsible for the final, rate-limiting, ATP-generating step of glycolysis in which phosphoenolpyruvate is converted to pyruvate (Mazurek et al., 2005). The PKM2 isoenzyme was found in self-renewing cells such as stem cells and is also expressed in many tumor cells. Interestingly, PKM2 is ineffective at promoting glycolysis (Mazurek et al., 2005; Christofk et al., 2008). Hence, this finding was ignored for many years because it seemed counterintuitive that there would be a tumor-specific isoenzyme that countered the Warburg effect. Closer examination eventually revealed that PKM2 provided an advantage to tumors because by inhibiting the final step in glycolysis, it promoted shunting of upstream metabolites to critical anabolic pathways such as the PPP, hexosamine biosynthetic pathway, UDP-glucose synthesis, glycerol synthesis, and the generating of NADPH reducing equivalents (Vander Heiden et al., 2009; Fang et al., 2010; Guertin and Sabatini, 2007).

Similar to mouse ES cells, cancer cells show increased activity in the PPP, generating

ribose 5-phosphate for de novo nucleotide synthesis as well as NADPH, which is required for reductive biomacromolecule synthesis and contributes to the defense of redox stress (Mayers and Vander Heiden, 2015). Glucose metabolites also provide components for fatty acid synthesis, glycosylation, and glycerol components of triacylglycerides and membrane phospholipids.

Not only is glucose used as a fuel and biomass supporter but glutamine also plays a significant role in supporting cellular proliferation. Glutamine is the most abundant free amino acid in human serum and is a requirement for proliferating cells *in vitro* (Cantor and Sabatini, 2012). With most of the glucose-derived carbon being shunted to the pentose phosphate pathway, hexosamine biosynthetic pathway, and lipid synthesis pathways, glutamine oxidation allows cells to sustain the TCA cycle by replenishing intermediates that are depleted. Moreover, in proliferating cells, glutamine is used as the nitrogen donor for biosynthesis of nucleotides, nonessential amino acids, and hexosamines (Hensley et al., 2013). Interestingly, oncogenic pathways can differentially regulate glucose and glutamine consumption to ensure a supply of energy and precursors for macromolecular synthesis. Mutant KRAS causes glutamine to be transaminated to alpha-ketoacids whereas increased MYC favors glutaminolysis with nitrogen released as ammonia (Mayers et al., 2014). This ability for oncogenic pathways to reprogram cellular metabolism brings questions as to other pathways central to growth and proliferation that could be influencing the cellular metabolic state.

1.2 The Hippo Signaling Pathway

1.2.1 The Core Signaling Cascade

The Hippo pathway was first identified in *Drosophila melanogaster* by genetic screens aimed to identify key regulators of tissue growth in which loss of function mutations in core components resulted in massively overgrown organs due to increased cell proliferation and resistance to pro-apoptotic signals (Justice et al., 1995; Xu et al., 1995; Tapon et al., 2002; Dong et al.,

2007). The first component of the Hippo pathway identified by these means was the kinase Warts (Wts; also known as Lats), which upon deletion caused cellular hyperproliferation and epithelial overgrowths (Justice et al., 1995; Xu et al., 1995). Additional studies identified the Sterile 20-like (STE20) kinase Hippo (Hpo) and the scaffolding proteins Salvador (Sav) and Mob as tumor suppressor (Mats) as tumor suppressor genes that resulted in similar overgrowth phenotypes from increased cellular proliferation and decreased apoptosis (Tapon et al., 2002; Harvey et al., 2003; Jia et al., 2003; Pantalacci et al., 2003; Udan et al., 2003; Wu et al., 2003; Lai et al., 2005). These four proteins were then identified through biochemical studies to form the core kinase cassette of the Hippo pathway (Figure 1.2.1) (Wu et al., 2003; Huang et al., 2005; Lai et al., 2005). Briefly, Sav and Mats mediate complex formation and propagate a cascade of phosphorylation leading to the activation and phosphorylation of Wts by Hpo (Pan, 2010; Varelas and Wrana, 2012). A yeast-two hybrid screen for Wts-interacting proteins identified the downstream effector of the Hippo kinase cascade to be the transcriptional co-activator Yorkie (Yki) (Huang et al., 2005). Gain-of-function mutations in Yki produce similar overgrowth phenotypes to the loss-of-function mutations seen in the upstream Hippo kinase cascade (Huang et al., 2005). Activated Wts directly phosphorylates Yki to inhibit its translocation to the nucleus by promoting its interaction with 14-3-3 proteins and its retention in the cytoplasm (Dong et al., 2007; Oh and Irvine, 2008). Yki, in its unphosphorylated state, associates with the transcription factor Scalloped (Sd) in the nucleus and activates a transcriptional profile promoting cellular proliferation and anti-apoptosis (Oh and Irvine, 2008; Goulev et al., 2008; Zhang et al., 2008).

The Hippo pathway is highly conserved, and all of the core components of the pathway have direct mammalian orthologs. Similar to *Drosophila*, the core of the signaling cascade in mammals consists of the STE20 protein kinases MST1 and MST2 (homologs of Hpo), which phosphorylate and activate the kinases LATS1 and LATS2 (homologs of Wts) with the aid of adaptor proteins SAV1 (homolog to Sav) and MOBKL1A and MOBKL1B (homologs of Mats) (Dong et al., 2007; Ramos and Camargo, 2012). Active LATS1 and LATS2

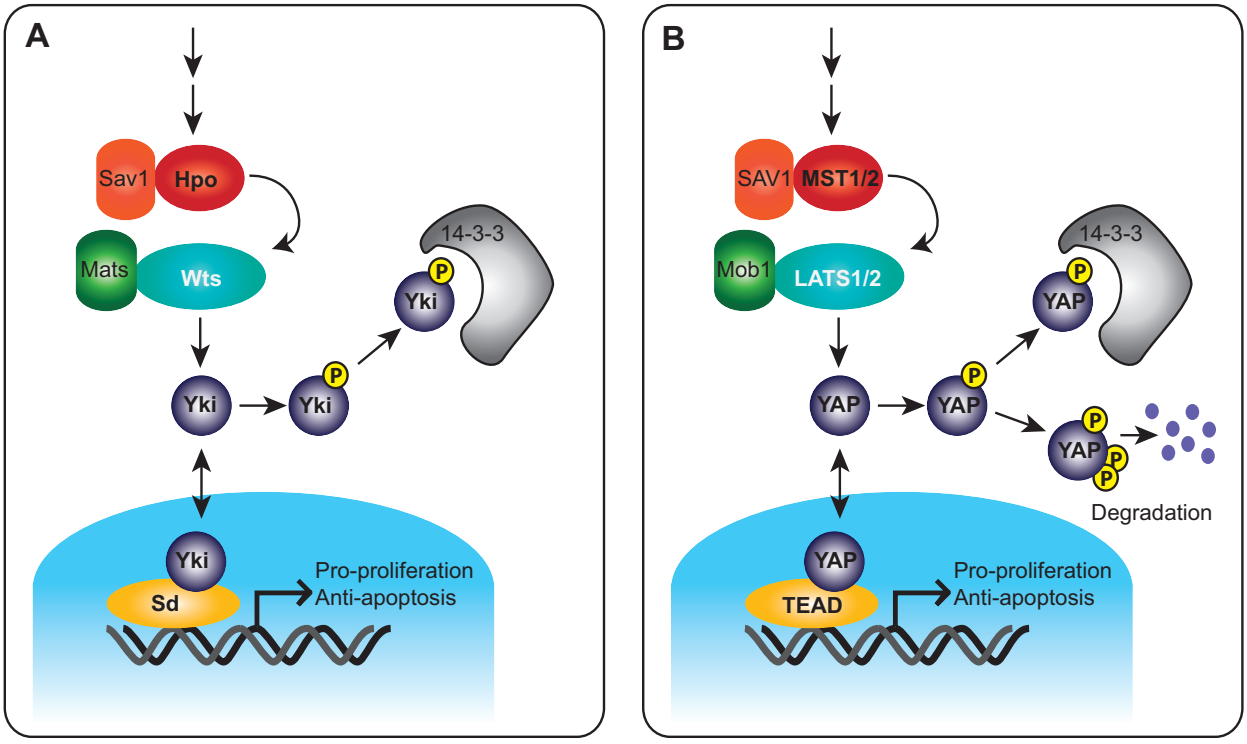

Figure 1.2.1: **Hippo Signaling in Drosophila and Mammals.** (A) The Hippo pathway in Drosophila melanogaster and (B) in mammals has more than 35 known proteins in the pathway. Multiple upstream pathways feed into the Hippo pathway. Here, the core signaling cascade is depicted. (A) The core kinase Hippo (Hpo) phosphorylates the kinase Warts (Wts) as well as the scaffolding proteins Salvador (Sav) and Mobs as tumor suppressor (Mats). Wts is then activated to phosphorylate the transcriptional co-activator Yorki (Yki), and phosphorylation at S168 causes it to be sequested in the cytoplasm and bind the 14-3-3 protein. When Yki is unphosphorylated, it translocates to the nucleus and binds its transcription factor Scalloped (Sd) and activates transcription that results in cell proliferation. (B) In mammals, signaling through the Hippo core kinase cassette is conserved. Mammalian MST1/2 phosphorlyates the kinase LATS1/2 to activate it, resulting in phosphorylation of Yap at multiple sites. Specifically, phosphorylation at S127 causes Yap to interact with the 14-3-3 protein and prevent translocation to the nucleus. Further, phosphorylation at S381 primes YAP for phosphorylation by CK1ε/δ, which further targets YAP for degradation. When the Hippo pathway is not active, YAP is able to localize to the nucleus and bind its transcriptional partner TEAD to drive transcription of pro-proliferative and anti-apoptotic genes.

phosphorylate the transcriptional co-activators Yes-associated protein (YAP) and transcriptional co-activator with PDZ-binding motif (TAZ), which are homologs to Yki. LATS1/2 phosphorylation of YAP and TAZ results in the cytoplasmic retention of the transcriptional co-activators by 14-3-3 binding, and thereby inhibits their nuclear translocation and activation. Similar to Yki, YAP and TAZ lack DNA binding domains and require association with transcription factors to execute their transcriptional activities. While a number of transcription factors have been found to interact with YAP and TAZ, the best described are those in the Transcriptional enhancer activator domain (TEAD) family (homologs to Sd). Further supporting the high degree of conservation of the Hippo kinase cascade, *Drosophila* lacking members of the core signaling cascade are able to be phenotypically rescued with expression of their respective human homologs (Wu et al., 2003; Huang et al., 2005; Lai et al., 2005).

1.2.2 YAP

The Hippo signaling cascade serves to regulate the activity of Yes-associated protein (YAP), a transcriptional co-activator. YAP was first identified as a binding partner of proto-oncogene Yes through its interaction with the Src homology (SH3) domain (Sudol, 1994). Subsequent cloning of the gene revealed a modular protein with various motif structures and identified for the first time the WW domain, a conserved domain characterized by the presence of two tryptophan residues spaced 20-22 amino acids apart (Figure 1.2.2) (Sudol, 1994; Sudol et al., 1995). These WW domains are important for mediating interactions with other proteins, specifically those containing PPxY motifs (Sudol and Harvey, 2010; Sudol et al., 2012). YAP also contains a transcriptional activation domain and a PDZ-binding motif. The transcriptional activation domain constitutes the carboxyl terminus of YAP and resembles that found in the herpesvirus VP16 protein (Yagi et al., 1999). When the DNA-binding domain of GAL4 is fused to the transcriptional activation domain of YAP, it demonstrates strong transcriptional activation (Yagi et al., 1999). Further, this domain is required for its transcriptional activation of the TEAD factors. Its acidic makeup suggests that it can

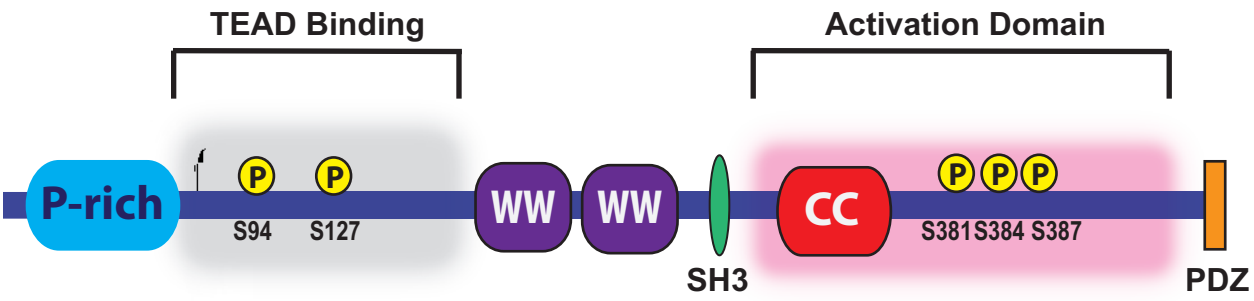

Figure 1.2.2: **Schematic of the modular domains of human YAP.** YAP is a 65 KDa protein with multiple distinct domains. YAP contains a proline-rich (P-rich) region at the N-terminus, tandem WW domains, a Src homology 3 (SH3) domain, a coiled-coil (CC) domain, and a PDZ-binding motif at the C-terminus. LATS1/2 phosphorylates a number of key residues, including S127 and S384. Phosphorylation of S127 promotes cytoplasmic retention of YAP and binding to 14-3-3. The N-terminus was mapped to be the TEAD family binding domain (shaded in gray), and S94 is a critical residue for this interaction. The C-terminus of YAP was found to be a strong transcriptional activator (shaded in pink). Phosphorylation of S381 primes YAP to be phosphorylated by CK1ε/δ at S384 and S87, targeting it for degradation.

similarly initiate transcription by interacting directly with components of the transcriptional machinery (Vassilev et al., 2001). In addition to the transcriptional activation domain, a PDZ-binding motif, which binds PDZ domains, is also found in the carboxyl terminus of YAP. This PDZ-binding motif, composed of the five terminal amino acids, is critical for its nuclear translocation (Oka and Sudol, 2009).

Importantly, YAP activity is modulated through a number of post-translational modifications, many of which have been studied and modified both *in vitro* and *in vivo*. Active LATS1/2, which contain PPxY motifs, interact with YAP through its WW domain and phosphorylate a number of residues on YAP, including the key serine residue S127 in human YAP (S112 in mouse YAP, S87 in zebrafish Yap) which is responsible for regulating YAP localization. Phosphorylation of S127 in human YAP, and its respective residues in its homologs, promotes the interaction of YAP with 14-3-3 and results in its cytoplasmic sequestration (Basu et al., 2003; Zhao et al., 2007). LATS1/2 also phosphorylates S61, S109, S164,

and S381. Phosphorylation of S381 primes YAP for further phosphorylation by CK1ε/δ kinases within a phosphodegron sequence. This additional phosphorylation then recruits the SCF$^{\beta\text{-TRCP}}$ ubiquitin ligase for subsequent ubiquitaination and degradation of YAP (Zhao et al., 2010).

1.2.3 The Role of Hippo Signaling in Development and Cancer

Emerging evidence has revealed that the Hippo pathway plays a critical role as a regulator of development, stem cell maintenance and tumorigenesis. Genetic ablation of various Hippo pathway members results in severe developmental defects in mice and demonstrates the importance of Hippo signaling in early embryonic development. Deletion of YAP in mice, for example, is embryonic lethal at approximately E8.5 with defects in yolk sac vasculogenesis, chorioallantoic fusion, and embryonic axis elongation (Morin-Kensicki et al., 2006). Deletion of TAZ, in contrast, results in a less dramatic phenotype of renal cysts and pulmonary emphysematous changes in mice that is not embryonic lethal (Hossain et al., 2007; Tian et al., 2007; Makita et al., 2008). However, when both YAP and TAZ are deleted, these double-knockout mice fail to develop past the 16-32 cell stage pre-implantation (Nishioka et al., 2009). YAP and TAZ normally are differentially nuclear localized to the less compacted outer cells of the blastocyst, and thereby activate TEAD to induce a trophectoderm-specific transcriptional program. With loss of YAP and TAZ, though, the embryo is unable to undergo this first cell fate decision, underscoring its importance in stem cell fate (Nishioka et al., 2009).

The role of YAP and TAZ in embryonic stem (ES) cells has been further studied *in vitro* and numerous studies have given evidence to support their role in cell fate specification and maintenance of pluripotency. In studies of mouse ES cells, Yap was required to maintain pluripotency, and its expression was reduced upon differentiation (Lian et al., 2010). Further, expression of a nuclear mutant Yap that is constitutively active prevented ES differentiation *in vitro* (Lian et al., 2010). YAP was also found to be essential for reprogramming mouse

embryonic fibroblasts into induced pluripotent stem (iPS) cells, which resemble embryonic stem cells in their pluripotency potential (Takahashi and Yamanaka, 2006). In human ES cells, studies have shown Yap to be integrated with critical growth factor signals required for maintaining the pluripotent state, specifically the transforming growth factor β (TGFβ) family. Yap forms a complex with TEADs as well as SMAD2/3, the downstream effectors of the TGFβ signaling pathway, and the core stem cell regulator OCT4 in human ES cells to regulate the expression of pluripotent target genes (Beyer et al., 2013).

Not only has the Hippo pathway been shown to be important in ES cells but it also has been implicated in the regulation of progenitor cell populations in a range of organs in line with its role as a key regulator of organ size. YAP has been found to be nuclear localized to progenitor cell compartments in a number of tissues, including the small intestine, developing brain, skin, and muscle (Ramos and Camargo, 2012). In the intestine, overexpression of YAP led to expansion of the progenitor stem cells in the crypts which was recapitulated in conditional deletions of MST1/2 or SAV1 (Camargo et al., 2007; Cai et al., 2010; Zhou et al., 2011). Similarly, in the skin, activation of YAP in the basal progenitors resulted in their extensive proliferation (Schlegelmilch et al., 2011; Zhang et al., 2011a). In contrast, the deletion of YAP in the epidermal stem cells resulted in a hypoplastic basal layer and failure of skin expansion (Schlegelmilch et al., 2011). In the developing heart, the Hippo pathway has been shown to be a regulator of cardiomyocyte proliferation and growth. Deletion of Hippo pathway members SAV1 or LATS2 dramatically increased heart size similar to that seen with nuclear activated Yap overexpression (Heallen et al., 2011; von Gise et al., 2012; Xin et al., 2011). Conversely, conditional YAP deletion in the heart caused decreased cardiomyocyte proliferation and lethal embryonic cardiac hypoplasia (von Gise et al., 2012; Xin et al., 2011).

The Hippo pathway has also been linked to tumorigenesis based on its ability to maintain "stemness" as well as its regulation of a number of cellular properties, such as proliferation and apoptosis, that are frequently deregulated in cancer. However, few mutations have been discovered in Hippo pathway members to date. Rather, YAP has frequently been reported to

be amplified and overexpressed (Harvey et al., 2013). Supporting this, YAP overexpression in differentiated murine tissues, including the liver, gastrointestinal tract, skin, and heart, cause significant hyperproliferation and overgrowth (Harvey et al., 2013). Tissue-specific genetic deletions of Hippo pathway core members in mice have revealed a number of tumor phenotypes, including cancers of the liver, breast, ovary, and skin (Harvey et al., 2013). In humans, deregulation of the Hippo pathway, measured by the abnormal detection of YAP in the nucleus, has been found in a number of different cancers, including hepatocellular carcinoma, colonic adenocarcinoma, lung adenocarcinoma, ovarian carcinoma, and ductal carcinoma of the breast (Zhao et al., 2007; Dong et al., 2007; Steinhardt et al., 2008; Harvey et al., 2013). More importantly, Hippo pathway abnormalities have been found to correlate with worse patient outcomes (Zhang et al., 2011; Xu et al., 2009; Wang et al., 2010).

While the Hippo pathway has been implicated in many of the hallmarks of cancer, namely limitless replicative potential, self-sufficiency in growth signals, evasion of apoptosis, and metastasis, the cellular mechanisms by which YAP sustains these abilities remain poorly understood. Investigating how the Hippo pathway can control unlimited cellular proliferation and drive cells to an undifferentiated state will further our understanding of the mechanisms driving and supporting tumor growth.

1.3 The Liver

The liver is a vital organ responsible for a wide range of functions including metabolism, glycogen storage, bile secretion, detoxification, protein synthesis, and digestion. The largest internal organ of the human body, the liver is a highly specialized tissue composed mainly of hepatocytes, which regulate hundreds of complex biochemical reactions necessary for life. Hepatocytes work in concert with a number of other cells, including biliary epithelial cells (cholangiocytes), endothelial cells, Kupffer cells, and hepatic stellate cells. The working unit of the liver is the hepatic lobule, which is defined at the histological level and consists of a

hexagonal plate of hepatocytes that are usually one cell thick. Each of the six corners of the lobule are bordered by a portal triad, which contains a hepatic artery, portal vein, and bile duct (Figure 1.3.1). Blood enters the lobule through branches of the hepatic artery and portal vein, supplying oxygen and nutrients to the organ, and then flows through a network of sinusoids before it leaves through the central vein located in the center of the lobule. Bile is generated by the hepatocytes and is collected first into bile caniculi that flow from the pericentral area to the periportal area and drain into bile ducts where it is then either secreted into the small intestine or stored in the gall bladder.

Disturbance of liver function from developmental defects, cirrhosis, or cancer results in significant morbidity and mortality. Primary liver and intrahepatic bile duct cancers are a global health problem, and in the United States, over 35,000 new cases will be diagnosed and approximately 24,000 will die of those cancers (Society, 2015). Hepatocellular carcinoma (HCC) is the most frequent malignant primary hepatic neoplasm followed by intrahepatic bile duct cancer, or cholangiocarcinoma (CC). While the risk factors are well known, including viral hepatitis, cirrhosis, diabetes, and alcohol consumption, the mechanisms contributing to HCC and CC remain unknown. These tumor types unfortunately carry a poor prognosis as we lack effective therapies to prevent or treat liver cancer. Continued investigation into the molecular mechanisms underlying HCC and CC pathogenesis is crucial as this will reveal new molecular targets for effective therapies.

1.3.1 Zebrafish as a Model

In order to better understand carcinogenesis, the study of organogenesis and stem/progenitor cells can provide important insights into the signaling pathways central to cancer. The zebrafish, *Danio rerio*, offers an ideal model for the study of this intersection between development and cancer in the liver. Native to the river basins in East India, the zebrafish was discovered in the Ganges river by Francis Hamilton in 1822 (Hamilton, 1822). The zebrafish is a small, striped vertebrate tropical fish that was pioneered as a model in the 1980s by

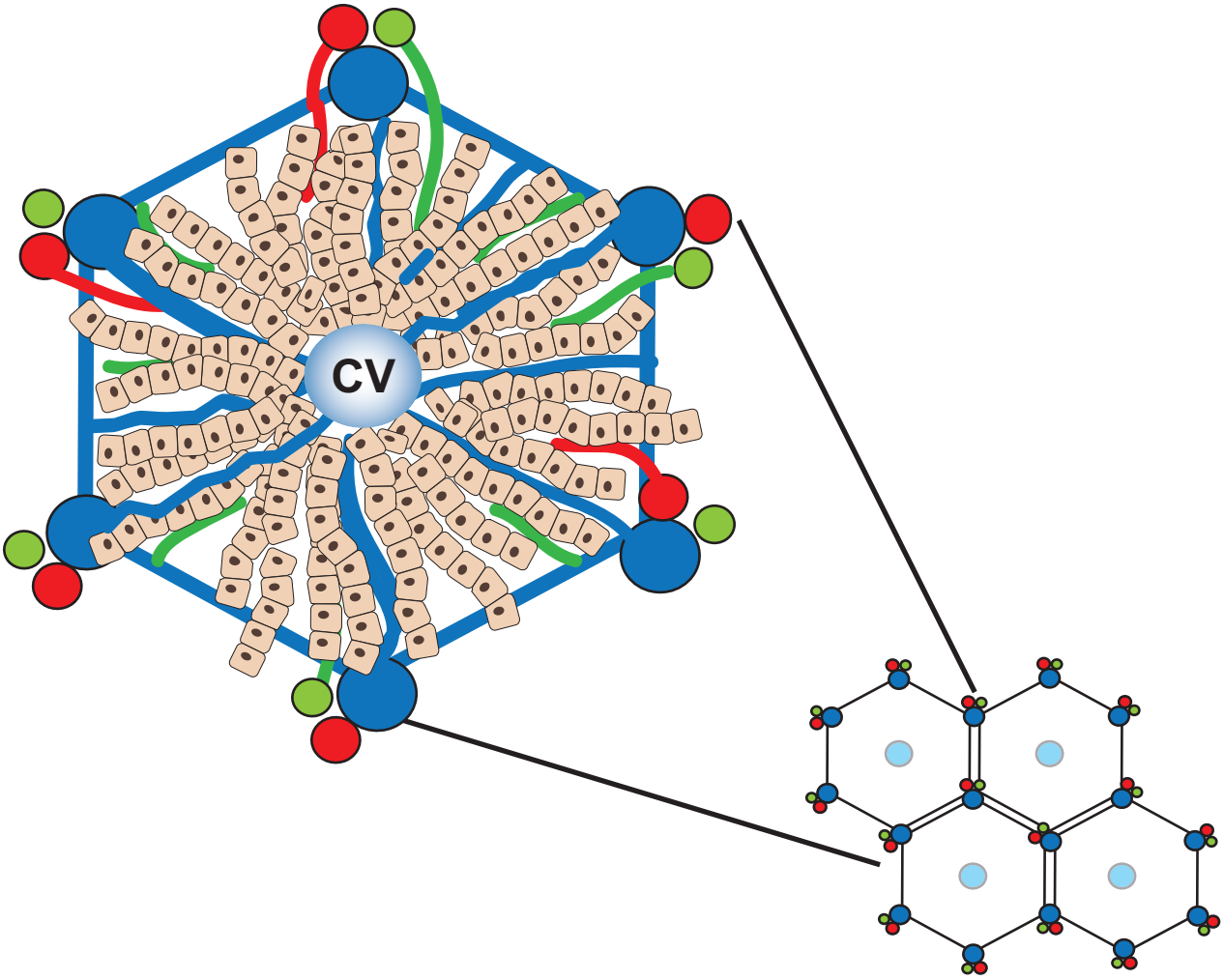

Figure 1.3.1: . **Schematic depicting the hepatic lobule of the human liver.** The portal triad, containing the hepatic artery (red), portal vein (blue), and bile duct (green) are located at the periphery. Bile made from the hepatocytes is collected by a network of intrahepatic bile ducts. Blood from the gastrointestinal system is drained through the central vein (CV).

George Streisinger at the University of Oregon, who described the generation of homozygous diploid zebrafish to facilitate neuronal development studies and broader mutant analysis (Streisinger et al., 1981). Genome-wide mutagenesis screens in the 1990s in Tubingen and Boston further uncovered the ability to use the zebrafish as a platform for invertebrate-style forward genetics to answer questions of vertebrate development (Lieschke and Currie, 2007). The zebrafish as a model offers a number of powerful advantages. First, they have a high fecundity and females can lay a few hundred eggs per week; secondly, embryos grow rapidly *ex utero* and are optically transparent allowing for ease in visualization during development; and thirdly, they share conservation of vertebrate organs, including the liver. Approximately 70% of human genes have zebrafish orthologs, and forward-mutagenesis screens have identified a number of conserved genes that correlate to human disease loci (Howe et al., 2013; Santoriello and Zon, 2012).

Zebrafish are also able to develop cancers that resemble human tumors at the histological, gene expression, and genomic levels (White et al., 2013). When zebrafish were first suggested to be a useful cancer model in 1982, it was known that zebrafish could form tumors in response to carcinogens, such as dimethylnitramine (White et al., 2013). The idea that zebrafish could be used as a cancer model was further expanded with other common carcinogens such as ethylnitrosurea (ENU), 7,12-dimethylbenz[a]anthracene (DMBA), and N-methyl-nitrosoguanadine (MNNG) causing various neoplasms, including skin papillomas, hepatocellular carcinomas, rhabdomyosarcoma, and seminoma (White et al., 2013). With the advent of transgenic technology, though, zebrafish became a formidable tool for cancer studies. Numerous transgenic zebrafish models have been created to model expression of oncogenes resulting in a range of cancers, including melanoma, leukemia, lymphoma, rhabdomyosarcoma, neuroblastoma, pancreatic, and hepatocellular carcinoma (Langenau et al., 2003; Patton et al., 2005; Sabaawy et al., 2006; Dovey et al., 2009; Santoriello et al., 2010; Liu and Leach, 2011; Nguyen et al., 2012; Zhu et al., 2012; Li et al., 2013).

In zebrafish, the liver is similarly comprised of hepatocytes, cholangiocytes, endothelial

cells, Kupffer cells, and stellate cells; however, unlike its mammalian counterparts, hepatocytes are not arranged into hepatic lobules as the portal veins, hepatic arteries, and biliary ducts are distributed throughout the liver in the zebrafish (Menke et al., 2011; Yao et al., 2012). Hepatocytes in the zebrafish liver are instead centralized around biliary cells. The zebrafish is also uniquely advantageous for studying liver development since the embryonic liver is not a site of hematopoiesis as it is in mammals, allowing for the study of developmental defects without complications from anemia or early lethality.

1.3.2 Liver Development

The liver is derived from the anterior endoderm, which itself is one of three germ layers established during gastrulation. In mice, cell fate studies showed three distinct domains of hepatic progenitor cells within the developing foregut that converge to generate the epithelial cells of the liver bud (Tremblay and Zaret, 2005). As the hepatic progenitor cells converge and bud into the surrounding stroma, they receive induction signals from the adjacent developing heart and septum transversum mesenchyme (STM) (Si-Tayeb et al., 2010). Fibroblast growth factor (FGF) family members FGF1 and FGF2 were found to be able to substitute for cardiac mesoderm in the induction of hepatoycte gene expression programs, such as albumin (Jung et al., 1999). From the STM, bone morphogenetic proteins (BMPs), activate genes important for induction of hepatic specification in part by affecting the GATA4 transcription factor (Rossi et al., 2001). In addition to FGF and BMP signaling, the WNT signaling pathway plays a complex role in hepatic endoderm specification and hepatocyte expansion (Si-Tayeb et al., 2010). Following specification of the hepatic endoderm, hematopoietically expressed homeobox (HHEX), a homeodomain transcription factor, is expressed in the ventral foregut endoderm and is the earliest known marker of the developing liver (Keng et al., 2000; Martinez Barbera et al., 2000). Prospero homeobox protein 1 (PROX1), another homeodomain transcription factor, is found in the hepatic bud and also promotes hepatoblast specification (Sosa-Pineda et al., 2000). Other transcription factors, such as members

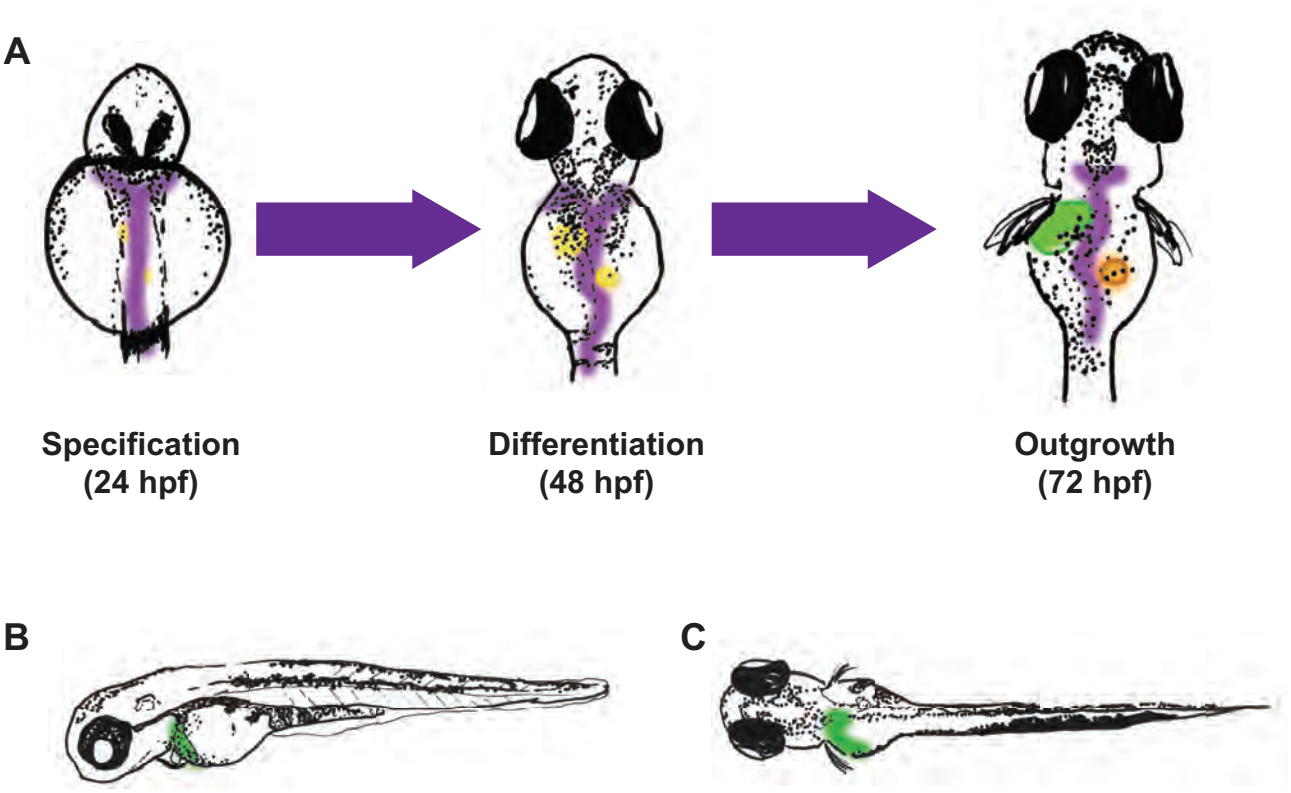

Figure 1.3.2: (A) Hepatic progenitors are specified in the gut tub by 24 hpf. *FoxA3* (purple) is expressed in the endoderm, and hepatocyte precursors aggregate at the anterior. The liver bud, marked by *hhex* (yellow), grows to the left of midline and expands outwardly at 48 hpf. By 72 hpf, the hepatocyte marker *lfabp* (green) marks the formed liver. (B) Lateral and (C) dorsal depictions of the expression of lfabp of the liver (green) at 72 hpf. Image courtesy of Diane Saunders.

of the *forkhead* box A (FOXA), GATA-binding factor (GATA) and hepatocyte nuclear factor (HNF) families, direct hepatic differentiation and control the onset of hepatic gene expression during liver bud formation (Si-Tayeb et al., 2010).

In the zebrafish, liver development occurs much more rapidly as a fully functioning liver is seen by 5 days post fertilization (dpf). Importantly, the same transcriptional networks and molecular signaling are conserved between terrestrial vertebrates and zebrafish. In zebrafish, liver development can be broken down into three stages: (1) specification, (2) differentiation, and (3) outgrowth (Figure 1.3.2). In specification, liver progenitors in the anterior endoderm

are first identifiable by *hhex* expression, and these hepatoblasts aggregate and appear as a prominent bud to the left of the midline between 24-28 hours post fertilization (hpf). These hepatic precursors also express *prox1* and *gata6*. Experiments utilizing heat shock-mediated expression of a dominant negative BMP receptor or FGF receptor in the zebrafish resulted in decreased expression of *hhex* and *prox1* in the liver region(Shin et al., 2007). In addition, *wnt2bb* and *adenomatous polyposis coli* (*APC*) zebrafish mutants demonstrated defective hepatic specification(Goessling et al., 2008; Ober et al., 2006). Together, these studies show that BMP, FGF, and WNT signaling are a conserved requirement in hepatoblast specification.

Hepatocyte differentiation in the zebrafish begins around 34 hpf, when markers of hepatoblast maturation begin to be expressed, such as the copper-binding protein gene, *ceuloplasmin* (*cp*), followed by the *selenoprotein P, plasma, 1b* (*sepp1b*). However, it is not until 48 hpf that the liver begins to be fully differentiated as hepatocytes begin to express genes indicative of mature hepatocyte function such as *liver fatty acid binding protein* (*lfabp*) and *group specific component* (*gc*). The vascular network in the liver begins to develop between 55-60 hpf as endothelial cells begin their invasion into the liver. Simultaneously, biliary cells in the liver begin to form, with cyotkeratin staining identifying the first cells between 50-60 hpf and biliary ducts by 70 hpf (North and Goessling, 2011). Proliferation accelerates as the hepatocytes differentiate in the outgrowth phase with a resulting mature liver that has three lobes (Menke et al., 2011; Yao et al., 2012).

1.3.3 Hippo Signaling and the Liver

In mammals, the initial studies linking the Hippo pathway with organ size control were conducted in the postnatal mouse liver, where conditional activation of a nuclear localized YAP mutant caused more than a three-fold increase in liver mass as a result of hepatocyte hyperproliferation, and with continued YAP overexpression, progressed to hepatocellular carcinoma (Camargo et al., 2007; Dong et al., 2007). Liver-specific deletions of upstream

Hippo pathway members resulted in similar hepatomegaly and development of hepatocellular carcinoma and cholangiocarcinoma (Lee et al., 2010; Benhamouche et al., 2010; Zhou et al., 2009). Further supporting the potential of YAP to be oncogenic in the liver, YAP is amplified and overexpressed in human hepatocellular carcinoma and cholangiocarcinoma (Zender et al., 2006; Kim et al., 2013).

Studies, though, have been conflicting in the role of YAP on hepatocyte differentiation and progenitor cells. In a conditional knockout model of YAP in the liver, loss of YAP led to decreased hepatocyte survival as well as defects in biliary development (Zhang et al., 2010). In a gain-of-function model, the conditional combined deletion of Hippo pathway members MST1 and MST2 in the liver showed an increase in nuclear YAP as well as increased cellular proliferation of both hepatocytes and oval cells, a poorly defined liver progenitor cell population (Lu et al., 2010). Another study examined the conditional deletion of SAV1 in the liver and found hyperproliferation of oval cells without a change in the proliferation of hepatocytes (Lee et al., 2010). In the context of bile-acid induced liver injury, hyperproliferation of hepatocytes and expansion of oval cells have been observed following increased nuclear YAP localization(Anakk et al., 2013). More recently, it has been suggested that activated YAP overexpression is able to directly dedifferentiate hepatocytes into progenitor oval cells(Yimlamai et al., 2014). However, the role of YAP in embryonic liver development has not been explored and could help elucidate its role in hepatocyte differentiation.

With the ability of YAP to induce rapid proliferation of hepatocytes, a major question concerning how it is able to support rapid cell division remains to be answered. Intriguingly, in heterozygous YAP mice, microarray analysis indicated that genes involved in metabolism may be deregulated (Septer et al., 2012). This opens the question as to whether YAP can can directly reprogram cellular metabolism to produce the necessary building blocks required for cellular proliferation and organ growth.

1.4 Overview of the Dissertation

In this dissertation, I examine the role of Yap in metabolically reprogramming cells for anabolic synthesis in order to sustain rapid proliferation. In Chapter 2, I utilize transgenic zebrafish that specifically express a constitutively active form of Yap in hepatocytes to show that Yap drives hepatocyte proliferation and hepatomegaly in the zebrafish. I demonstrate that Yap, in these transgenic livers, upregulates glutamine synthetase expression and activity in order to drive nitrogen flux into *de novo* nucleotide biosynthesis. I also show that chemical treatment with a glutamine synthetase chemical inhibitor reduces Yap-induced liver growth. In Chapter 3, I describe the role of Yap in early liver development using yap knockout zebrafish and heat shock inducible zebrafish that can modulate Yap transcriptional activity. Here, I find that loss of Yap results in decreased glucose transporter expression and cellular reprogramming of the carbon backbone of glucose into purine and pyrimidine synthesis *in vivo*. In the final chapter, I discuss our conclusions and the current model of the role of Yap in cellular metabolic reprogramming. I also discuss future directions and unknown questions as to the role of Yap as a central regulator of organ growth.

Chapter 2

The Role of Yap in Glutamine Metabolism During Liver Development and Tumorigenesis

2.1 Abstract

The Hippo pathway has emerged as a master regulator of organ size and tumorigenesis. It is unclear, however, how the Hippo pathway affects cellular metabolism to provide the energy and cellular building blocks required for rapid cell growth. Here, we utilize transgenic zebrafish with liver-specific expression of the Hippo pathway effector Yap to demonstrate that Yap promotes hepatomegaly, liver dysplasia and increased susceptibility to chemical hepatocarcinogenesis. Transcriptomic and metabolomic profiling identified glutamine metabolism as a predominant target of Yap. Yap activation enhances glutamine synthetase (Glul) expression and activity. This results in elevated steady-state levels of glutamine and enhanced nitrogen flux into *de novo* purine and pyrimidine biosynthesis. *In vitro* studies in human liver cancer cells identify Glul as a direct target of Yap. Yap-mediated activation of Glul is required for rapid cell and organ growth, as Glul knockdown or intervention studies with the Glul inhibitor methionine sulfoximine diminish Glul activity, inhibit nitrogen flux into nucleotide biosynthesis and suppress liver growth observed in Yap transgenics. We conclude that Yap regulates Glul expression and reprograms nitrogen metabolism to enhance liver growth during development and tumorigenesis. Our findings demonstrate that Yap inte-

grates the anabolic demands of rapid cell proliferation by increasing the flux of glutamine into nucleotide biosynthesis.

2.2 Introduction

Many signaling pathways have been identified to govern liver growth during organ development and tumor formation. It is often unclear, however, how these signals provide energy and cellular building blocks to enable rapid cell division and organ growth. The Hippo signaling pathway has emerged as an evolutionarily conserved master regulator of organ size and tissue growth (Yu and Guan, 2013; Piccolo et al., 2014). The Hippo kinase cascade regulates the transcriptional co-activator Yap that binds the Tead family of transcription factors to enhance cell proliferation, inhibit cell death and alter cell fate (Pan, 2010; Yu et al., 2015). The Hippo pathway is frequently perturbed in human cancer(Harvey et al., 2013). Recent studies have shown that many oncogenic pathways including Wnt (Imajo et al., 2012; Rosenbluh et al., 2012; Azzolin et al., 2012), Ras (Zhang et al., 2014; Shao et al., 2014; Kapoor et al., 2014), PI3K/mTOR (Liang et al., 2014; Tumaneng et al., 2012b), TGFβ (Alarcon et al., 2009; Varelas et al., 2010b; Fujii et al., 2012), Hedgehog (Fernandez et al., 2009; Huang and Kalderon, 2014; Amoyel et al., 2014), Rb (Nicolay et al., 2010; Tschop et al., 2011; Ehmer et al., 2014) and LKB1 (Mohseni et al., 2014; Nguyen et al., 2013) feed into the Hippo pathway and sustain growth in a Yap-dependent manner. While many upstream regulators of Yap are now well defined, the molecular mechanisms by which Yap target genes enable rapid cell proliferation to modulate organ size remain elusive.

Altered cellular metabolism is a hallmark of cancer cells (Hanahan and Weinberg, 2011). Until recently, a number of studies had focused attention on the alternate means by which cancer cells produce ATP, including aerobic glycolysis (Vander Heiden et al., 2009) or the anaplerotic use of alternate fuel sources such as glutamine (Deberardinis et al., 2008; Hensley et al., 2013). However, new findings have elaborated on mechanisms by which oncogenic

pathways, such as mTOR, enhance de novo synthesis of building blocks and macromolecules required for cell growth (Dibble and Manning, 2013). Despite the substantial progress in our understanding of metabolic reprogramming in cancer, it is unknown whether the Hippo pathway can rewire cellular metabolism to match the demands for rapid cell growth.

Here, we investigate transgenic zebrafish expressing activated Yap in the liver that develop hepatomegaly and are prone to liver tumor formation. Transcriptomic and metabolomic analyses reveal that Yap induces glutamine synthase (Glul), to elevate glutamine flux into anabolic processes, particularly nucleotide synthesis. We demonstrate that Yap-dependent regulation of Glul is conserved in humans. Finally, we identify Glul as a primary target of Yap activation, which is required for maximal proliferation during the development of hepatomegaly. Treatment studies in larval and adult zebrafish demonstrate that Glul inhibition diminishes Yap-induced liver growth. Our studies define a new role of Yap to rewire cellular metabolism to provide the anabolic requirements for rapid cell growth and illustrate the therapeutic promise of targeting Yap-driven alterations in metabolism.

2.3 Materials and Methods

Zebrafish Husbandry

Zebrafish were maintained according to institutional animal care and use committee (IACUC-BIDMC) protocols. Lines used in this study include WT (AB) and *Tg(-2.8fabp10a:eGFP)*^{as3} as previously described (Her et al., 2003b,a). *Tg(−2.8fabp10:Yap1*^{S87A}; *−0.8cryaa:Venus*, abbreviated *lf:Yap*) express a constitutively activate form of Yap (Yap1^{S87A}) driven by the hepatocyte-specific promoter fabp10a. This line also contained the selection marker Venus, driven by the cryaa promoter, which produced green fluorescence in the lens of the eye.

Chemical Exposure

Embryos and adult zebrafish were exposed to methionine sulfoximine (MSO, 1 mM) and dimethylbenzanthracene (DMBA, 5 ppm) as described. Where necessary, chemicals were dissolved in DMSO. Chemicals were obtained from Sigma-Aldrich (St. Louis, MO, USA).

Morpholino Injection

Morpholinos (MO) (GeneTools, PhiloMath, OR, USA) designed against exon2-intron2 splice sites of *glula* (5'- ATAGTTCAAGTCCAGCTTACCTTCA -3') and *glulb* (5'- AATACAA-CAACTACCTTCAACAGAT -3') or mismatched controls glula-MM (5'- ATAcTTaAAcTC-CAcCTTAaCTTCA -3') and glulb-MM (5'- AATAaAAaAACTACaTTCAAaAcAT -3') were injected into *Tg(-2.8fabp10a:eGFP)* and *Tg(-2.8fabp10a:eGFP)*; *lf:Yap* embryos at the one-cell-stage.

Fluorescence Microscopy

Fluorescent liver reporter *Tg(-2.8fabp10a:eGFP)* embryos were put under anesthesia with 0.04 mg/ml Tricaine-S and microscopy was performed. Embryos were imaged using a Zeiss Discovery V8/Axio Cam MRC with the Axiovision software suite (Carl Zeiss). Lightsheet microscopy was performed using a Zeiss Lightsheet Z.1 at the Harvard Center for Biological Imaging (HCBI) core and analyzed using FIJI (NIH) as previously described (Weber et al., 2014; Schindelin et al., 2012).

Histology

Paraformaldehyde (PFA)-fixed embryos, fish or mice livers were paraffin-embedded, cut into serial sections and stained with Hematoxylin and Eosin (H&E) using standard techniques.

FACS Analysis

Fluorescent liver reporter *Tg(-2.8fabp10a:eGFP)* embryos were dissociated by enzymatic disaggregation in TrypLETM Express (Invitrogen, CO, USA) combined with manual disruption. Upon addition of DMEM with 10% FCS, the cells were strained through a 35 μM nylon mesh and then analyzed using a BD FACSAria II flow cytometer (BD Biosciences, San Jose, CA, USA).

DMBA-induced carcinogenesis

WT and *lf:Yap* transgenic fry were exposed to 5 ppm DMBA dissolved in DMSO for 24 hr at 3, 4 and 5 weeks of age. Following exposure fry were rinsed several times in aquarium water before being returned to the aquarium tanks. Fish were monitored closely for tumor development over the subsequent 6 months.

RNA Transcriptomic Analysis

Livers were isolated from adult WT and *lf:Yap* transgenic adults and RNA was extracted in Trizol (Life Technologies) and purified using the RNease Mini Kit (Qiagen) according to the manufacturers instructions. RNA quality was checked using an Agilent Bioanalyzer and sequenced using an Illumina platform. polyA sequence data was annotated on a genomic reference (ZV9) to identify differentially affected genes (Collins et al., 2012).

qPCR analysis

RNA was isolated from pooled zebrafish embryos or isolated livers using Trizol (Life Technologies). Following DNAse treatment, cDNA synthesis was performed using the SuperScript III First-Strand Synthesis kit (Life Technologies). Quantitative RT-PCR was performed on biological triplicates using an iCycler (BioRad) with iQ SYBR green (BioRad). Gene expression was analyzed with Ef1α as the reference gene. Primer sequences can be found in Table 2.3.1.

Table 2.3.1: **qPCR Primer Sequences**

Gene	Forward Primer	Reverse Primer
ef1a	GCGTCATCAAGAGCGTTGAG	TTGGAACGGTGTGATTGAGG
ctgfa	CTACGGCTCCCCAAGTAACC	TCCACTGCGGTACACCATTC
cyr61	ACAAGCTGCAACCTACCACT	AGAGTATTCATTCTACTCACACTCA
amotl2b	TCCCAGCACAACAGACTTCC	CCGTTTGTCCCTCTAGCTCC
glula	ATGGTGGACTGAAATGTATTGAGG	AATGTTGGAGGTTTCATGGTGG
glulb	GCCCGCTTCCTCCTACACA	CTCCTCAATATGCTTCAAACCTCC
axin2	GGACACTTCAAGGAACAACTAC	CCTCATACATTGGCAGAACTG
cyclinD1	GGAACTGCTGGCGCTTAAATA	GACTTGCGAGAGGAAGTTGG

ChIP analysis

Chromatin Immunoprecipitation was performed essentially as previously described (Galli et al., 2012). Briefly, cells were cross-linked in 1% formaldehyde for 10 min at room temperature after which the reaction was stopped by addition of 0.125M glycine. Cells were lysed and harvested in ChIP buffer (100 mM Tris at pH 8.6, 0.3% SDS, 1.7% Triton X-100, and 5 mM EDTA) and the chromatin disrupted by sonication using a Diagenode Bioruptor sonicator UCD-200 to obtain fragments of average 200-500 bp in size. Suitable amounts of chromatin were incubated with specific antibodies overnight. Antibodies used were IgG (Sigma, I8140), Yap (a kind gift of Joseph Avruch, MGH, Boston), Tead4 (Abcam Ab58310). Immunoprecipitated complexes were recovered on Protein-A/G agarose beads (Pierce) and, after extensive washes, DNA was recovered by reverse crosslinking and purification using QIAquick PCR purification kit (QIAGEN).

Luciferase assay

HEK293 cells were cotransfected with glutamine synthetase reporter constructs (van der Vos et al., 2012), the Renilla plasmid, and pCMV-EGFP, pCMV-Yap-S127A (Addgene, #17794), or pCMV-Yap-S94A. Cells were harvested 48 hr later using the Dual-Glo Luciferase Assay System (Promega) and assayed according to the manufacturer's directions.

Cell culture and lentiviral infection

HEK293, HepG2 and Huh7 cells were grown in high glucose Dulbecco's modified Eagle's medium supplemented with 10% fetal bovine serum and maintained at 37 °C in a humidified atmosphere with 5% CO2. HEK293T cells were transiently transfected with polyethylenimine (PEI) gene transfer reagent (Boussif et al., 1995) in its 25-kDa linear form (Polysciences, Warrington, PA). pLKO.1 plasmid constructs were co-transfected in HEK293T cells with packaging vectors pCMV-Δ8.2 and pCMV-VSVG using polyethyleimine. Two days post-transfection, virus-containing media was harvested, 5 μg of Polybrene added, passed through a 0.45 μM filter, and used to infect target cells. Target cells at approximately 70% confluence were infected for 24 hr followed by selection in 2 μg/mL puromycin for 48 hr prior to stimulation and cell lysis.

Immunoblot analysis

Cultured cells were collected and lysates were prepared using RIPA buffer. Lysates were resolved by SDS-PAGE and electrophoretically transferred onto nitrocellulose. Membranes were probed with anti-Yap (AbCam), anti-Glul (Cell Signaling) or a overnight and detected with secondary antibody conjugated with HRP. Antibody complexes were visualized by enhanced chemiluminescence using X-ray film.

Steady-state metabolomics analysis

Livers were isolated from adult WT and *lf:Yap* transgenic adults and a methanol extraction was performed. Polar metabolites were isolated and enriched using the methodology outlined by Yuan et al (Yuan et al., 2012). Polar metabolites were quantified using selected reaction monitoring on a 5500 QTRAP hybrid triple quadrupole mass spectrometer.

Glul activity assay

Glul activity was assayed using the γ-glutamyltransferase assay as previously described (Deuel et al., 1978). Briefly, WT and *lf:Yap* transgenic embryos or adult livers were lysed in 50 mM imidazole. Lysates were run on micro bio-spin gel p-6 columns (BioRad) and protein quantification was performed using the DCTM assay (BioRad). Lysates were incubated in activity buffer (50 mM imidazole, 50 mM L-glutamine, 25 mM hydroxylamine, 25 mM sodium arsenate, 2mM manganese chloride, 0.16 mM adenosine diphosphate) at 27 °C for 30 min. The reactions were quenched in stop solution (2.42% iron chloride and 1.45% trichloroacetic acid in 1.82 N hydrochloric acid). Absorbance was read at 520 nm and a calibration curve of glutamyl-γ-hydroxamate (Sigma) was used to calculate nmol of product formed.

Determination of ammonia excretion rate

The rate of ammonia excretion was determined by placing individual fish into small water containers and monitoring ammonia buildup over time using methods previously established (Bucking et al., 2013) and an ammonia detection kit (Biovision Inc.) according to the manufacturers instructions.

Analysis of $^{15}NH_4Cl$ flux in liver lysates

Ammonia incorporation into nucleotide precursors was measured using adaptations to previously established methods (Skaper et al., 1978; Monks et al., 1985). Briefly, livers were isolated from adult WT and *lf:Yap* transgenic adults and liver homogenates were prepared in lysis buffer (100mM NaCl, 25mM Imidazole, 25mM HEPES, 1mM MgCl2, 1mM MnCl2, 0.1mM KCl and 1% NP-40 pH 7.4 supplemented with Complete protease inhibitors (Roche)). Liver homogenates (90 µl) containing the same amount of protein were incubated a reaction cocktail (10 µl) containing 10 mM $^{15}NH_4Cl$ (Cambridge Isotopes Laboratories, Inc.), 10 mM ATP and 10 mM sodium glutamate and incubated at 37 °C for 20 min before the reaction was

quenched in 80% Methanol (900 µl). Polar metabolites were enriched using the methodology outlined by Yuan *et al.* (Yuan et al., 2012) and quantified using selected reaction monitoring on a 5500 QTRAP hybrid triple quadrupole mass spectrometer using a protocol to detect ^{15}N-labelled isotopomers of nucleotide precursors.

^{15}N-Spirulina feeding protocol

^{15}N-labelled Spirulina (98%) (Cambridge Isotopes Laboratories, Inc.) gels containing 50 mg/ml ^{15}N-labelled Spirulina, 5 mg/ml Gemma Micro 300 (Skretting) and 1% agar were aliquoted into 30 µl pellets. Individual WT and *lf:Yap* transgenic adults were given a ^{15}N-labelled Spirulina gel pellet twice a week over a 4 week period.

Analysis of ^{15}N-Spirulina nutritional flux into genomic DNA

Livers were isolated from adult WT and *lf:Yap* transgenic adults and genomic DNA was isolated using Quick-gDNA™ MiniPrep (Zymo Research) according to the manufacturers instructions and re-purified by sodium acetate precipitation. DNA from ^{15}N-labeled spirulina and unlabeled spirulina was extracted as previously described (Morin et al., 2010). Purified DNA was quantified with PicoGreen (Life Technologies), and 100 ng of DNA was treated with DNA Degradase Plus (Zymo Research) for 24 hours. Completion of DNAse digestion was measured by PicoGreen quantification. Hydrolyzed nucleotides were enriched using the methodology outlined by Yuan *et al.* (Yuan et al., 2012) and quantified using selected reaction monitoring on a 5500 QTRAP hybrid triple quadrupole mass spectrometer using a protocol to detect ^{15}N-labelled isotopomers of nucleotides.

Figure 2.4.1: **Schematic of *lf:Yap* construct.** Diagram of the construct used to generate transgenic fish with hepatocyte-specific expression of Yap1^{S87A}, abbreviated to *lf:Yap*.

2.4 Results

Hepatocyte-specific overexpression of Yap causes hepatomegaly and accelerates DMBA-induced liver tumor formation

To address the impact of Yap activation on liver growth in the zebrafish embryo, we generated transgenic zebrafish *Tg(-2.8fabp10:Yap1^{S87A})* (*lf:Yap*) with hepatocyte-specific expression of a constitutively active form of Yap, homologous to human YAP1^{S127A} (Figure 2.4.1). Liver development was visualized using an established hepatocyte reporter line, *Tg(-2.8fabp10:eGFP)*, referred to as *lf:GFP*. By 5 dpf, which is within 2 days of transgene induction, *lf:Yap;lf:GFP* fish exhibit a 36% increased liver area (Figure 2.4.2 A,B) compared to their wild type (WT) siblings. Single-plane illumination confocal microscopy was performed to produce a 3D-rendering of WT and *lf:Yap* transgenic livers and this confirmed liver enlargement and preservation of gross architectural features of the bi-lobed embryonic liver (Figure 2.4.2 C,D). Histological and FACS analysis revealed that increased liver size in the transgenic animals is accompanied by hepatocyte hyperproliferation without significant increase in liver cell size (Figures 2.4.2 E,F). Increased liver size was maintained in *lf:Yap* fish into adulthood at 16 weeks post fertilization (wpf) (Figure 2.4.3 A,B): liver-to-body weight ratio was two-fold increased in *lf:Yap* transgenics (Figure 2.4.3 C). Adult *lf:Yap* livers are hyperplastic with increased cellularity and a significant increase in cell proliferation, increased bile duct density and a decreased amount of glycogen deposition (Figure 2.4.3 D). These data demonstrate that Yap induces hepatomegaly and promotes liver hyperplasia in zebrafish.

Liver hyperplasia did not spontaneously progress to frank cancer even in 2 year-old fish

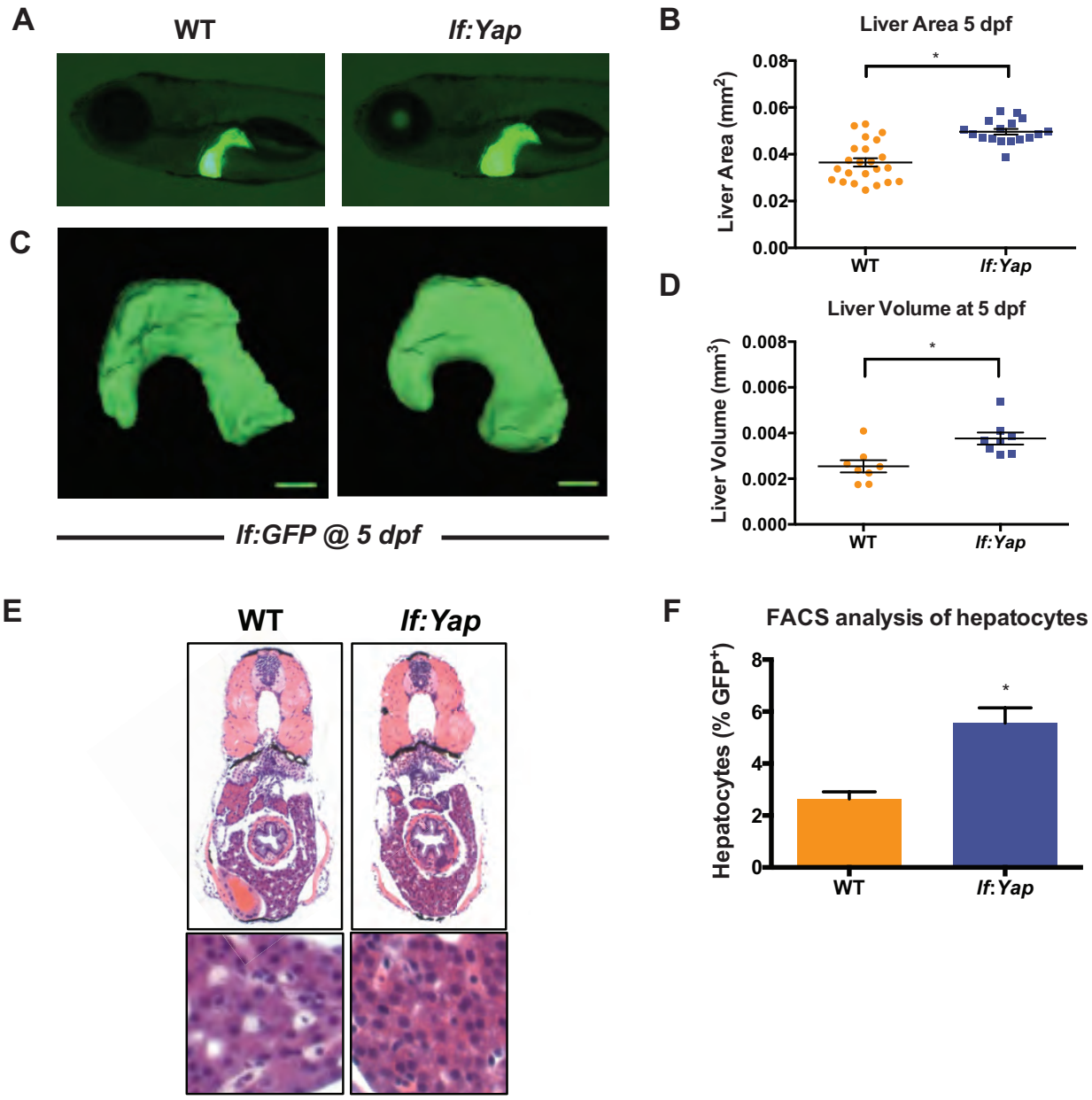

Figure 2.4.2: **Hepatocyte-specific overexpression of Yap causes embryonic hepatomegaly.** (A) Fluorescence microscopic analysis of hepatomegaly in *lf:Yap;lf:GFP* compound transgenic embryos at 5 dpf. (B) Quantitative analysis of fluorescent liver area in WT and *lf:Yap* transgenic embryos at 5 dpf. (C) Confocal tomography of liver morphology in WT and *lf:Yap* transgenic embryos at 5 dpf. (D) Quantitative analysis of liver volume in WT and *lf:Yap* transgenic embryos at 5 dpf. (E) Histological evaluation of liver morphology in WT and *lf:Yap* transgenic embryos at 5 dpf. (F) FACS analysis of the percentage of differentiated hepatocytes in WT and *lf:Yap* transgenic embryos at 10 dpf. $n > 17$, $p < 0.0001$.

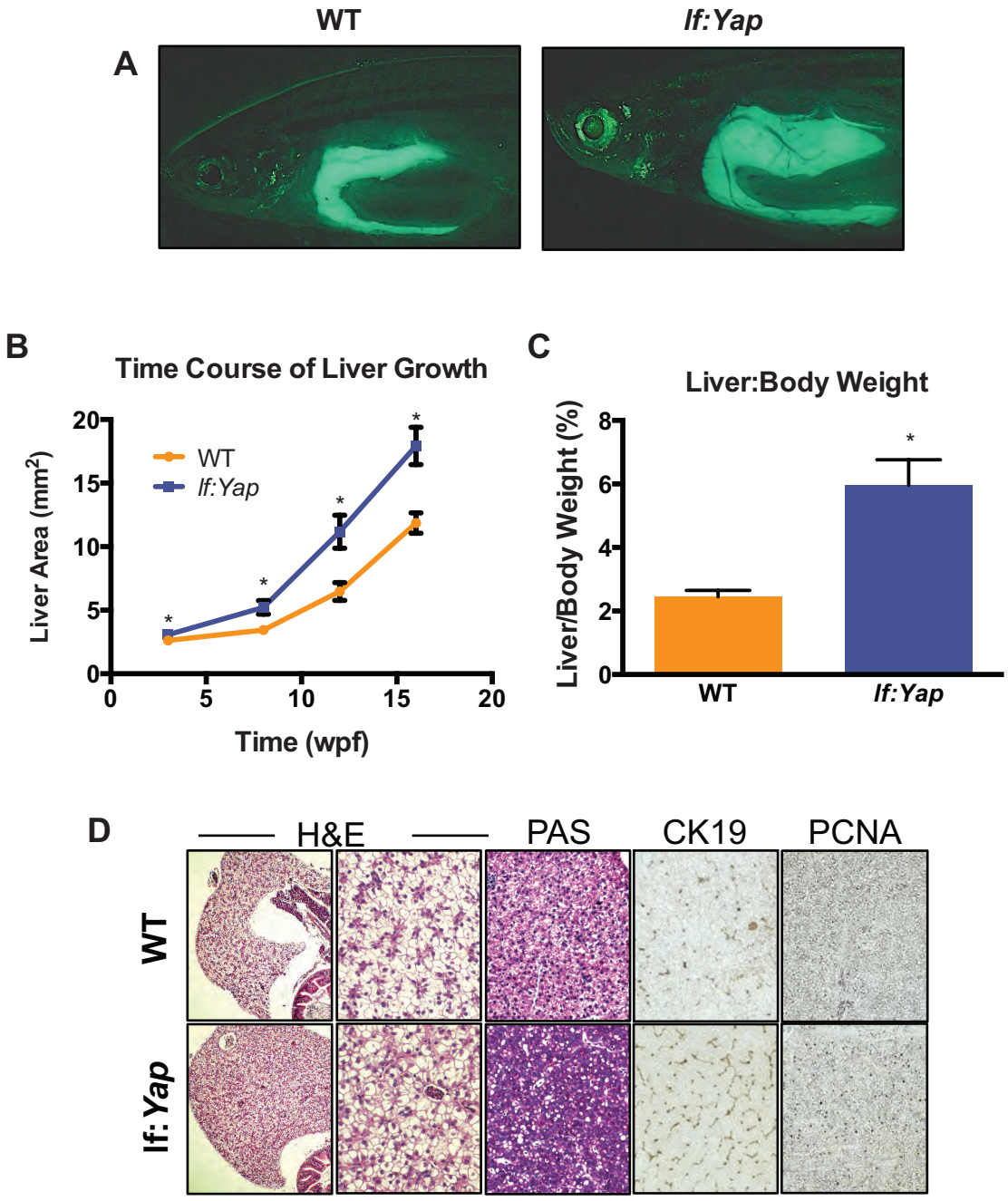

Figure 2.4.3: **Hepatocyte-specific overexpression of Yap causes adult hepatomegaly.** (A) Fluorescence microscopic analysis of hepatomegaly in dissected *lf:Yap* transgenics at 12 weeks post fertilization (wpf). (B) Timecourse of hepatomegaly during early adulthood as determined by quantification of fluorescent liver area. (C) Quantitative determination of hepatomegaly in WT and *lf:Yap* as determined by liver:body weight ratio. n = 6. p $\leq$ 0.01. (D) H&E staining of histological sections from liver of WT and *lf:Yap* transgenics at low (10x) and high magnification (25x). Periodic-acid Schiff (PAS) stain for hepatic glycogen (pink inclusions) in liver sections from WT and *lf:Yap* transgenics. Bile duct morphogenesis (2F11) in liver sections from WT and *lf:Yap* transgenics.

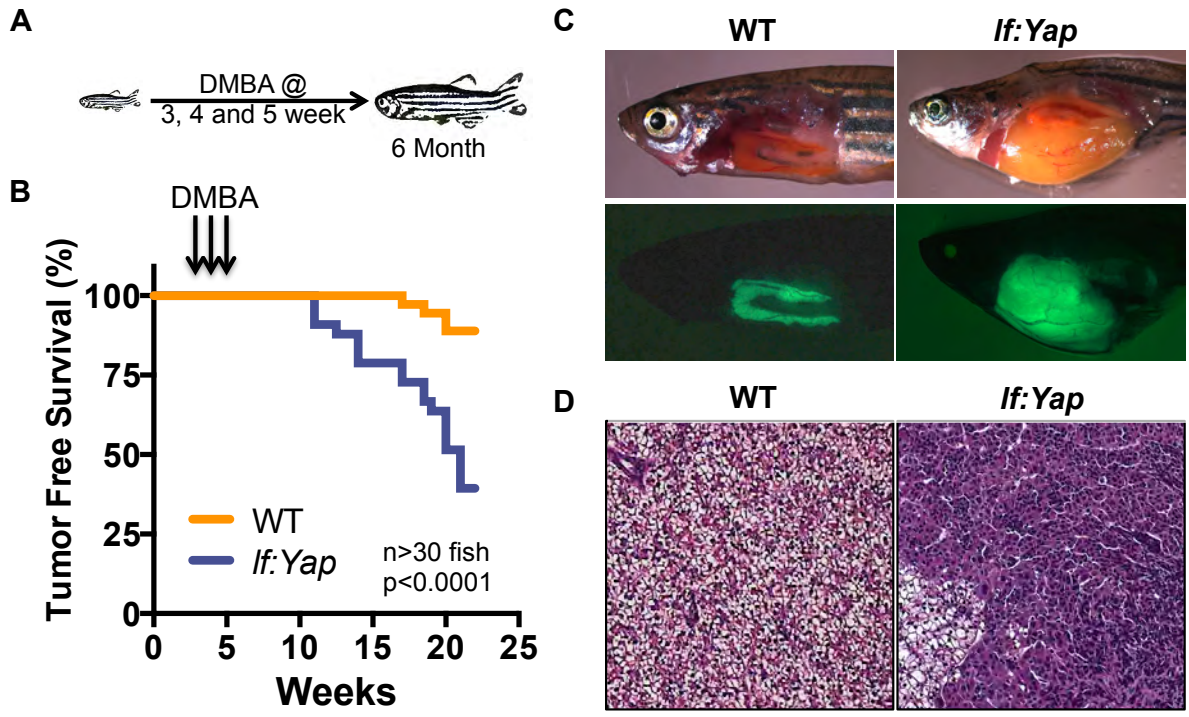

Figure 2.4.4: **Yap overexpression accelerates DMBA-induced liver tumor formation.** (A) Schematic illustrating the exposure of zebrafish to the chemical carcinogen DMBA. (B) Kaplan-Meier survival plot showing tumor-free survival of WT and *lf:Yap* transgenics exposed to DMBA. n $>$ 35 fish, p $<$ 0.0001 by Log rank Mantel-Cox test. (C) Fluorescence microscopy examination of gross liver morphology of WT and *lf:Yap* transgenic tumors following dissection. (D) Histological evaluation (H&E stain) of liver sections in WT and *lf:Yap* transgenics harboring tumors.

(data not shown). To examine whether Yap predisposes to liver tumor formation, WT and *lf:Yap* transgenics were exposed to the carcinogen dimethylbenzanthracene (DMBA) (Figure 2.4.4 A). *lf:Yap* transgenics formed liver tumors earlier and with greater frequency than their wild type siblings (Figure 2.4.4 B). Tumors were evident as abdominal enlargements showed liver masses taking up the entirety of the abdominal cavity (Figures 2.4.4 C, D). Examination by immunohistochemistry revealed a spectrum of liver cancer subtypes ranging from hepatocellular carcinoma (HCC) to cholangiocarcinoma (CCA) with features of peliosis hepatis, fibrosis, sarcomatoid cytology and ascites (Figure 2.4.5 and Table 2.4.1). These data demonstrate that Yap is a potent oncogene that can accelerate and exacerbate chemically induced hepatocarcinogenesis.

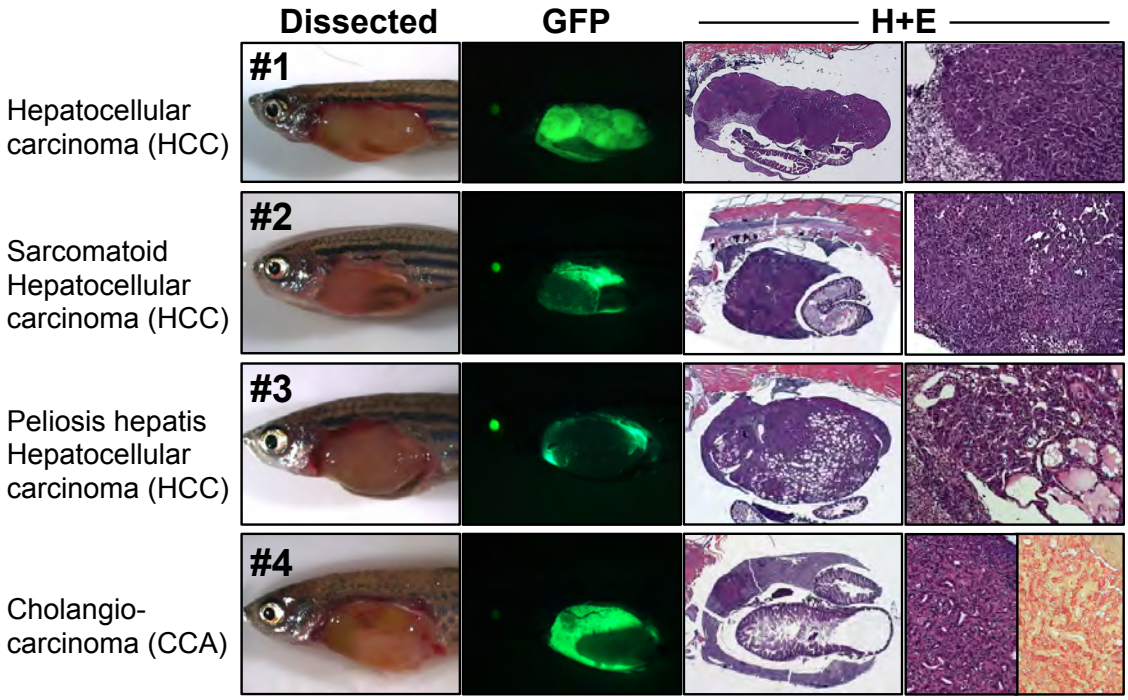

Figure 2.4.5: **Tumor heterogeneity in *lf:Yap* transgenics exposed to DMBA.** *lf:Yap* tumors include Hepatocellular carcinoma (HCC), Sarcamatoid HCC, Peliosis hepatis HCC and Cholangiocarcinoma (CCA).

Table 2.4.1: **Tumor subtype frequency in DMBA exposed WT and *lf:Yap* transgenics.** Table illustrating the incidence of fibrosis, glycogen, sarcomatoid cytology, peliosis hepatis and ascites in DMBA-induced liver tumors.

	Tumor subtype	Fibrosis	Glycogen poor	Sarcomatoid cytology	Peliosis hepatis	Ascites
WT	HCC	50% (2/4)	100% (4/4)	25% (1/4)	25% (1/4)	0% (0/4)
	CCA	100% (1/1)	100% (1/1)	N/A	N/A	0% (0/1)
Yap^{S87A}	HCC	47% (9/19)	84% (16/19)	21% (4/19)	58% (11/19)	32% (6/19)
	CCA	100% (4/4)	100% (4/4)	N/A	N/A	25% (1/4)

Yap alters expression of metabolism-related genes and enhances Glul expression

To identify downstream pathways responsible for Yap-driven liver hyperplasia, we performed transcriptional profiling in WT and *lf:Yap* transgenic adult livers, revealing a large number of differentially expressed genes (Figure 2.4.6 A). Gene set enrichment analysis (GSEA) confirmed consistency with a previously published mammalian Hippo signature (Figure 2.4.7 A) (Cordenonsi et al., 2011), including upregulation of the bona fide Yap target genes *amotl2*, *ctgf* and *cyr61* (Figure 2.4.6 C). Intriguingly, gene ontology (GO) analysis revealed that 60% of the top 20 biological processes upregulated by Yap were related to metabolism (Figure 2.4.6 B). Amongst the most differentially upregulated genes were glutamine synthetase (Glul) orthologs Glula and Glulb (Figure 2.4.6 C), which play a key role in nitrogen assimilation in the liver. Quantitative PCR (qPCR) verified induction of *ctgf*, *cyr61*, *amotl2*, *glula* and *glulb* in *lf:Yap* livers (Figure 2.4.6 D,E). While Glul expression has been reported to be regulated by Wnt activity, no activation of the Wnt target genes *cyclinD1*, *axin2* and *cd44* was seen in the *lf:Yap* transgenics (Figure 2.4.7 B,C).

Yap transcriptionally upregulates Glul and is evolutionarily conserved

Chromatin immunoprecipitation (ChIP) was performed to determine whether Yap transcriptionally regulates Glul directly. We found Yap was enriched at the promoter region of the actively transcribed gene *glula* as avidly as *ctgf* (Figures 2.4.8 A,B). To determine whether Yap-dependent regulation of Glul is evolutionarily conserved in humans, a luciferase reporter assay was utilized in HEK293 cells. This demonstrated that a constitutively active form of human Yap (Yap^{S127A}) activates Glul expression, whereas a Yap mutant lacking the ability to co-activate Tead (Yap^{S94A}) did not induce Glul (Figure 2.4.8 C). Promoter fragment analysis revealed that several promoter regions contributed to the total Yap-induced increase in activity (Figure 2.4.9). ChIP analysis in HepG2 cells revealed Yap occupation of the Glul promoter in the region associated with luciferase activation (Figure 2.4.8 D). shRNA-mediated knockdown of Yap in HepG2 liver cancer cell lines led to reduction in Glul

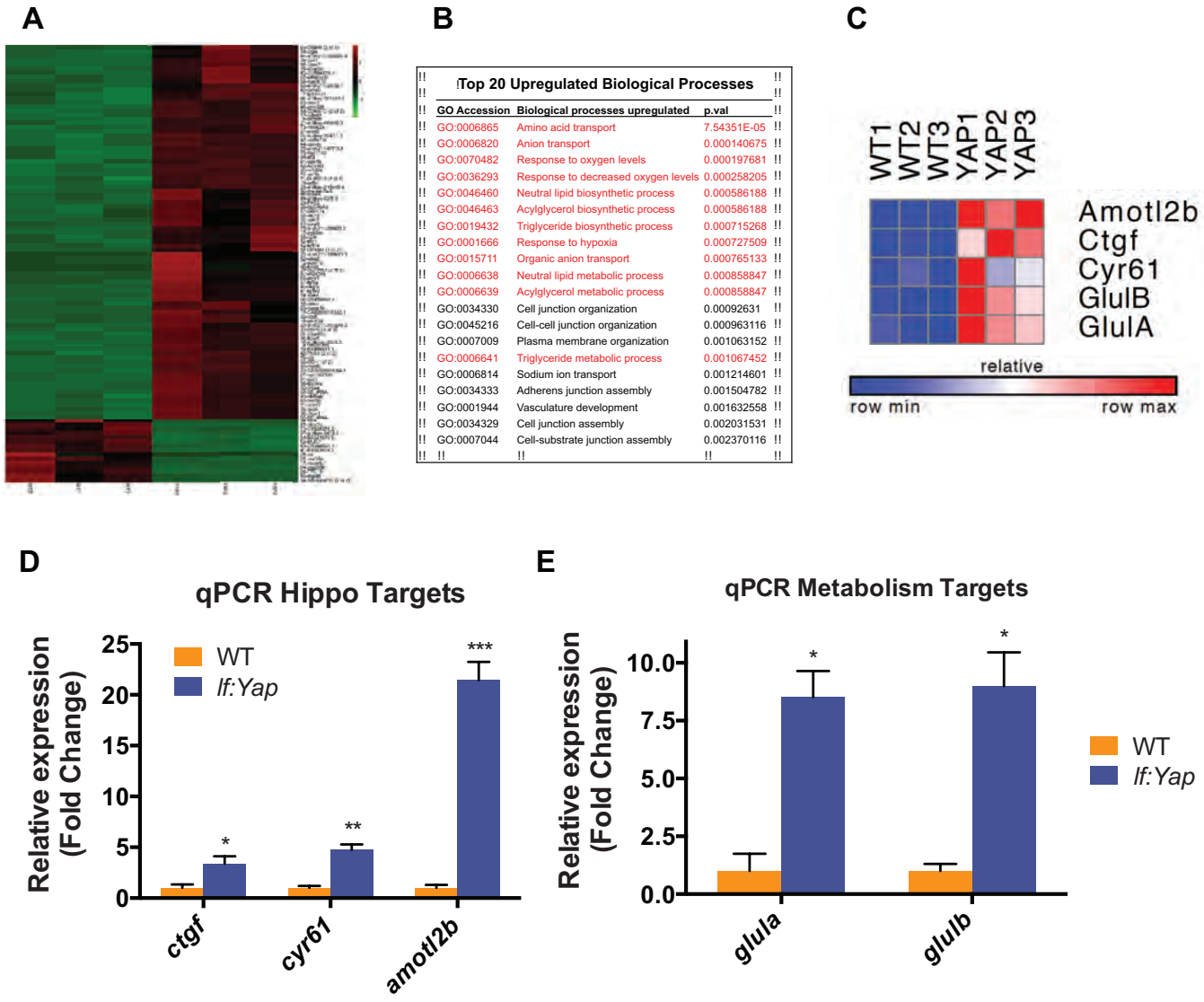

Figure 2.4.6: **Yap alters expression of metabolism-related genes and enhances Glul expression.** (A) RNA-seq analysis identifies differential gene expression between dissected WT and *lf:Yap* transgenic livers. (B) Gene ontology (GO) analysis of the top 20 biological processes upregulated by Yap. Biological processes related to metabolism are highlighted in red. (C) Heat Map analysis of RNA-seq data illustrates the induction of Yap target genes (*ctfg*, *amotl2b*, *cyr61*) and genes related to nitrogen metabolism (*glula*, *glulb*). (D) qPCR validation of Yap target gene expression in dissected WT and *lf:Yap* transgenic livers. (E) qPCR validation of Glul induction in dissected WT and *lf:Yap* transgenic livers. mean ± S.E.M, biological triplicates, $^{*}p \leq 0.05$, $^{**}p \leq 0.01$, $^{***}p \leq 0.001$.

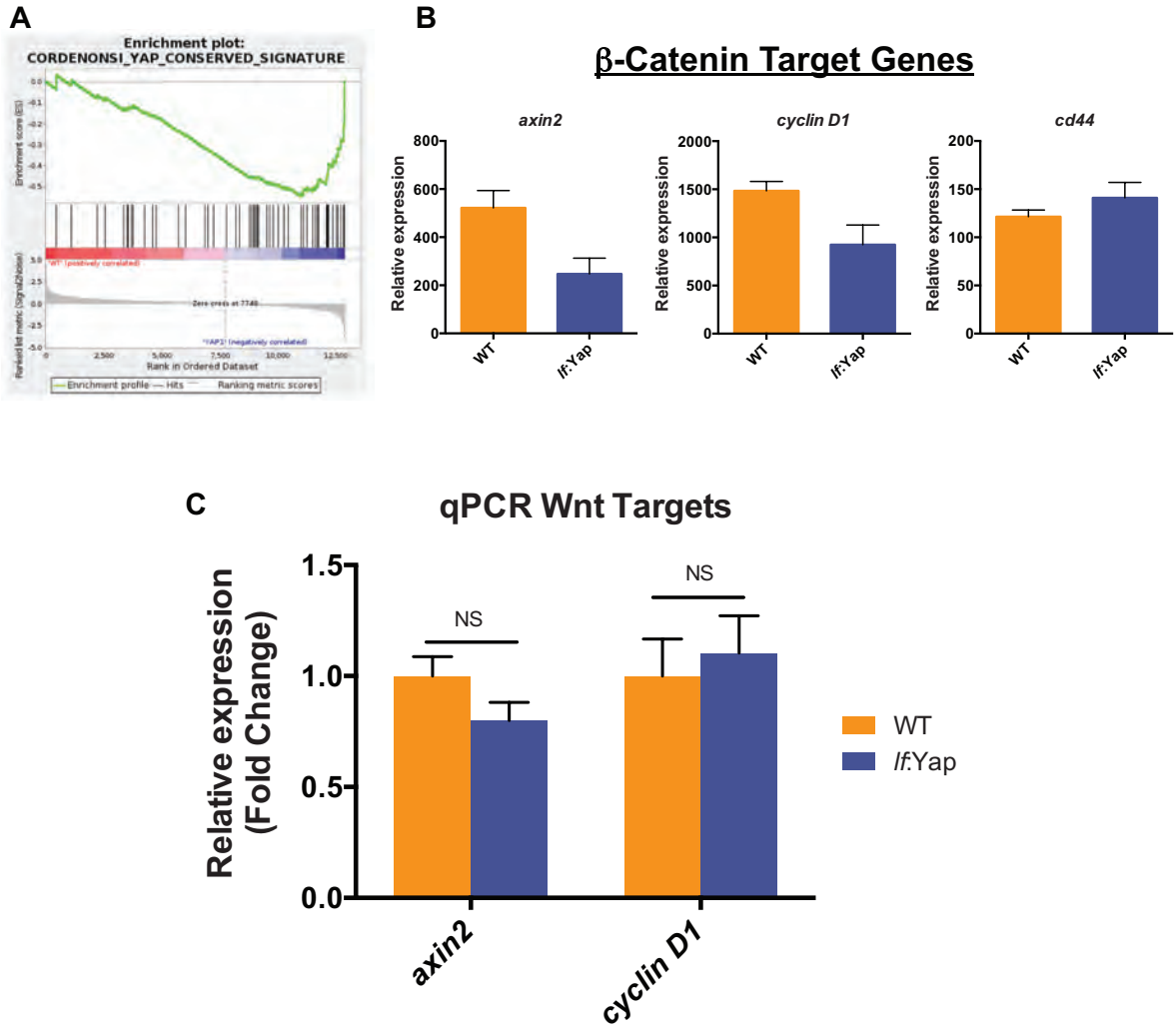

Figure 2.4.7: **Yap expression in the zebrafish demonstrates features of a Hippo target gene signature without Wnt features.** (A) Gene set enrichment (GSEA) derived from RNA-seq of WT and *lf:Yap* transgenic livers identifies a conserved Yap target gene signature. (B) RNA-seq analysis of the Wnt target genes CyclinD1, Axin2, Cd44 in dissected WT and *lf:Yap* transgenic livers. (C) qPCR validation of Wnt target genes *axin2* and *cyclinD1* in dissected WT and *lf:Yap* transgenic livers. Data are represented as mean ± S.E.M, biological triplicates, N.S. = not significant.

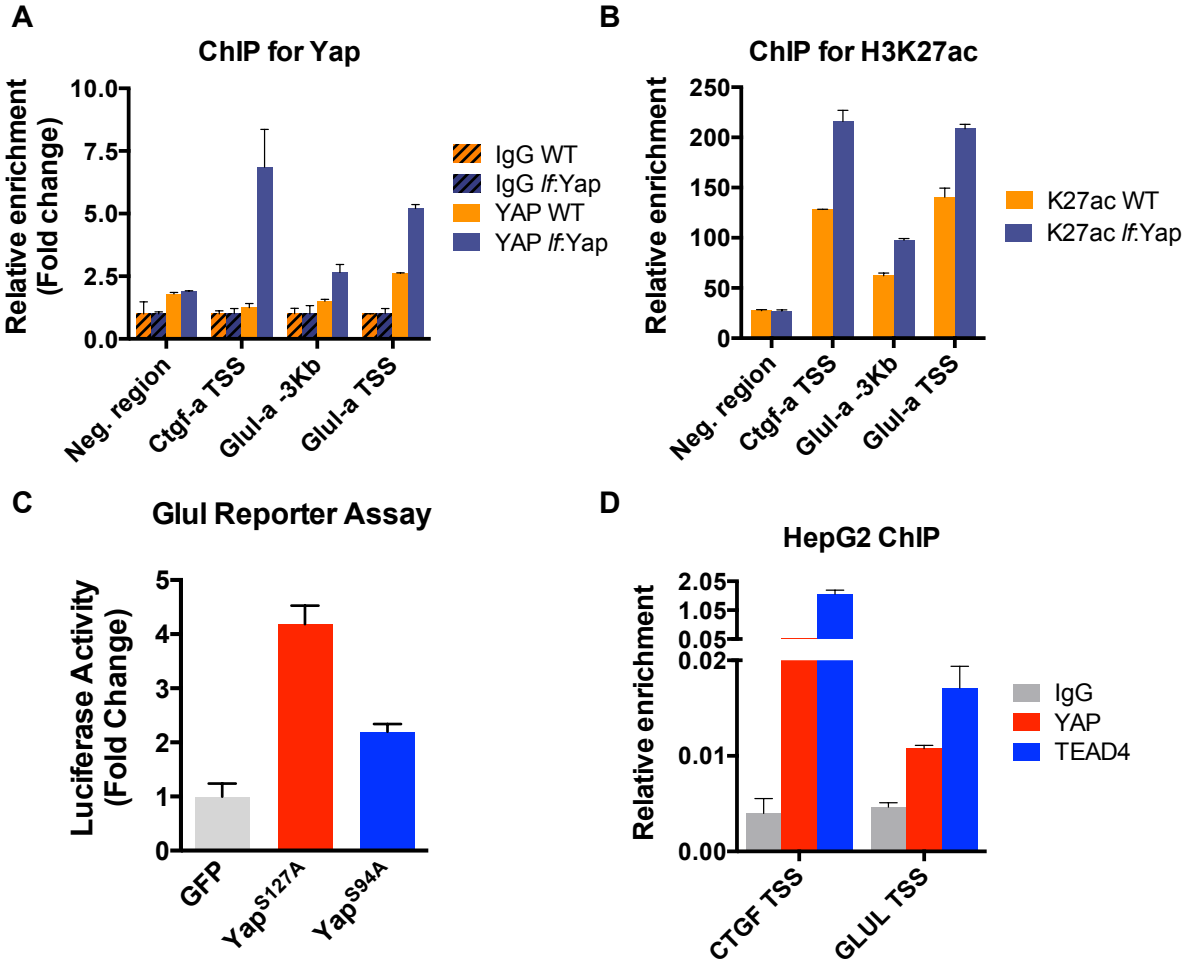

Figure 2.4.8: **Yap transcriptionally upregulates Glul and is evolutionarily conserved.** (A) Chromatin Immunoprecipitation (ChIP)-qPCR analysis of Yap enrichment at Glula promoter in dissected WT and *lf:Yap* transgenic livers. (B) ChIP-qPCR analysis of transcriptional activity (H3K27ac) at the Glula promoter in dissected WT and *lf:Yap* transgenic livers. (C) Luciferase Glul reporter assay in cultured HEK293 cells expressing GFP, $Yap1^{S127A}$ or $Yap1^{S94A}$, n = 3. (D) ChIP-qPCR analysis of Yao and Tead4 enrichment at the Glul promoter in HepG2 cells.

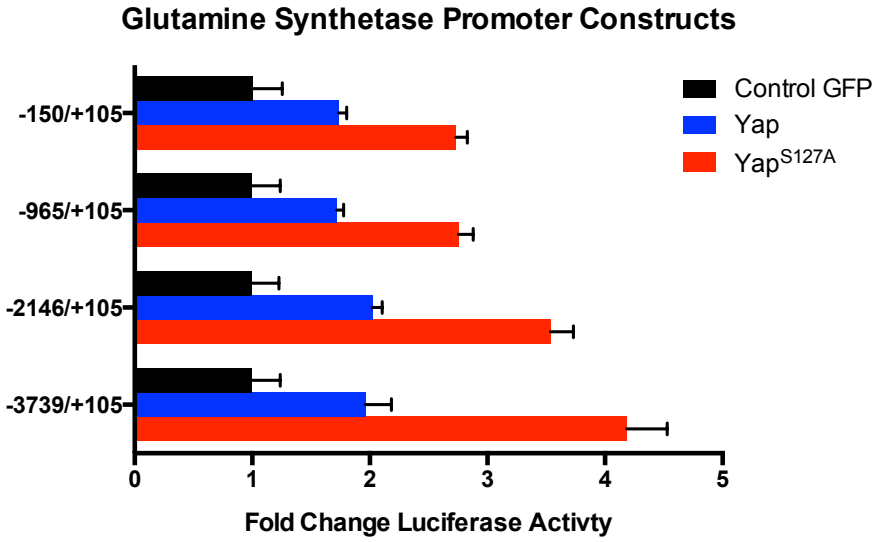

Figure 2.4.9: **Luciferase reporter assay shows Glul promoter is directly regulated by Yap**. Luciferase Glul reporter assay using truncated promoter constructs were co-transfected into HEK293 cells with GFP, Yap or Yap1^{S127A}, n = 3.

expression (Figure 2.4.10 A). As in zebrafish, β-catenin levels did not change, and expression of Wnt target genes was not affected (Figure 2.4.10 A). Regions of hepatocellular carcinomas with high Glul expression also demonstrated high nuclear expression of Yap (Figure 2.4.10 B). Together, these studies demonstrate that the regulation of Glul by Yap is evolutionarily conserved in humans.

Yap reprograms nitrogen metabolism by enhancing Glul-dependent anabolic assimilation of ammonia for de novo nucleotide biosynthesis

To examine the effect of Yap expression on cellular metabolism, polar metabolomics by LC-MS on isolated adult livers determined distinct metabolite profiles between transgenic *lf:Yap* and WT livers. Metabolite clustergram analysis revealed regulation of many metabolite steady-state levels (Figure 2.4.11 A), including enrichment of metabolites associated with protein biosynthesis, purine metabolism and pyrimidine metabolism (Figure 2.4.11 B). *lf:Yap* transgenic livers had a steady-state concentration of glutamine that was twice as much as WT livers (Figure 2.4.11 C). Glul enzyme activity in *lf:Yap* transgenic liver homogenate was

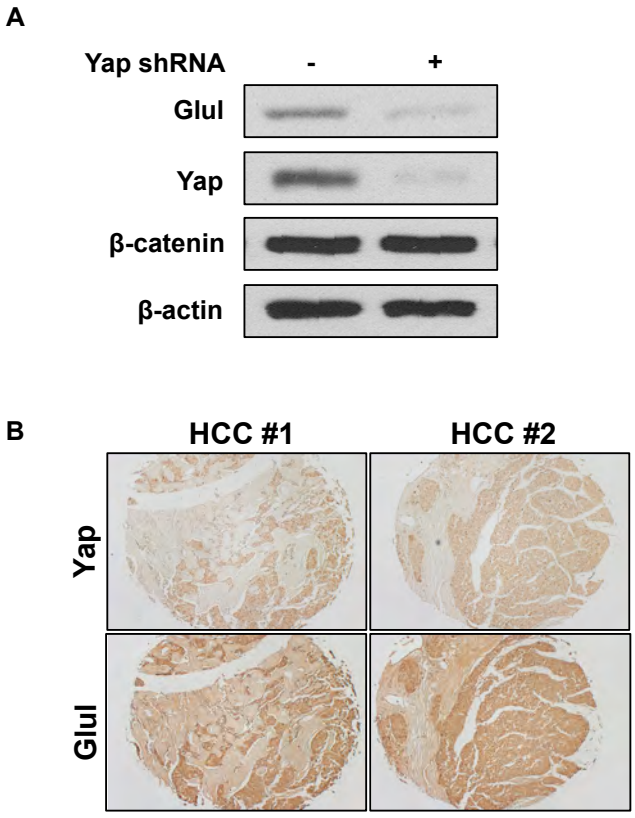

Figure 2.4.10: **Glul expression is decreased in HepG2 cells with knockdown of Yap.** (A) Immunoblot analysis of Glul, Yap and β-catenin expression in HepG2 cells infected with shYap retrovirus. (B) Immunohistochemical staining of Yap and Glul in Tissue Microarray (TMA) sections derived from human HCC.

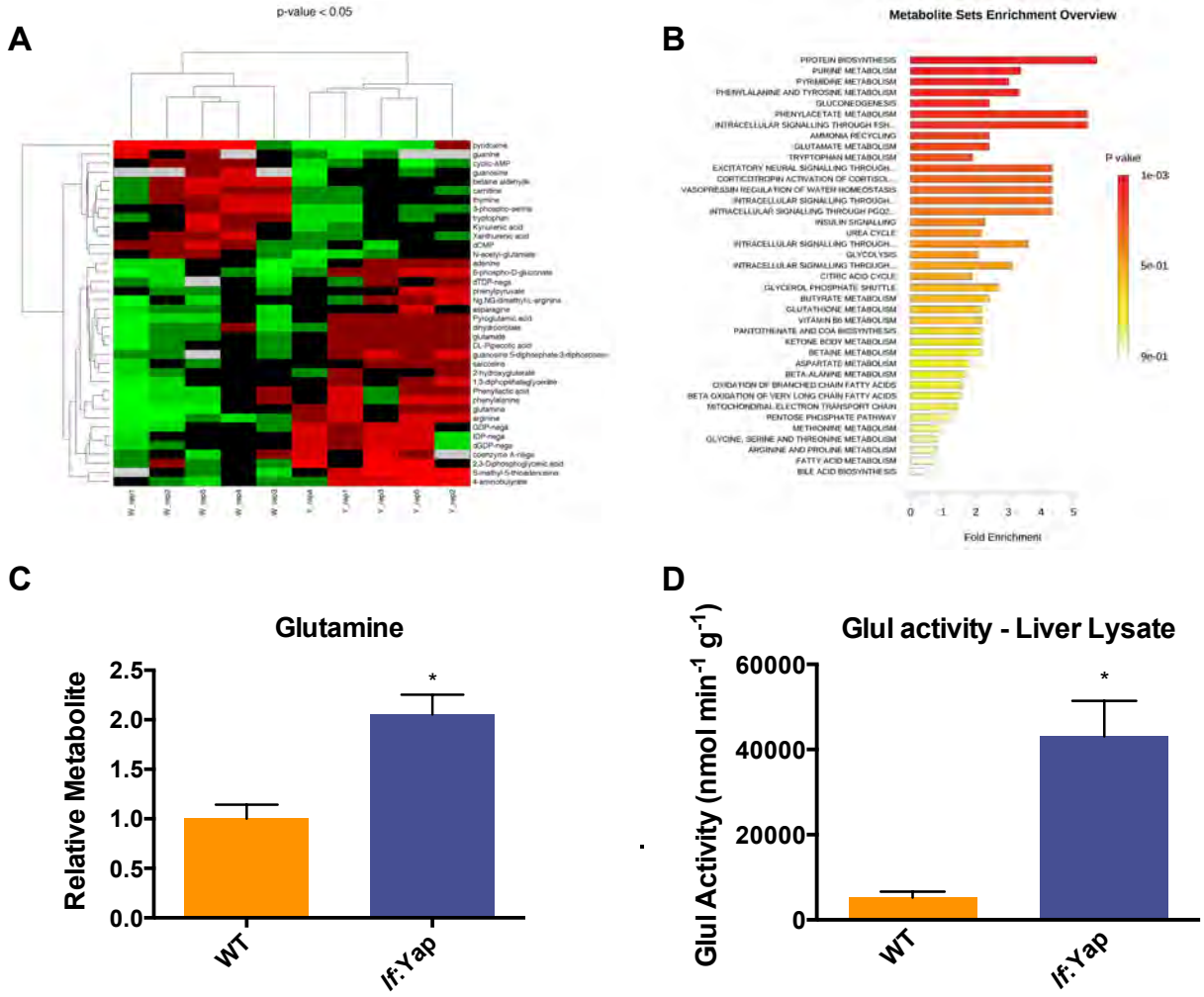

Figure 2.4.11: **Yap reprograms nitrogen metabolism by enhancing Glul acitivity.** (A) Clustergram analysis of polar metabolite abundance from dissected WT and *lf:Yap* transgenic livers as determined by LC-MS/MS selected reaction monitoring (SRM) analysis. (B) Metabolite Set Enrichment of polar metabolites from WT and *lf:Yap* transgenic livers as determined by SRM analysis. (C) Steady state abundance of glutamine in WT and *lf:Yap* transgenic livers as determined by SRM analysis. (D) Enzymatic assay of glutamine synthase activity in dissected WT and *lf:Yap* transgenic livers. n = 3, p $\leq$ 0.001.

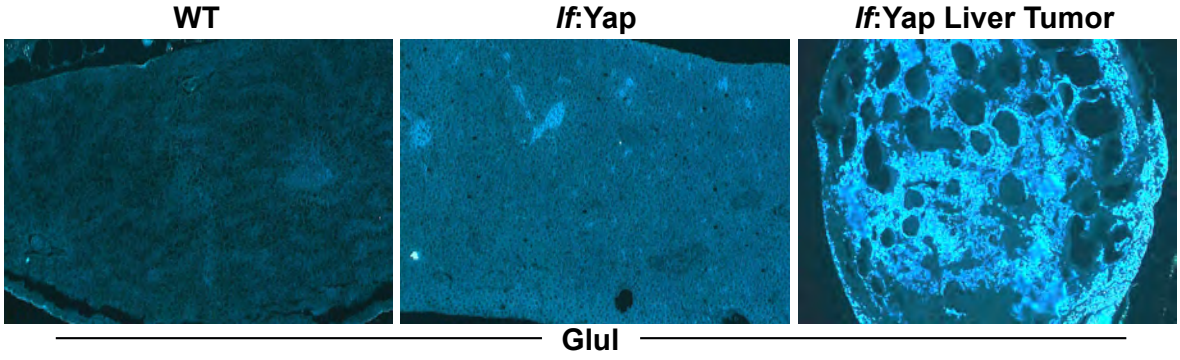

Figure 2.4.12: **Immunohistochemical detection of Glul.** Glul expression in WT, *lf:Yap* transgenic livers and DMBA-induced *lf:Yap* liver tumors.

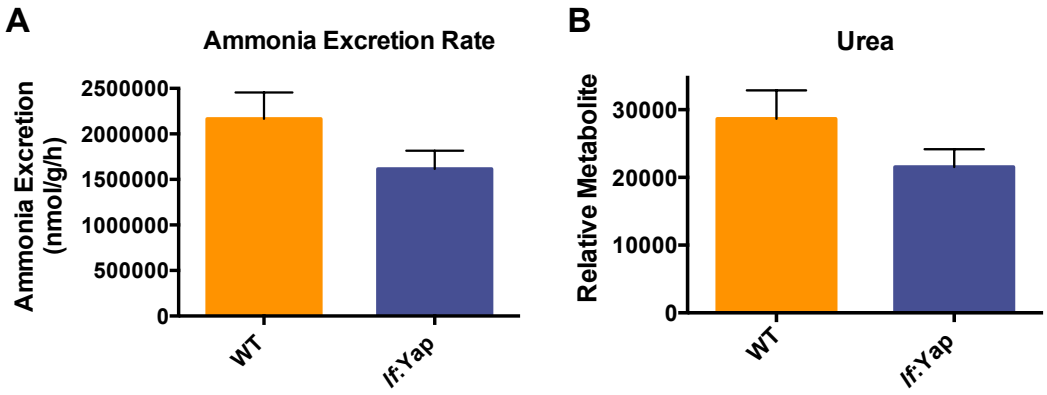

Figure 2.4.13: **Ammonia excretion rates and urea abundance in individual WT and *lf:Yap* transgenics.** (A) Ammonia excretion rates in individual WT and *lf:Yap* transgenics. (B) Steady state abundance of urea in WT and *lf:Yap* transgenic livers as determined by SRM analysis.

increased 10-fold compared to WT (Figure 2.4.11 D). Consequently, immunohistochemistry demonstrated uniform Glul overexpression in *lf:Yap* transgenic hepatocytes (Figure 2.4.12). Glul expression was also elevated, but heterogeneously expressed in Yap-driven liver tumors (Figure 2.4.12). To demonstrate changes in ammonia assimilation on the organism level, the rate of ammonia excretion in adult zebrafish was measured in an *in vivo* assay, revealing decreased ammonia excretion rates in *lf:Yap* transgenic fish, consistent with nitrogen retention (Figure 2.4.13 A). Similarly, metabolomics analysis revealed that *lf:Yap* transgenic livers contained decreased steady-state levels of urea compared with WT (Figure 2.4.13 B). To more precisely determine the fate of ammonia in *lf:Yap* transgenics livers overexpressing

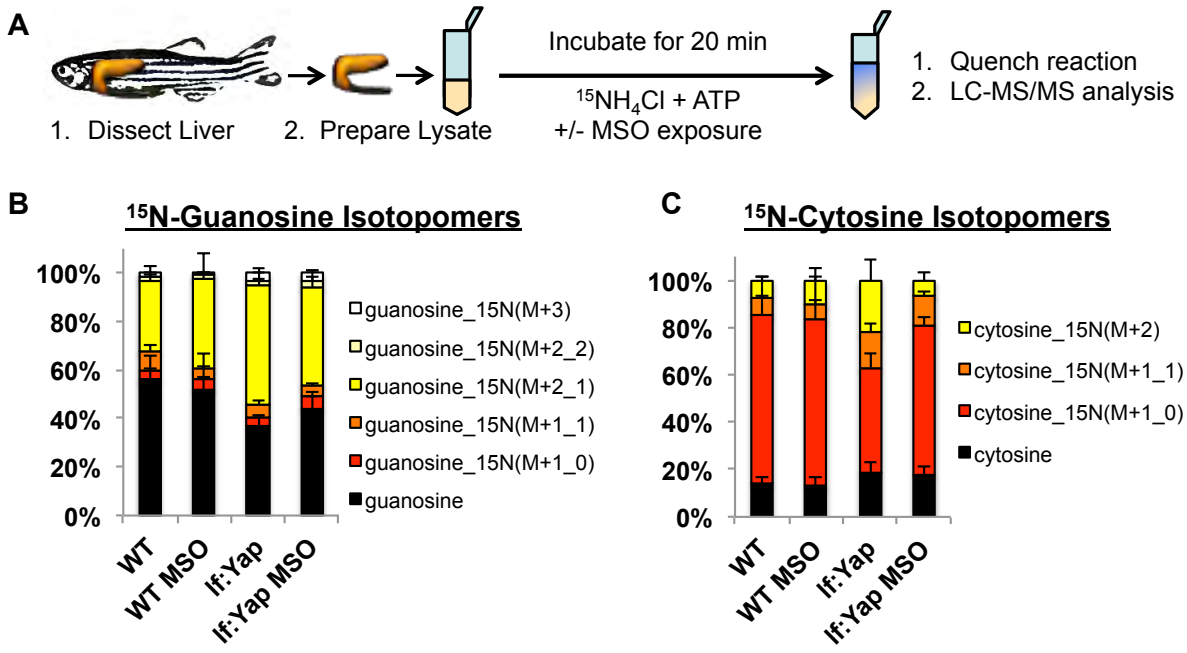

Figure 2.4.14: **Yap reprograms $^{15}NH_4Cl$ flux in liver lysates.** (A) Scheme to monitor the flux of $^{15}NH_4Cl$ in the presence or absence of MSO in liver lysates from WT and *lf:Yap* transgenics. (B) Percentage of ^{15}N-labelled Guanosine isotopomers in WT and *lf:Yap* transgenic liver lysates following ammonia assimilation in the presence or absence or MSO. (C) Percentage of ^{15}N-labelled Cytosine isotopomers in WT and *lf:Yap* transgenic liver lysates following ammonia assimilation in the presence or absence or MSO.

Glul, extracted zebrafish liver were briefly incubated with ^{15}N-labelled NH_4Cl and ATP in the presence or absence of the Glul inhibitor, methionine sulfoximine (MSO) (Figure 2.4.14 A). Glutamine is required for *de novo* nucleotide biosynthesis as it provides the nitrogen atoms present on both purines and pyrimidines. Incorporation of ^{15}N into nucleotide precursors was monitored by LC-MS, revealing that ^{15}N-labelled isotopomers of Guanosine and Cytosine, derived from ^{15}N-labelled glutamine, were increased in the *lf:Yap* liver lysates and this was inhibited in the presence of MSO (Figure 2.4.14 B,C). Altogether, these results demonstrate that Yap reprograms nitrogen metabolism by activating Glul and promoting the assimilation of ammonia via glutamine into precursors for nucleotide biosynthesis.

Elevated Glul activity contributes to Yap-induced hepatomegaly

Given the dramatic impact of Yap on Glul expression and activity and the subsequent metabolic changes, the requirement of Glul for mediating Yap-induced rapid liver growth was examined utilizing genetic knockdown of Glula and Glulb (Figure 2.4.15 A,B). Yap-induced increase in liver size at 120 hpf was partially mitigated in combined Glula/Glulb morphants (Figure 2.4.16 A). Quantification of liver size confirmed that Glula/Glulb knockdown significantly inhibited Yap-driven embryonic hepatomegaly (Figure 2.4.16 B, $n > 34$, $p = 0.0237$). To complement these studies and to demonstrate potential therapeutic implications, embryos were exposed to MSO during the outgrowth phase of liver development from 3-5 dpf. MSO effectively inhibited Glul activity in whole larvae extracts (Figure 2.4.15 C) and significantly inhibited Yap-driven hepatomegaly (Figure 2.4.16 C, $n > 88$, $p = 0.0215$). Importantly, both Glula/Glulb knockdown and MSO treatment had no effect on liver size or morphology in WT embryos (Figure 2.4.16 A,B,C). Together, these studies suggest that Glul is conditionally required for the rapid cell proliferation leading to hepatomegaly in Yap transgenics.

Yap reprograms nutritional nitrogen flux into nucleotide biosynthesis in a Glul-dependent manner to support liver growth

The steady-state metabolomics data indicated that Yap altered nitrogen metabolism, but it did not define how nitrogen is being utilized to contribute to accelerated cell growth. To examine the fate of the increased glutamine present in the *lf:Yap* transgenics we developed a novel feeding methodology to enable metabolic flux analysis. ^{15}N-labelled Spirulina gel pellets were prepared to provide fish with a defined and consistent amount of ^{15}N-labelled nutrition. Individual WT and *lf:Yap* transgenic fish were fed twice a week and maintained in the presence or absence of MSO (twice a week for 48 hr) for 4 weeks (Figure 2.4.17 A). Liver DNA was extracted and hydrolyzed into nucleotides for analysis (Figure 2.4.17 B). *lf:Yap* transgenic livers contained a significantly higher amount of ^{15}N-labelled nucleotides

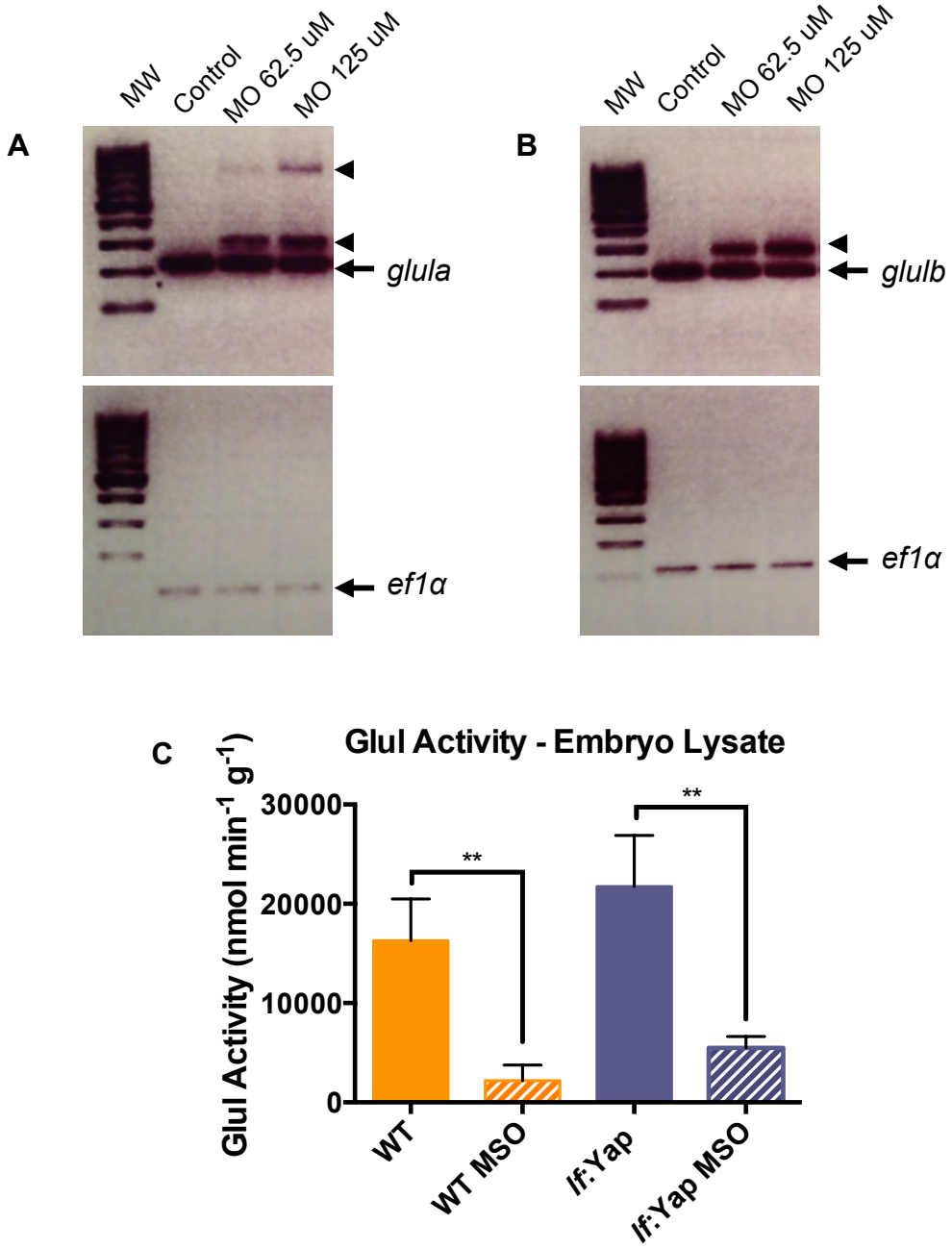

Figure 2.4.15: **Validation of morpholinos and glutamine synthetase inhibition.** Morpholinos targeting splice sites in (A) *glula* and (B) *glulb* were validated by RT-PCR with increasing amounts of morpholino. *Ef1a* was used as a control. MW = 100 bp ladder, Arrow indicates expected spliced product, Arrowheads indicate splice variants. (C) Glul activity in WT and *lf:Yap* embryonic extracts derived from embryos exposed to MSO from 3-5 dpf.

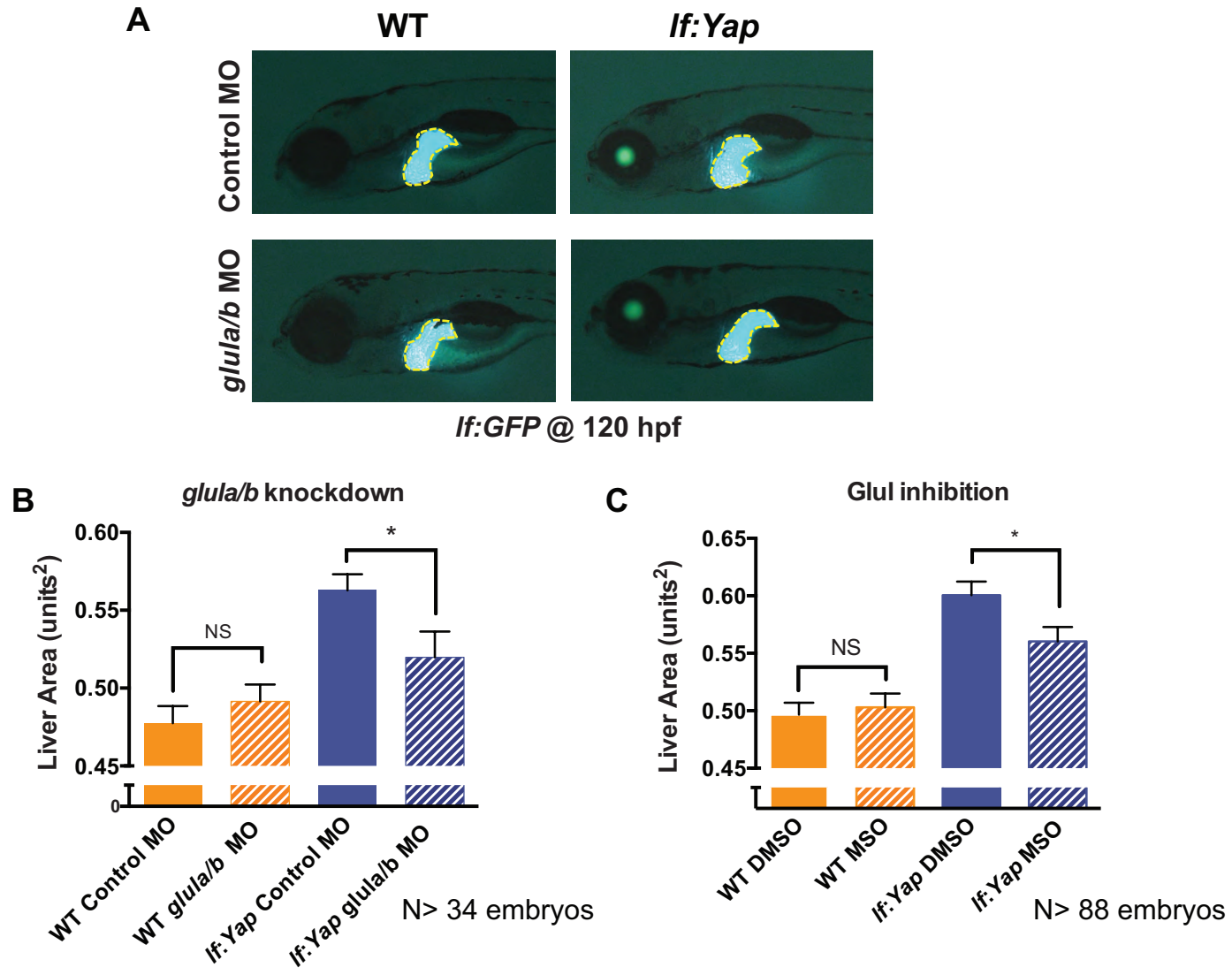

Figure 2.4.16: **Elevated Glutamine synthase activity contributes to Yap-induced hepatomegaly.** (A) Morpholino knockdown of Glula/b in WT and *lf:Yap* embryos showed a decrease in Yap-induced hepatomegaly as determined by fluorescence microscopy at 5 dpf. (B) Quantitative analysis of the effect of Glula/b morpholino knockdown on liver size. (C) Quantitative analysis of the effect of MSO treatment from 3-5 dpf on liver size as determined by fluorescence microscopy. $p < 0.05$.

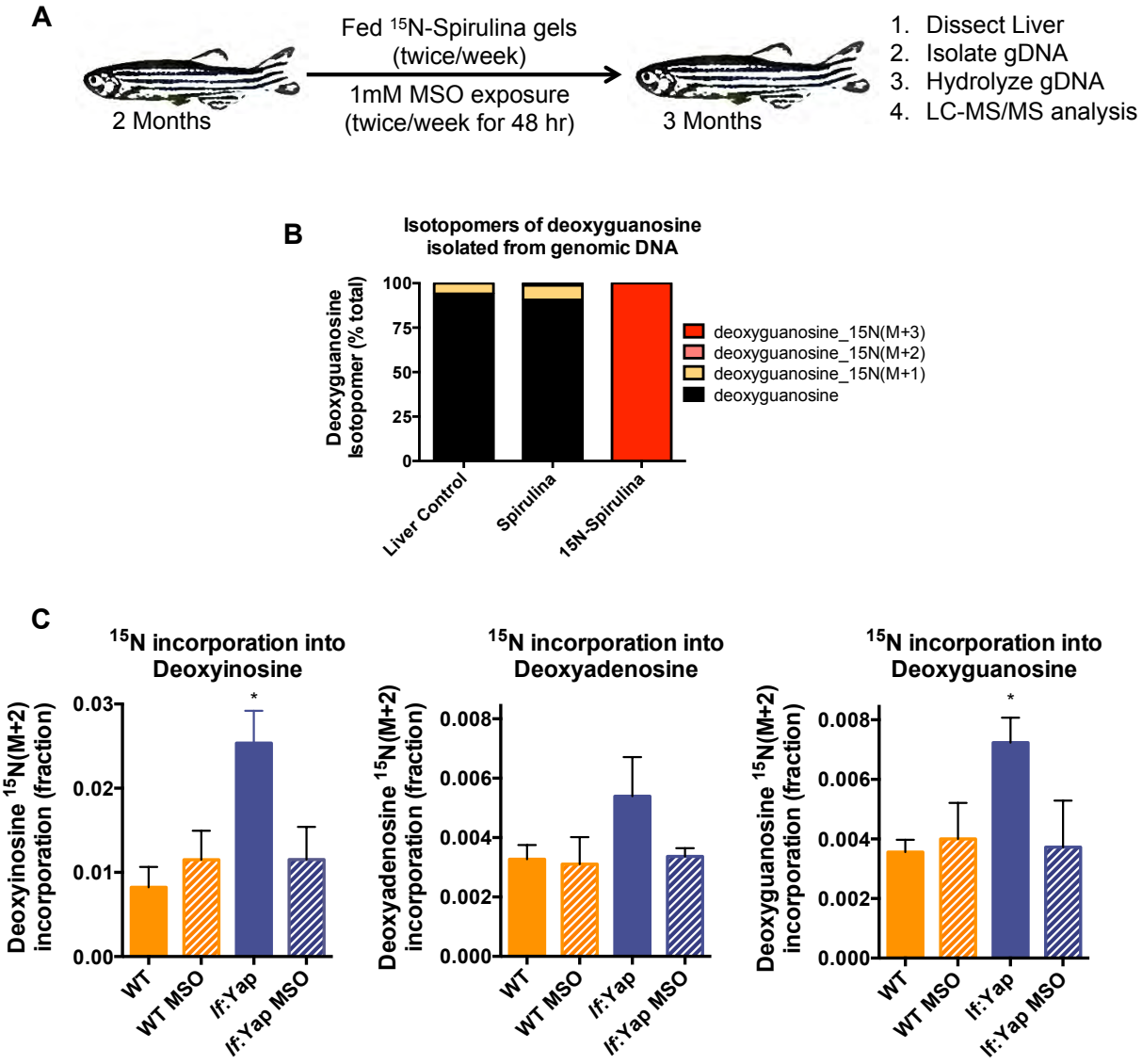

Figure 2.4.17: **Yap reprograms nutritional nitrogen flux into nucleotide biosynthesis in a Glul-dependent manner to support liver growth.** (A) Scheme describing the long-term ^{15}N-Spirulina feeding studies in adult fish. (B) ^{15}N flux analysis of deoxyguanosine isotopomers derived from hydrolyzed genomic DNA of liver and spirulina as determined by LC-MS. (C) Abundance of ^{15}N-labelled nucleotide (Deoxyinosine, Deoxyadenosine and Deoxyguanosine) isotopomers (M+2 fraction) from hydrolyzed genomic DNA of dissected livers from WT and *lf:Yap* fish as determined by LC-MS. $p < 0.05$.

incorporated into the DNA than WT controls, with 3 times more deoxyinosine, twice as much deoxyguanosine and 65% more deoxyadenosine (Figure 2.4.17 C). This Yap-dependent increase was mitigated to baseline levels by exposure to MSO. The ^{15}N flux data suggest that Yap reprograms nitrogen metabolism by stimulating anabolic incorporation of glutamine into nucleotides in a Glul-dependent manner. In order to evaluate the potential therapeutic impact of Glul inhibition on adult liver hyperplasia, fish were exposed to MSO (twice a week for 48 hr) over a 4-week period (Figure 2.4.18 A). This regimen efficiently inhibited Glul activity (Figure 2.4.18 B, $n = 3$, $p < 0.001$) and significantly reduced hepatomegaly in *lf:Yap* transgenics (Figure 2.4.18 C, $n > 9$, $p < 0.05$). MSO exposure had no effect on liver size in WT fish and overall fish appearance, suggesting that Glul is conditionally required for hepatic growth. MSO exposure did not cause cell death as determined by TUNEL staining (Figure2.4.18 D). Collectively, these data show that Yap elevates Glul activity and produces glutamine that is essential for the biosynthesis of nucleotides required for DNA synthesis during rapid liver growth.

2.5 Discussion

In this study, we generated transgenic zebrafish that express activated Yap in hepatocytes and demonstrate the rapid onset of embryonic hepatomegaly that persists into adulthood, with a high susceptibility to DMBA-induced hepatocarcinogenesis. Using a combination of transcriptomic and metabolomic analyses, we discover that Yap reprograms nitrogen metabolism by inducing Glul and elevating the steady-state level of glutamine available for biosynthetic growth. The transcriptional regulation of Glul by Yap is evolutionarily conserved in human cell lines and cancers. Therapeutic studies with the Glul inhibitor MSO revealed that elevated Glul activity contributes to Yap-driven hepatomegaly, making this the first example documenting suppression of an oncogene-induced adult phenotype by manipulation of a metabolic enzyme using zebrafish as a model system. Collectively, our data

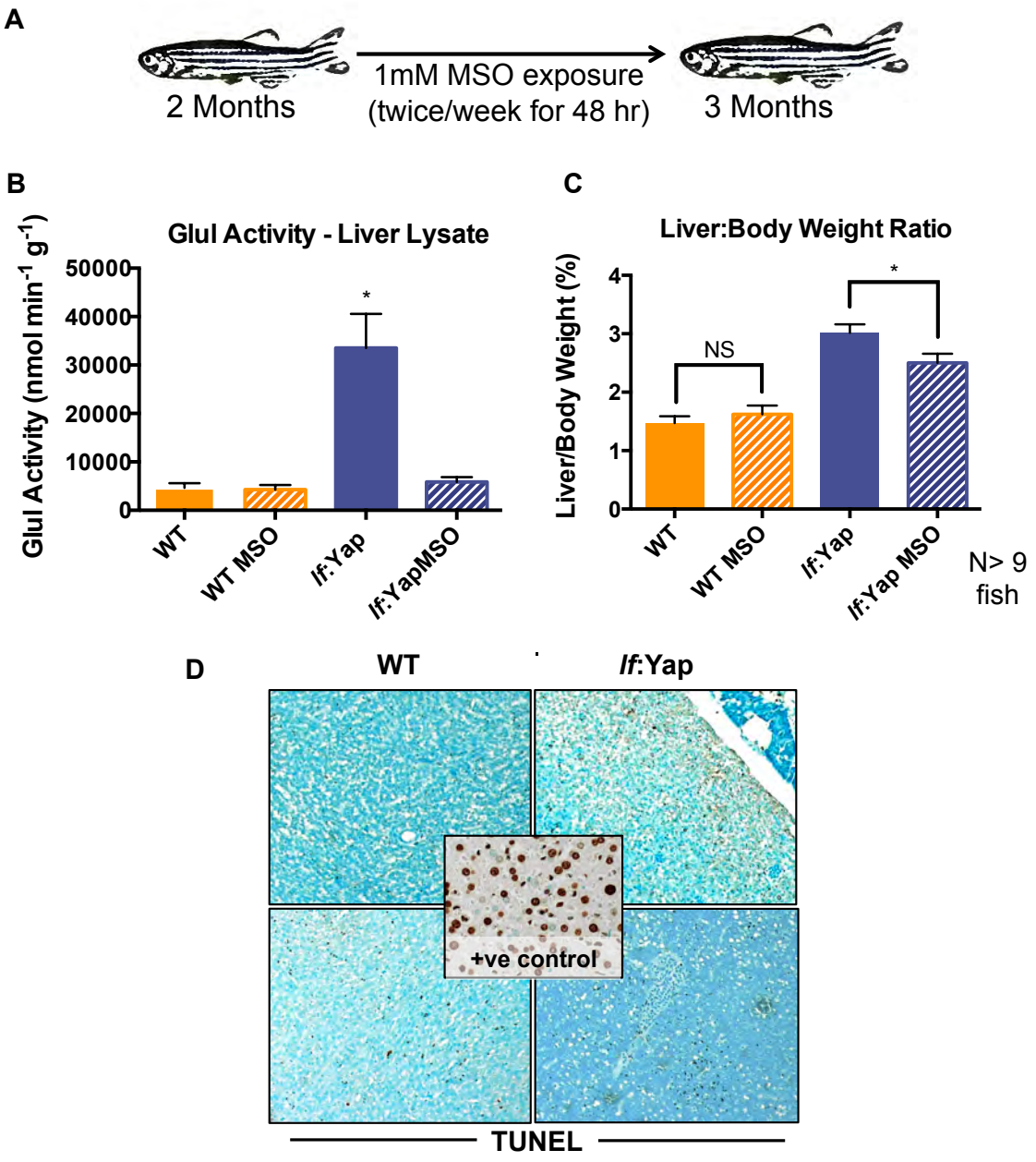

Figure 2.4.18: **Chemical Glul inhibition in adult zebrafish reduces Yap-induced hepatomegaly.** (A) Scheme describing the long-term intervention studies with MSO in adult fish. (B) Glul activity in liver lysates extracted from WT and *lf:Yap* fish in the presence or absence of MSO. (C) Effect of MSO intervention on Liver:Body weight ratios in WT and *lf:Yap* adult fish. (D) Histological analysis of cell death (TUNEL) from WT and *lf:Yap* transgenics derived from the long-term MSO intervention studies. The positive control showing DAB-stained nuclei is derived from a murine liver section. $p < 0.05$.

reveals that the Hippo pathway reprograms glutamine metabolism to provide cellular building blocks crucial for Yap-driven hepatic growth. Given that the Hippo pathway is frequently deregulated in cancer, targeting the metabolic alterations caused by Yap activation may be an attractive and rational therapeutic avenue.

Hippo pathway involvement in liver growth and tumorigenesis

Previous investigations in mice have demonstrated that Yap can alter liver cell fate, induce hepatomegaly and promote tumorigenesis (Dong et al., 2007; Camargo et al., 2007; Zhou et al., 2009; Benhamouche et al., 2010; Lee et al., 2010). Recent insights have shown that Yap can reprogram mature hepatocytes into progenitor cells by activation of the Notch pathway (Yimlamai et al., 2014). Yap promotes dedifferentiation of mature hepatocytes by influencing Hnf4a and Foxa2 binding site choice and activating the expression of embryonic target genes (Alder et al., 2014). Furthermore, Yap activation antagonizes the hepatic differentiation programs directed by HNF4a and β-catenin, whereas loss of Yap function in murine HCC causes tumor differentiation and regression (Fitamant et al., 2015). In the current study, we expand this emerging area of research by discovering that the Hippo effector Yap reprograms glutamine metabolism through induction of Glul, resulting in enhanced de novo nucleotide biosynthesis to meet the anabolic demands of rapid cell proliferation. Interestingly, previous ChIP-seq studies examining Yap and Tead target genes in MCF7 cells and embryonic stem cells have also found that Yap was bound to the Glul promoter (Zhao et al., 2008; Lian et al., 2010). Unlike other developmental signaling cascades, the Hippo pathway is not activated by a single receptor, instead mounting evidence supports the notion that the Hippo pathway is regulated by the integration of a plethora of environmental cues including cell-cell contact (Zhao et al., 2007), cell polarity (Boggiano and Fehon, 2012), GPCR stimulation (Yu et al., 2012), mechanical forces (Dupont et al., 2011; Aragona et al., 2013) and the activation of other oncogenic pathways (Harvey et al., 2013). Consequently, it is possible

that environmental cues in the early stages of liver disease, including the development of fibrosis, activate Yap and provide a growth advantage for the initiation of cancer.

Crosstalk between the Hippo and Wnt pathways in the context of cancer

In the current study, we found that overexpression of Yap in zebrafish lead to the direct induction of Glul. Previous work in mice has characterized Glul as a bone-fide Wnt target gene (Benhamouche et al., 2006; Lachenmayer et al., 2012); however, in our study overexpression of Yap directly induced Glul expression, while it did not modulate Wnt/β-catenin target gene expression. The Hippo and Wnt pathways appear to have a very complex context-dependent relationship. Pioneering studies found that Yap and Taz inhibit the Wnt pathway by binding to Dvl or β-catenin directly (Imajo et al., 2012; Varelas et al., 2010a). Building on these studies, elegant work using transgenic mice has shown that intestinal-driven expression of Yap inhibits the Wnt pathway and causes a rapid loss of intestinal crypts, whereas Yap depletion activates Wnt and expands the stem cell niche (Barry et al., 2013). However, other studies have reported that Yap activation enhances β-catenin activity. For example, in the context of murine heart development, Yap binds β-catenin and they act in a coordinated fashion to activate target genes to induce cardiomegaly (Heallen et al., 2011; Xin et al., 2011). Studies in cultured cancer cells have found that Yap is essential for the transformation and survival of β-catenin-driven intestinal tumors (Rosenbluh et al., 2012; Konsavage Jr. et al., 2012). Recent insights from the Piccolo group have led to a model in which the authors propose that Yap and Taz are sequestered in the β-catenin destruction complex and are released to enter the nucleus upon Wnt stimulation (Aragona et al., 2013; Azzolin et al., 2012). Elegant studies by Monga and colleagues have shown that Yap binds and activates β-catenin target genes in the context of hepatoblastoma (HB), but not hepatocellular carcinoma (HCC) (Tao et al., 2014). In summary, these studies highlight that the crosstalk between the Hippo and Wnt pathways is nuanced, depending on cell type, the activation status of other signaling cascades as well as microenvironmental factors that impinge upon each pathway.

Our study provides clear evidence that the Hippo pathway can regulate Glul expression in zebrafish and human hepatocytes independently of Wnt. Interestingly, we were unable to observe a similar phenotype in mice because in our current experimental systems, Yap rapidly reprograms murine hepatocyte cell fate (data not shown) (Yimlamai et al., 2014). Previous studies have identified that Glul is overexpressed in human HB (Schmidt et al., 2011), hepatocellular adenoma56 and early stage HCC (Nault et al., 2014; Christa et al., 1994; Roskams and Kojiro, 2010). Groundbreaking studies by Colnot and colleagues used conditional mouse mutants to demonstrate that the Wnt/β-catenin pathway plays a key role in regulating Glul expression (Benhamouche et al., 2006; Lachenmayer et al., 2012; Colnot et al., 2004). Subsequent genomic studies have revealed that components of the Wnt pathway are frequently mutated in liver cancer (Guichard et al., 2012). In spite of this, there are a subset of HCCs that overexpress Glul, which do not harbor mutations in the Wnt pathway (Lachenmayer et al., 2012), suggesting that alternative pathways may converge on the regulation of Glul expression. Additional factors that have been implicated in Glul induction in other contexts include Met (Yuneva et al., 2012), Gata3 (Kung et al., 2011), the Glucocorticoid receptor (Abcouwer et al., 1995, 1996; Chandrasekhar et al., 1999; Labow et al., 2001) and Foxo van der Vos et al. (2012). Given the pivotal role that Glul plays in nitrogen metabolism, it is likely there is redundancy with alternative signaling pathways capable of regulating Glul expression. Our work together with previous studies provide support for the hypothesis that Glul overexpression in liver tumor cells may provide a competitive advantage by fulfilling the biosynthetic demands for rapid cell proliferation.

Metabolic reprogramming in cancer

One of the key features of malignancy is altered cellular metabolism. Tumor cells exploit metabolic pathways to increase nutrient uptake and bioenergetic output. Aerobic glycolysis ("Warburg effect") and glutaminolysis are among the most well described metabolic changes in cancer (Vander Heiden et al., 2009; Hensley et al., 2013). Interestingly, recent insights

have shown that stem cells exploit metabolism in a similar manner to cancer cells by elevating glycolytic flux and becoming more dependent on glutamine for lineage specification (Shyh-Chang et al., 2013a,b; Oburoglu et al., 2014). An often-overlooked aspect of cancer cell metabolism is the need to rewire carbon and nitrogen flux to generate the building blocks required to fulfill the biosynthetic (anabolic) needs of rapid cell growth (Howell et al., 2013). Recent studies examining the metabolic profiles of the NCI-60 cell line panel (Jain et al., 2012), Kras-induced pancreatic cancer (Ying et al., 2012) and Myc-driven lymphomas (Cunningham et al., 2014) have identified that a common theme in metabolic reprogramming is the production of precursors that stimulate de novo nucleotide biosynthesis. In the current study, we revealed that Yap reprograms glutamine metabolism and stimulates de novo nucleotide biosynthesis. Although we focused our attention on the fate of glutamine, we predict that Yap can alter the expression of other metabolic enzymes to remodel cellular metabolism. It will be of interest in future studies to examine whether Yap-driven metabolic reprogramming is coupled to cellular reprogramming to a progenitor-like cell fate. Together, these data provide compelling evidence illustrating how oncogenic pathways co-opt metabolism to promote tumor growth.

Parallels between how the mTOR and Hippo pathways integrate nutrient status and anabolic cell growth

It is well established that functional crosstalk exists between the mTOR and Hippo pathways during cell growth (Tumaneng et al., 2012a). The mTOR pathway plays a key role in linking nutrient status with metabolic processes underlying anabolic cell growth (Dibble and Manning, 2013). Intracellular nutrients like glucose and amino acids activate mTOR and this alters the metabolic flux to generate the lipids, protein and nucleic acids required for cell proliferation. For example, mTOR stimulates de novo lipid and protein synthesis via activation of SREBP and inhibition of 4E-BP1 respectively (Duvel et al., 2010; Li et al., 2010; Laplante and Sabatini, 2012). More recently, elegant studies have provided evidence that

the mTOR pathway phosphorylates and thereby activates CAD, the rate-limiting enzyme in de novo pyrimidine biosynthesis (Ben-Sahra et al., 2013; Robitaille et al., 2013). Similarly, emerging work supports the notion that the Hippo pathway effector Yap is regulated by nutrient cues in the cellular environment. The role that Yap plays in "sensing" nutrient status was first revealed in studies identifying that serum-borne lipids such as lysophosphatidic acid and sphingosine 1-phosphate regulate Yap (Yu et al., 2012; Miller et al., 2012). At the mechanistic level, serum starvation activates Amot130, which binds Yap and facilitates its degradation by recruiting the E3 ubiquitin ligase Aip4 (Miller et al., 2012; Adler et al., 2013). In addition to serum starvation, recent work has shown that glucose deprivation and bioenergetic stress inhibit Yap activation via AMPK (DeRan et al., 2014; Wang et al., 2015; Mo et al., 2015; Enzo et al., 2015). Innovative studies by Sorrentino et al. have demonstrated that the mevalonate pathway is required for Yap activation (Sorrentino et al., 2014). In the context of liver growth, recent studies have shown that bile acids activate Yap to promote carcinogenesis (Anakk et al., 2013). In light of these studies and the new insights provided by our work, we hypothesize that Yap functions to "sense" the nutrient status of the environment and initiate an appropriate growth response. Given the striking similarities between the mTOR and Hippo pathways as networks that integrate metabolite availability to anabolic cell growth, it would be interesting to further explore these links in the context of cancer.

In summary, our study provides compelling evidence that metabolic reprogramming contributes to the hyperplastic growth phenotype imbued by Yap. A greater understanding of the metabolic perturbations specific to malignant cells may provide new pharmacological approaches to combat cancer.

2.6 Acknowledgements

This work was done in equal collaboration with Andrew G. Cox. Contributors to this work were also: Kimberley Evason, Kristin K. Brown, Sebastian Beltz, Keelin O'Connor, Giorgio G. Galli, Allison Tsomides, Dean Yimlamai, Sagar Chhangawala, Min Yuan, Evan Lien, Julia Wucherpfennig, Sahar Nissim, Akihiro Minami, David E. Cohen, Fernando D. Camargo, John Asara, Yariv Houvras, Didier Y. Stainier, and Wolfram Goessling. A.G.C, K.L.H, and W.G. designed experiments, reviewed results and wrote the manuscript. A.G.C. and K.L.H. performed the majority of the experiments. K.E. generated the Yap transgenic fish and performed pathological analysis of liver tumors. K.K.B. performed cell culture experiments and immunoblotting. S.B., K.O., A.T. and S.N. assisted in zebrafish experiments. G.G.G. performed CHIP experiments. D.Y. provided murine tissue sections. S.C. and Y.H. analyzed RNA-seq datasets. E.L. analyzed metabolomics dataset. F.D.C., J.A., Y.H., and D.Y.S. provided intellectual support.

Chapter 3

The Role of Yap in Glucose Metabolism During Liver Development

3.1 Abstract

The metabolic state of stem and progenitor cells is an important regulator of self-renewal and proliferation; however, how these metabolic processes contribute to development and organ growth remains poorly understood. One particular question is how cells are able to turn on metabolic pathways as they meet the demands of rapid cellular growth and halt these processes as the organ reaches its final size. In order to understand these basic mechanisms, developmental metabolism studies are needed. This is of particular interest since tumor cells have been shown to display these same metabolic properties of rapidly proliferating cells but fail to stop growth and instead exploit these processes for their proliferative advantage.

In organ development, the Hippo signaling pathway has emerged as a central regulator of organ size by controlling cell proliferation and growth. How it is able to coordinate normal development and the metabolic demands of its proliferative capacity, though, has not been explored. Here, we utilize the zebrafish to investigate the role of Yap, the transcriptional co-activator and downstream target of the Hippo pathway, in liver organogenesis and embryonic metabolism. Using a viable *yap* knockout zebrafish model and heat shock inducible *yap* modulating transgenic fish lines, we show that Yap plays a role in hepatic progenitor cell populations that is critical for liver growth. Transcriptome analysis revealed that *glucose*

transporters 1 and *2* (*glut1/2*) expression are decreased in *yap* knockout embryos. Further metabolomic analysis revealed that Yap plays a critical role in nucleotide biosynthesis and glucose metabolism in the developing embryo, and *in vivo* flux labeling showed Yap channels glucose into purine and pyrimidine precursors. In order to determine whether glucose uptake is critical for Yap-induced proliferation, we chemically inhibited *glut1* glucose transport with WZB117, and showed that *glut1* is critical for Yap-induced hepatomegaly. We propose that Yap regulates glycolytic flux into the biosynthesis of nucleotides required for anabolic growth in the developing embryo.

3.2 Introduction

Development of a multicellular organism with specialized tissues from a single cell requires complex signals and rapid decisions of proliferation and differentiation while maintaining ample bioenergetics and macromolecular building blocks for rapid cell growth. Features of rapidly dividing cells have been elucidated through cancer studies and have shown some common metabolic features, mainly increased rates of glucose uptake, increased rates of glucose metabolism by anaerobic glycolysis even with oxygen present (aerobic glycolysis), and shunting of glycolytic intermediates into anabolic pathways for biomass production (Vander Heiden et al., 2009; Mayers and Vander Heiden, 2015). Moreover, embryonic stem cells, which proliferate rapidly, show these same characteristics (Shyh-Chang et al., 2013a). This brings about the question as to how rapidly dividing cells in the embryo coordinate their highly anabolic cellular needs with developmental pathways.

In the developing liver, many studies have examined the transcriptional and signaling pathways required for hepatogenesis; however, little is known as to how these pathways regulate cellular metabolism (North and Goessling, 2011). In the zebrafish, liver organogenesis begins with endoderm specification which is a result of multiple signaling pathways and transcription factors that are integrated. Hepatic progenitors from this multipotent precursor

population are specified and bud, eventually differentiating into hepatocytes and proliferating to form the matured organ. The zebrafish liver develops from the anterior endodermal rod by 24 hours post fertilization (hpf) identifiable by the progenitor markers *prospero-related homoebox 1* (*prox1*) and *hematopoietically expressed homeobox* (*hhex*) (Field et al., 2003; Shin et al., 2007; Chu and Sadler, 2009; North and Goessling, 2011). By 48 hpf, the liver primordium is fully distinguishable as a bud to the left of the midline and hepatocytes begin to differentiate, indicated by markers of *liver fatty acid binding protein* (*lfabp*) and *group specific component* (*gc*) (Her et al., 2003b,a; Noël et al., 2010). Hepatic outgrowth then commences between 60-72 hpf and continues until it achieves its appropriate size (Chu and Sadler, 2009).

The Hippo signaling pathway has emerged as a major regulator of post-natal liver growth and organ size determination. Yap, the downstream transcriptional co-activator of the Hippo pathway, has been shown to regulate cell proliferation, growth, and survival and has been implicated as a key regulator of stem and progenitor cells (Ramos and Camargo, 2012). Originally discovered in *Drosophila*, the Hippo pathway has been found to be widely conserved, with homologs of Yap in human, mouse, and zebrafish. The core components of the pathway in mammalian systems include the kinases MST1/2 and Lats1/2, the adaptor proteins Sav1 and Mob1, the transcriptional co-activators Yap and Taz, and the Tead family transcription factors (Harvey et al., 2003; Udan et al., 2003; Pantalacci et al., 2003; Wu et al., 2003; Tapon et al., 2002; Taguchi et al., 2010; Xu et al., 1995; Huang et al., 2005). Activation of the signaling cascade results in Lats1/2 phosphorylating Yap and rendering it to the cytoplasm, thereby inactivating its transcriptional activity (Zhao et al., 2007; Dong et al., 2007). Yap hyperactivation causes uncontrolled cellular proliferation and oncogenic transformation (Harvey et al., 2013). While many studies have elucidated functional roles of Yap and its upstream regulators, how Yap coordinates the bioenergetic demands of forming the cellular metabolic building blocks for proliferation has not been explored. Studies of the role of Yap in development have been especially challenging as Yap knockout mice

are embryonic lethal at E8.5, prior to the formation of many organs (Morin-Kensicki et al., 2006). Utilizing, $Yap^{+/-}$ heterozygous mice, Yap has been found to have a critical effect on post-natal liver proliferation and hepatic differentiation (Septer et al., 2012). Additionally, a mouse model with liver specific conditional knockout of Yap revealed Yap is important for hepatocyte survival and bile duct development (Zhang et al., 2010).

Here, to look at early liver development, we use *yap* knockout zebrafish that are able to survive through embryonic development as well as newly developed heat shock inducible transgenics to modulate Yap transcriptional activity. Utilizing these models, we probe the role of Yap in hepatogenesis and discover that Yap plays an integral role in liver development. Further studies to determine the underlying mechanisms of Yap driven proliferation and organ growth control, through transcriptional and metabolomic studies, revealed Yap regulates glucose metabolism and the *de novo* synthesis of purine and pyrimidines. We show that loss of Yap downregulates glucose transporters, *glut1* and *glut2*, and that glucose transport is critical for Yap dependent growth and cellular proliferation. Together, our data reveal that Yap is central in the modulation of glucose metabolism and glycolytic flux into the anabolic nucleotide synthesis pathways in the developing embryo, and we hypothesize this ability to direct glycolytic metabolites into DNA building blocks plays a crucial role in the proliferation of progenitor populations critical for organogenesis.

3.3 Methods

Generation of transgenic fish lines and zebrafish husbandry

Zebrafish embryos, larvae, and adult fish were maintained according to Institutional Animal Care and Use Committee (IACUC-BIDMC) protocols. Lines used in this study include wild-type (AB), *Tg(-2.8fabp10a:eGFP)*^{as3}referred to as *lf:GFP* as previously described (Her et al., 2003b,a), *Tg(l-fabp:CFP-NTR)*^{s891} referred to as *lf:CFP-NTR* as previously described (Curado et al., 2007a), and *Tg(lf:Yap)* referred to as *lf:Yap*. For this study, we gener-

ated *Tg(hsp70:mCherry-2A-Flag-Yap^{S87A})* referred to as *hs:Yap^{S87A}* and *Tg(hs:dnYap-2A-mCherry)* referred to as *hs:dnYap*. We used the plasmids pME-YapS87A and pME-NLS-YapDN generously provided by Dr. Brian Link (Medical College of Wisconsin, Milwaukee, WI) to generate the heat shock inducibile transgenics. Yap^{S87A} was amplified from pME-YapS87A using the forward (5'-AAA AGA ATT CAg act aca aag acg atg acg aca agG ATC CGA ACC AGC ACA ACC-3') and reverse (5'-AAA AAG AAT TCC TAT AGC CAG GTT AGA AAG TTC TCC-3') primers to add a Flag-tag (lower case) and EcoRI restriction digest sites (underline). The resulting product was digested with EcoRI-HF (NEB) and cloned into the Tol2 kit vector p3E-2A-pCS2MCS-pA previously digested with EcoRI-HF and calf intestine phosphatase treated (Kwan et al., 2007). The resulting plasmid was recombined by Gateway (Life Technologies) recombination with Tol2 kit plasmids pDestTol2pA, p5E-hsp70i and pME-mCherry-nostop to place the heat shock cognate promoter (*hsp70i*) upstream of the constitutively active Yap^{S87A} followed by a 2A self cleaving linker sequence and mCherry reporter gene. To create the *Tg(hs:dnYap-2A-mCherry)*, QuikChange lightning site-directed mutagenesis (Agilent Technologies) was used to delete the stop codon from the plasmid pME-NLS-YapDN with the oligos 5'-AGA AGG AGA GAC TGA GGA ACC CAG CTT TCT TGT A-3' and 5'-TAC AAG AAA GCT GGG TTC CTC AGT CTC TCC TTC T-3'. The resulting plasmid pME-NLS-YapDN-nostop was recombined by Gateway cloning with Tol2 kit plasmids pDestTol2pA, p5E-hsp70i and p3E-2A-mCherry-pA. To generate stable transgenic lines, we co-injected our newly generated plasmids with Tol2 Transposase RNA into one-cell AB embryos. Adult founders (F_0) were identified by screening their progeny for heat shock inducible mCherry expression. The F1 generation's progeny were then screened for Mendelian inheritance, inducible mCherry expression and brightness, and quantification of mCherry Hippo target gene mRNA expression.

Heat shock conditions

Embryos were heat shocked by transferring them into pre-warmed 38 °C E3 (fish) water and incubating them at 38 °C for 30 min. Genotype was determined by the presence of mCherry fluorescence at 3 hours post heat-shock. Sorted non-fluorescent (wild-type) siblings were used as controls.

Fluorescence microscopy and quantification

Live fluorescence microscopy was performed on *lf:GFP* and *lf:CFP-NTR* embryos that were put under anesthesia with 0.04 mg/ml Tricaine-S. Embryos were imaged using a Zeiss Discovery V8/Axio Cam MRC with the Axiovision software suite (Carl Zeiss). Fluorescent images obtained of embryonic livers were processed and quantified using the freeware FIJI (Schindelin et al., 2012).

Histology

Paraformaldehyde-fixed embryos were paraffin-embedded, cut into serial sections and stained with Hematoxylin and Eosin (H&E) using standard techniques.

Whole mount *in situ* hybridization

Zebrafish embryos were fixed in 4% paraformaldehyde (PFA) at the specified stages, and *in situ* hybridization was performed according to established protocols (http://zfin.org/ZFIN/Methods/ThisseProtocol.html). RNA probes for *ifabp*, *trypsin*, *gc*, *lfabp*, *prox1*, *hhex*, and *foxA3* were used. Embryos were imaged in glycerol with a Zeiss Discovery V8/Axio Cam MRC with the Axiovision software suite (Carl Zeiss). *Prox1* and *lfabp* expression areas were quantified using FIJI.

RNA-seq and GSEA and GO analysis

Embryos were collected from incrossed *yap*$^{-/-}$zebrafish and sorted based on phenotype at 72 hpf. RNA was extracted with Trizol (Life Technologies) and purified using the Qiagen Rneasy kit (Qiagen) according to the manufacturers instructions. RNA quality was checked using an Agilent Bioanalyzer and sequenced using an Illumina platform. polyA sequence data was annotated on a genomic reference (ZV9) to identify differentially affected genes. Raw data files were first QC'd using FASTQC. Almost all reads from all the samples were of good quality (phred quality score > 30). The reads were then aligned with STAR in paired-end mode. After sorting and indexing, the aligned files were used with bedtools and Ensembl zebrafish transcriptome to generate read counts for genes for all samples. These read counts were used with DESeq for differential expression and orthology was determined. Read counts were also normalized with limma and orthologous human gene names were used with GSEA for gene set enrichment analysis. Gage and pathview was used for pathway analysis and GO Term enrichment on normalized reads counts.

Quantitative PCR

RNA was isolated from pooled zebrafish embryos (n = 30) using Trizol (Life Technologies) and purified with Direct-zol RNA MiniPrep (Zymo Research). Following Turbo DNAse treatment (Life Technologies), cDNA synthesis was performed using the iScript cDNA synthesis kit (BioRad). Quantitative PCR (qPCR) was performed with technical triplicates on biological triplicates using a CFX96 Touch cycler (BioRad) with iTaq SYBR green supermix (BioRad). Relative expression levels were determined using the $\Delta\Delta C_t$ method and Ef1α was used as the reference gene. Primer sets for *ef1a*, *mCherry*, *ctgf*a, *amotl2b*, *glut1* and *glut2* can be found in Table 3.3.1.

Table 3.3.1: **Sequences of qPCR primers.**

Gene	Forward Primer	Reverse Primer
ef1a	GCGTCATCAAGAGCGTTGAG	TTGGAACGGTGTGATTGAGG
mCherry	GAACGGCCACGAGTTCGAGA	CTTGGAGCCGTACATGAACTGAGG
ctgfa	CTACGGCTCCCCAAGTAACC	TCCACTGCGGTACACCATTC
amotl2b	TCCCAGCACAACAGACTTCC	CCGTTTGTCCCTCTAGCTCC
glut1	AAGCCAAGAGCGTGCTAAAG	CGGTACAGTGATGAGCGGAA
glut2	TTAACAGGCACGCTCGCTCT	TTCATGCTCTGTGCCATTTCC

Chemical exposure

Embryos were exposed to either 10 μM or 20μM WZB117, a Glut1 inhibitor (Liu et al., 2012), (Sigma-Aldrich) in DMSO as described.

Steady-state metabolomics

WT and *yap*$^{-/-}$embryos were collected at 72 hpf and a methanol extraction was performed. Polar metabolites were isolated and enriched using the methodology outlined by Yuan et al (Yuan et al., 2012). Polar metabolites were quantified using selected reaction monitoring on a 5500 QTRAP hybrid triple quadrupole mass spectrometer.

Flux analysis of ^{13}C-glucose

WT and *yap*$^{-/-}$ embryos were incubated in E3 (fish) water with 1% U-^{13}C-glucose for 24 hours and then harvested.

3.4 Results

Yap knockout zebrafish are able to survive through embryogenesis and display defects in liver development

In mice, genetic deletion of Yap is embryonic lethal, making it impossible to study the role of Yap in early liver development (Morin-Kensicki et al., 2006). In order to characterize the role of Yap in early hepatic development, we utilized Yap knockout zebrafish (*yap*$^{-/-}$) generated

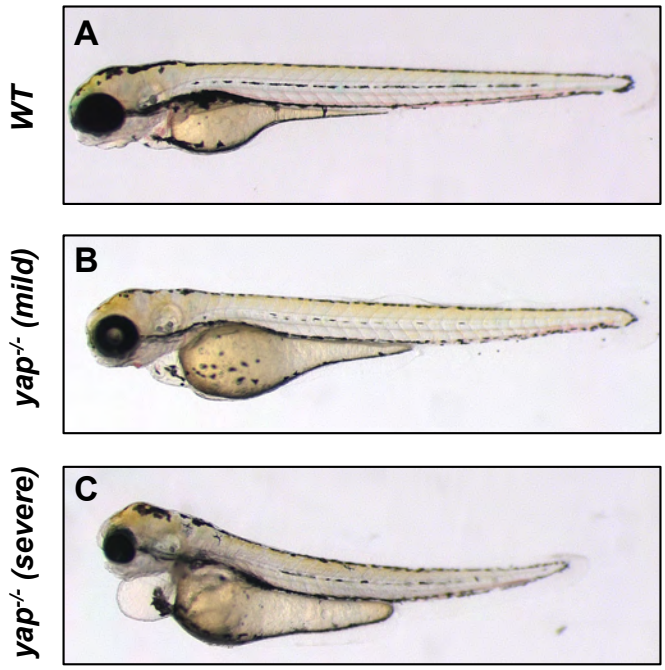

Figure 3.4.1: **Yap knockout zebrafish display developmental defects.** Lateral view of live (A) WT, (B) *yap*$^{-/-}$mutant zebrafish with the mild phenotype, and (C) *yap*$^{-/-}$mutant zebrafish with the severe phenotype at 72 hpf.

by TALENs. These *yap*$^{-/-}$ zebrafish contain a 4 bp deletion in exon 1 at amino acid 53 leading to frameshift mutations and a premature stop codon 47 amino acids downstream. We found the *yap* knockout zebrafish were able to survive gastrulation, and they displayed a distinct phenotype with a range of severity (mild and severe). Notably, knockout embryos at 72 hours post fertilization (hpf) exhibit hypopigmented eyes, cardiac edema, shortened body axis, defects in yolk resorption, and curled tails (Figure 3.4.1). When raised at lower, permissive temperatures (22 ^{o}C instead of 28.5 ^{o}C), some of the severe phenotypes were suppressed. We noted that the *yap*$^{-/-}$ embryos with the mild phenotype were able to survive past 5 dpf, and monitoring of the embryonic survival rate showed a similar survival of *yap* knockout embryos compared to their phenotypic wild type (WT) siblings (one-third *yap*$^{+/+}$

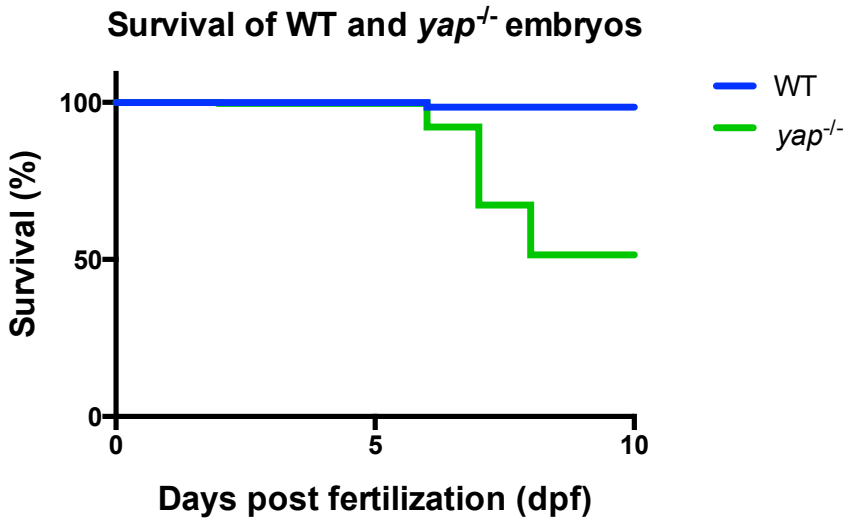

Figure 3.4.2: . **Survival rates for embryonic *yap*$^{-/-}$ zebrafish and their wild type siblings.** n > 200 embryos.

and two-third *yap*$^{+/-}$) up through 5 dpf. At 6 dpf, *yap*$^{-/-}$ survival began to decrease, reaching approximately 50% survival by 8 dpf (Figure 3.4.2).

A subset of our *yap*$^{-/-}$ zebrafish not only were able to survive through embryogenesis but they also were able to to survive to adulthood. Of adult zebrafish generated from intercrossing *yap*$^{+/-}$ heterozygotes, 12.1% were homozygous knockouts, 56.1% were heterozygous, and 31.8% were wild type (n = 264). This ability to survive through embryogenesis into adulthood provides an advantageous model for examining the mechanisms of Yap in organogenesis.

To determine whether Yap was having an effect on endoderm organ development, we performed *in situ* analysis for the hepatocyte marker *group specific component (gc),* the intestinal marker *intestinal fatty acid binding protein (ifabp),* and the pancreatic marker *trypsin* at 72 hpf. Uniformly, endoderm development was stunted and decreased liver, intestine and pancreas sizes were observed. As we have shown the liver to be greatly influenced by hepatocyte-specific Yap overexpression and transcritpional activation, we were interested in understanding the role of Yap loss in liver development. To quantify the effect of Yap loss on liver size, we crossed *yap*$^{+/-}$ heterozygotes into the reporter transgenic line *Tg(lfabp:CFP-*

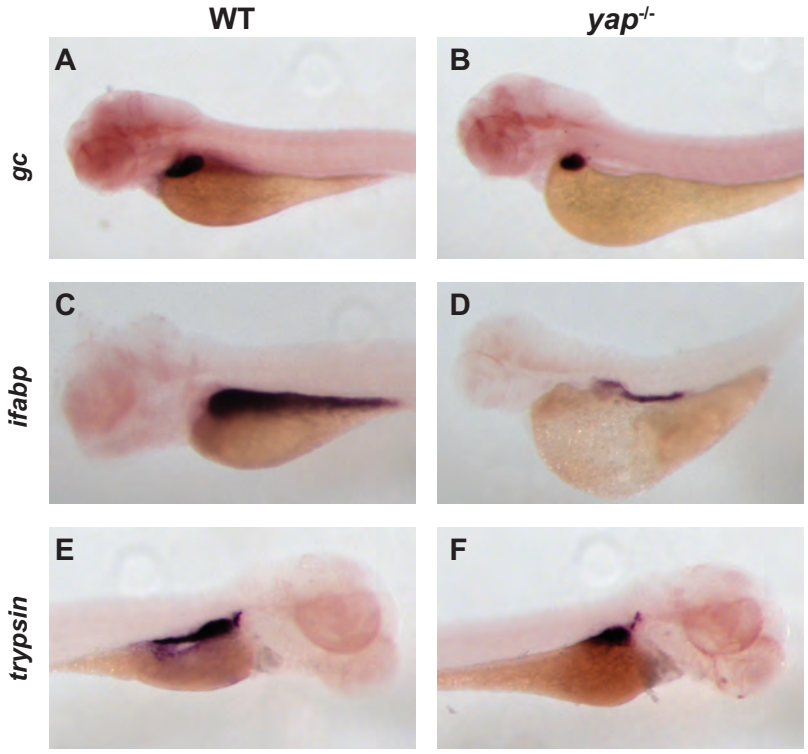

Figure 3.4.3: ***Yap* knockout embryos display stunted growth of endoderm organs.** *In situ* analysis of endoderm organ makers (A,B) *gc* (liver), (C,D) *ifabp* (intestine), and (E,F) *trypsin* (pancreas) show a marked decrease of organ size in *yap*$^{-/-}$ embryos (B,D,F) compared to their phenotypic wild type siblings (A,C,E) at 72 hpf. n $\geq$ 30.

NTR), referred to as *lf:CFP-NTR*, which specifically drives expression of cyan fluorescent protein in hepatocytes. At 72 hpf, *yap*$^{-/-}$;*lf:CFP-NTR* embryos display a 1.7-fold reduction in liver outgrowth compared to their WT siblings when measured by fluorescent microscopy (Figure 3.4.4 A,B). This decrease in liver size persists to 120 hpf with a 1.3-fold decrease (Figure 3.4.4 C,D). Histological examination revealed that *yap*$^{-/-}$livers are comprised of fewer hepatocytes with a decrease in overall cellularity (Figure 3.4.5 A-C). In addition, we observed that the liver appeared more midline at 72 hpf in *yap*$^{-/-}$ embryos, and by 5 dpf, a more midline lobe was retained. These results suggest that Yap plays a crucial role in the development of normal endoderm organ size, and this can be especially observed in liver development.

To gain further insight into whether Yap is affecting liver progenitor formation in liver development, we performed *in situ* hybridizations for endoderm, hepatoblast, and hepatocyte markers. *yap*$^{-/-}$embryos displayed decreased endoderm budding and gut looping at 48 hpf as measured by *foxA3* expression as well as decreased expression of *prox1* and *hhex* in the liver region (Figure 3.4.6). These data demonstrate that Yap plays a crucial role in endoderm and hepatoblast development.

Yap signaling during hepatoblast specification and expansion is required for liver development

In order to complement these studies and dissect the temporal role of Yap transcriptional activation on liver development, we developed heat shock inducible transgenic lines that are driven by the heat shock cognate 70-kd protein promoter, *hsp70*, and express either a Flag-tagged constitutively activated, nuclear localized form of Yap (*hsp70:mCherry-2A-Yap*^{S87A} , "*hs:Yap*^{S87A} ") or a nuclear localized, dominant negative Yap (*hs:dnYap-2A-mCherry*, "*hs:dnYap*") with the red fluorescent reporter protein mCherry separated by a self-cleavable viral 2A peptide linker sequence (Figure 3.4.7).

The dnYap was created by deleting the transcriptional transactivation domain and adding a nuclear localization signal at the N-terminus to localize dnYap to the nucleus as otherwise

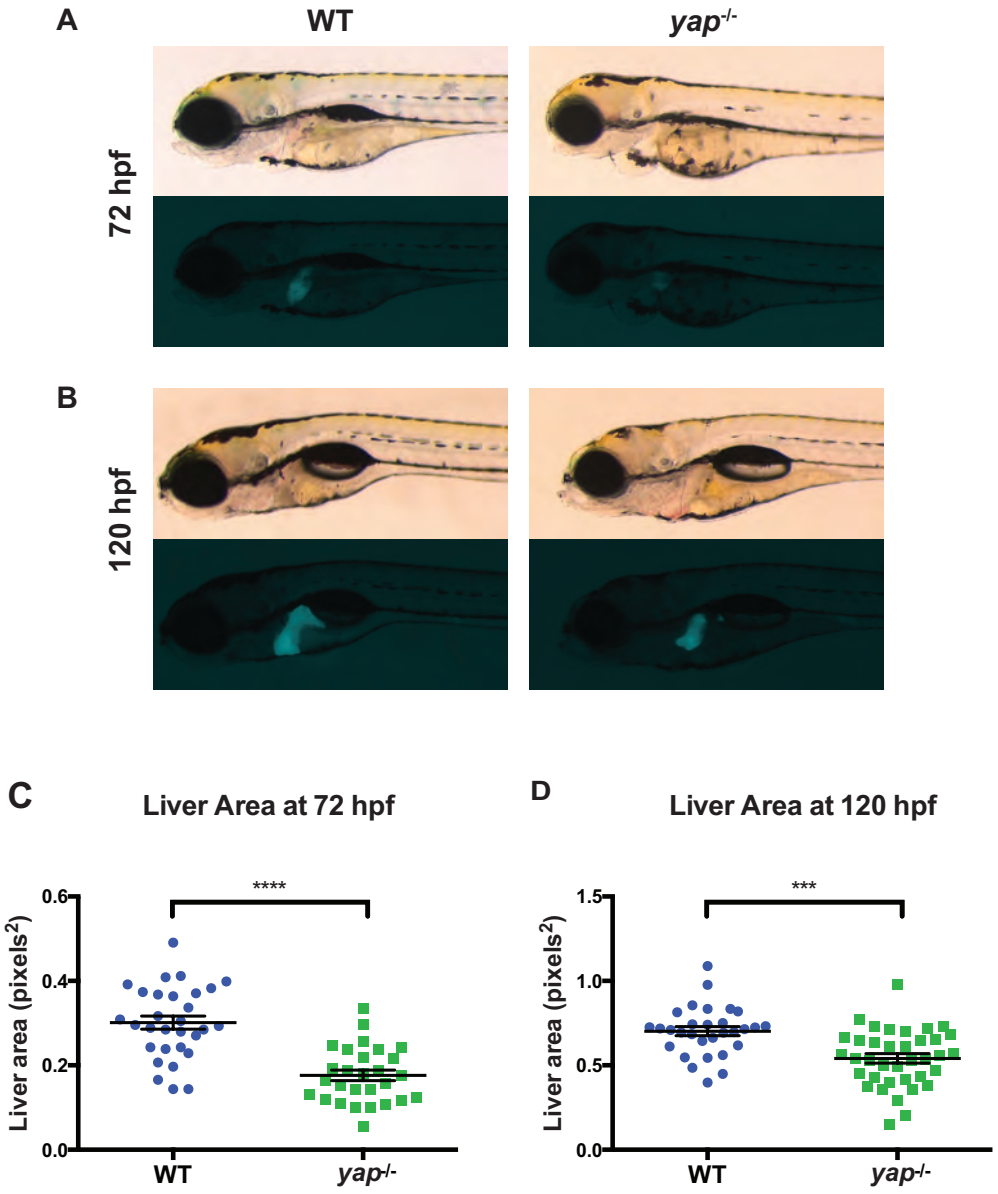

Figure 3.4.4: **Embryonic *yap*$^{-/-}$embryos display decreased liver size.** Embryos resulting from an incross of *yap*$^{+/-}$;*lf:CFP-NTR* zebrafish display reduced liver size at (A) 72 hpf and (B) 120 hpf as demonstrated by fluorescence microscopy. Quantification of liver area as measured by fluorescence at (C) 72 hpf and (D) 120 hpf. Data are represented as individual points with the horizontal line representing the mean ± S.E.M.; n ≥ 30 for each condition; significant by t test comparing *yap*$^{-/-}$ to WT siblings; $^{***}p \leq 0.001$, $^{****}p < 0.0001$.

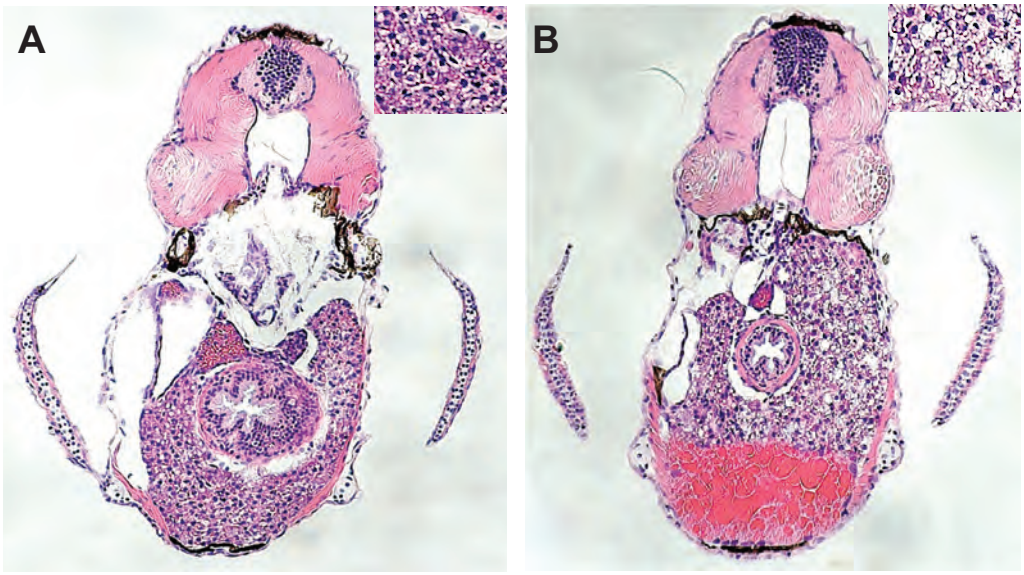

Figure 3.4.5: **Histology of embryonic livers at 120 hpf.** (A) Hematoxylin and eosin (H&E) staining in transverse sections of 120 hpf WT and (B) *yap*$^{-/-}$embryos demonstrate decreased hepatocytes in knockout embryos. Insets show magnified liver area.

deletion of the C-terminal PDZ domain results in cytoplasmic retention. A similar ortholog construct has been utilized in human cell culture which was capable of effectively suppressing TEAD activation (Cao et al., 2008; Nishioka et al., 2009). In order to determine the induction of the heat shock response, embryos were heat shocked for 30 min at 38 ^{o}C at 24 hpf. Heat shock inducible hemizygous embryos were observed to have detectable mCherry fluorescence beginning at 2 hours post heat shock and were able to be sorted from their wild type siblings. Quantification of mCherry, which is transcribed at equimolar amounts to the Yap induced transcript, by quantitative PCR (qPCR) showed effective expression of mCherry from 3 hours post heat shock to 10 hours post heat shock with mCherry expression returning to baseline at 24 hours post heat shock (Figure 3.4.8 A). In order to determine the transcriptional activation or suppression of *hs:Yap*^{S87A} or *hs:dnYap*, respectively, we quantified known Yap target genes, *ctgf* and *amotl2b* from 3 hours post heat shock to 24 hours post heat shock (Figure 3.4.8 B,C).

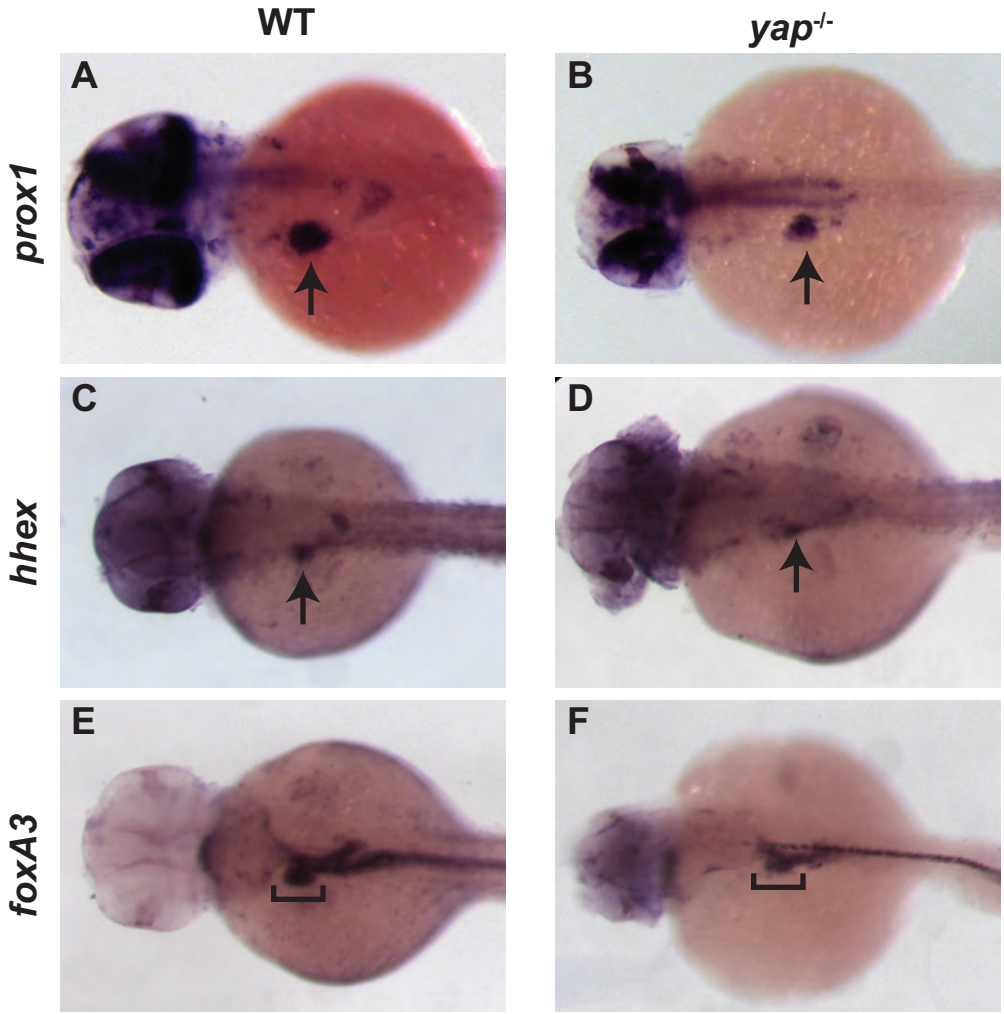

Figure 3.4.6: **Yap is required for early liver development**. WT and *yap*$^{-/-}$ embryos were analyzed for *prox1* (A,B), *hhex* (C,D) and *foxA3* (E,F) expression by *in situ* hybridization at 48 hpf. *prox1* and *hhex* expression in the liver region (arrows) was diminished in the mutant *yap*$^{-/-}$ embryos. Intestinal endoderm (brackets) marked by *foxA3* expression also showed diminished gut looping in the mutants. All images are representative dorsal views, anterior left. n $\geq$ 30.

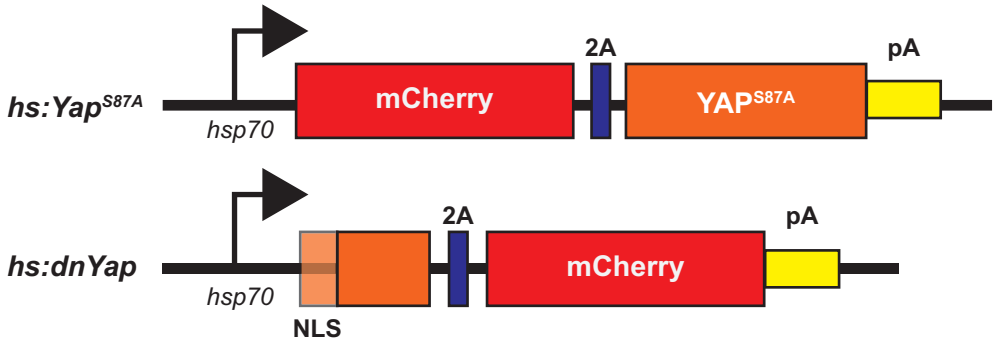

Figure 3.4.7: **Schematic of heat shock inducible transgenic constructs.** Construct *hs:Yap*^{S87A} contains the heat shock promoter, *hsp70*, that drives the red fluorescent protein, mCherry, separated by a viral 2A linker that encodes a self-cleavable peptide, and the zebrafish Yap gene with a S87A mutation that localizes it to the nucleus and remain transcriptionally active. The *hs:dnYap* construct is similarly driven by the *hsp70* promoter and an ectopic nuclear localization signal (NLS) was added to the N-terminus of the dominant negative Yap which is missing the C-terminus transactivation domain.

In the *hs:Yap*^{S87A} transgenic fish, the constitutively activated form of Yap increased expression of both *ctgf* and *amotl2b* from 6 hours post heat shock to 10 hours post heat shock. Conversely, the *hs:dnYap* transgenic zebrafish suppressed expression of *ctgf* and *amotl2b* at 6 hours post heat shock. However, this suppression was relieved and a concomitant increase in *ctgf* and *amotl2b* at 8 hours post heat shock was observed. This could be a result of other unknown mechanisms compensating for the repression of these traditional Hippo target genes in the developing embryo. These data demonstrate that we have an effective, rapid and transient system for activating and reducing Yap transcriptional signaling in the zebrafish embryo.

We next utilized our heat shock inducible transgenic zebrafish to probe whether Yap transcriptional signaling is essential for hepatoblast formation. *Prox1* and *hhex* are among the earliest markers of hepatoblast differentiation from endoderm in the zebrafish, and their expression initiates at approximately 22 hours post fertilization (Shin et al., 2007, 2011). To determine whether Yap transcriptional activation is required for hepatoblast specification, we outcrossed hemizygous *hs:Yap*^{S87A} or *hs:dnYap* zebrafish and heat shocked the resulting embryos at 18 hpf prior to expression of *hhex* or *prox1*. *In situ* analysis of these heat shocked

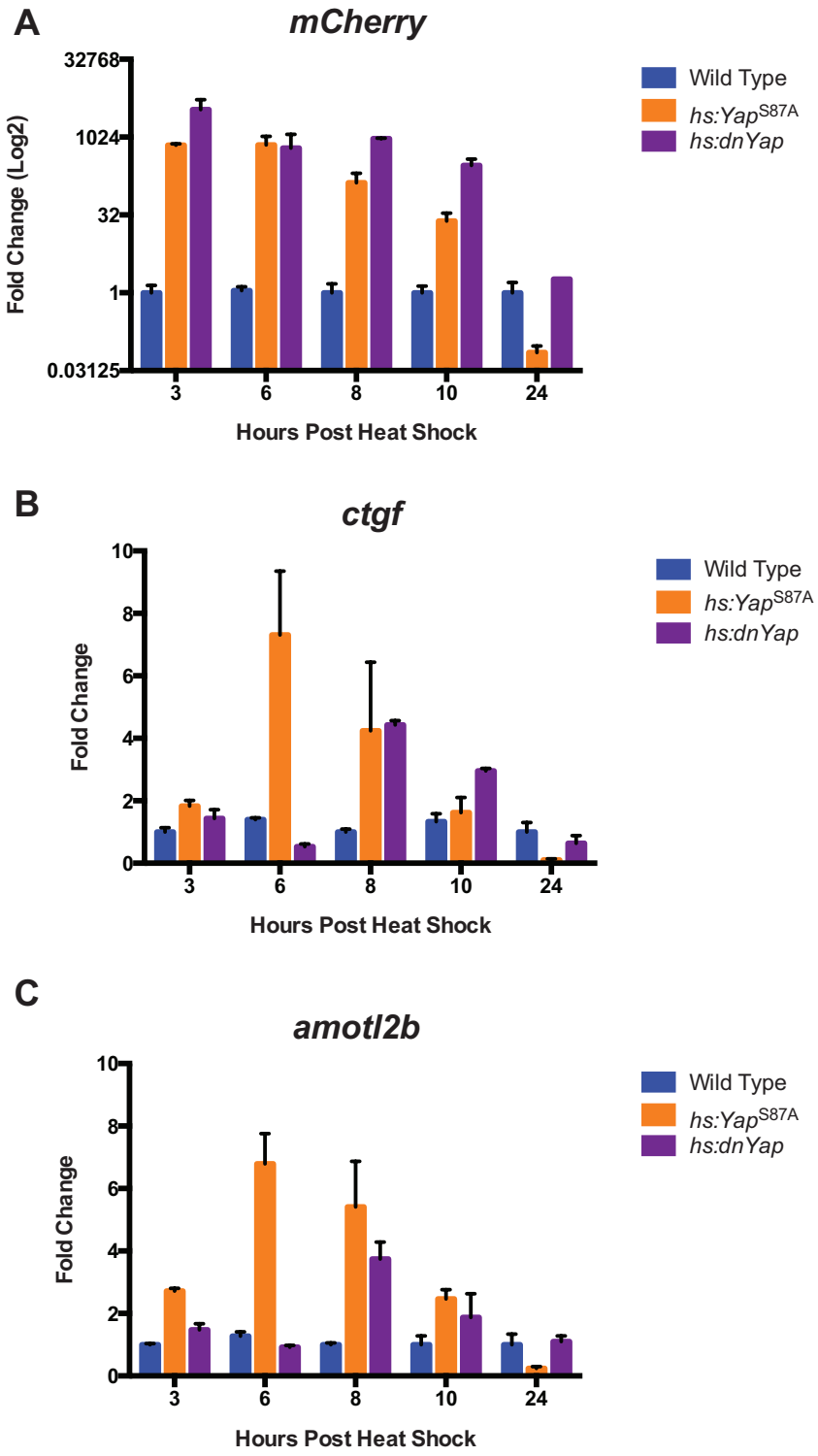

Figure 3.4.8: **Time course of the transcriptional response following heat shock induction.** (A) Relative mCherry levels to *ef1a* of *hs:Yap*^{S87A} and *hs:dnYap* from 3 hours post heat shock to 24 hours post heat shock measured by qPCR. Fold change of (B) *ctgf* or (C) *amotl2b* relative to 0 hours heat shock were measured from 3 hours post heat shock to 24 hours post heat shock by qPCR with *ef1a* as the reference gene. All experiments were done in biological triplicate. Data are represented as the mean ± S.E.M.

embryos at 36 hours post fertilization revealed a decrease in expression of *prox1* and *hhex* in *hs:dnYap* embryos whereas activation of Yap increased *prox1* and *hhex* expression (Figure 3.4.9 A-F).

Quantification of the *prox1* hepatoblast area confirmed this decrease in hepatoblast size in dominant negative Yap embryos and increased hepatoblast size in activated Yap embryos. (Figure 3.4.9 J). Gut looping visualized by *foxA3* expression also showed defective leftward bending in dominant negative embryos whereas the constitutively active form of Yap showed no change (Figure 3.4.9 G-I). These data suggest that Yap transcriptional activation is required for hepatoblast proliferation and expansion.

We next investigated whether this decrease in hepatocyte precursor cell population due to decreased Yap activity could affect liver size. To test this, we outcrossed outcrossed hemizygous heat shock liver reporter fish *hs:Yap*^{S87A}*;lf:CFP-NTR* or *hs:dnYap;lf:CFP-NTR* zebrafish and heat shocked the resulting embryos at 18 hpf. However, in the *hs:dnYap;lf:CFP-NTR* outcross, we noted that the Mendelian inheritance of the CFP reporter gene with the dominant negative Yap was less than expected (~25%), whereas the inheritance of CFP and the constitutively active Yap was as expected (~56%), making us suspect that the decreased number of hepatoblasts was resulting in decreased hepatocyte formation. To test this, we performed *in situ* analysis for expression of the hepatocyte markers *lfabp* in hemizygous *hs:Yap*^{S87A} and *hs:dnYap* embryos heat shocked at 18 hpf and measured at 72 hpf. We analyzed liver area by *lfabp* expression area, and *hs:dnYap* embryos showed a significant decrease in liver area with the majority showing no expression of *lfabp;* however, *hs:Yap*^{S87A} embryos showed no change in liver size (Figure 3.4.10 A-C). To confirm the loss of expression in *hs:dnYap* embryos was due to lack of hepatocytes and not only a result of decreased *lfabp* expression, we performed *in situ* analysis for the hepatocyte marker *gc* (Figure 3.4.10 D-F). The *hs:dnYap* embryos again showed a significant decrease in liver size and 56% of embryos had no appreciable expression of *gc*. This suggests that a reduction in hepatoblast size from decreased Yap activity in early liver development results in a decrease in liver formation and

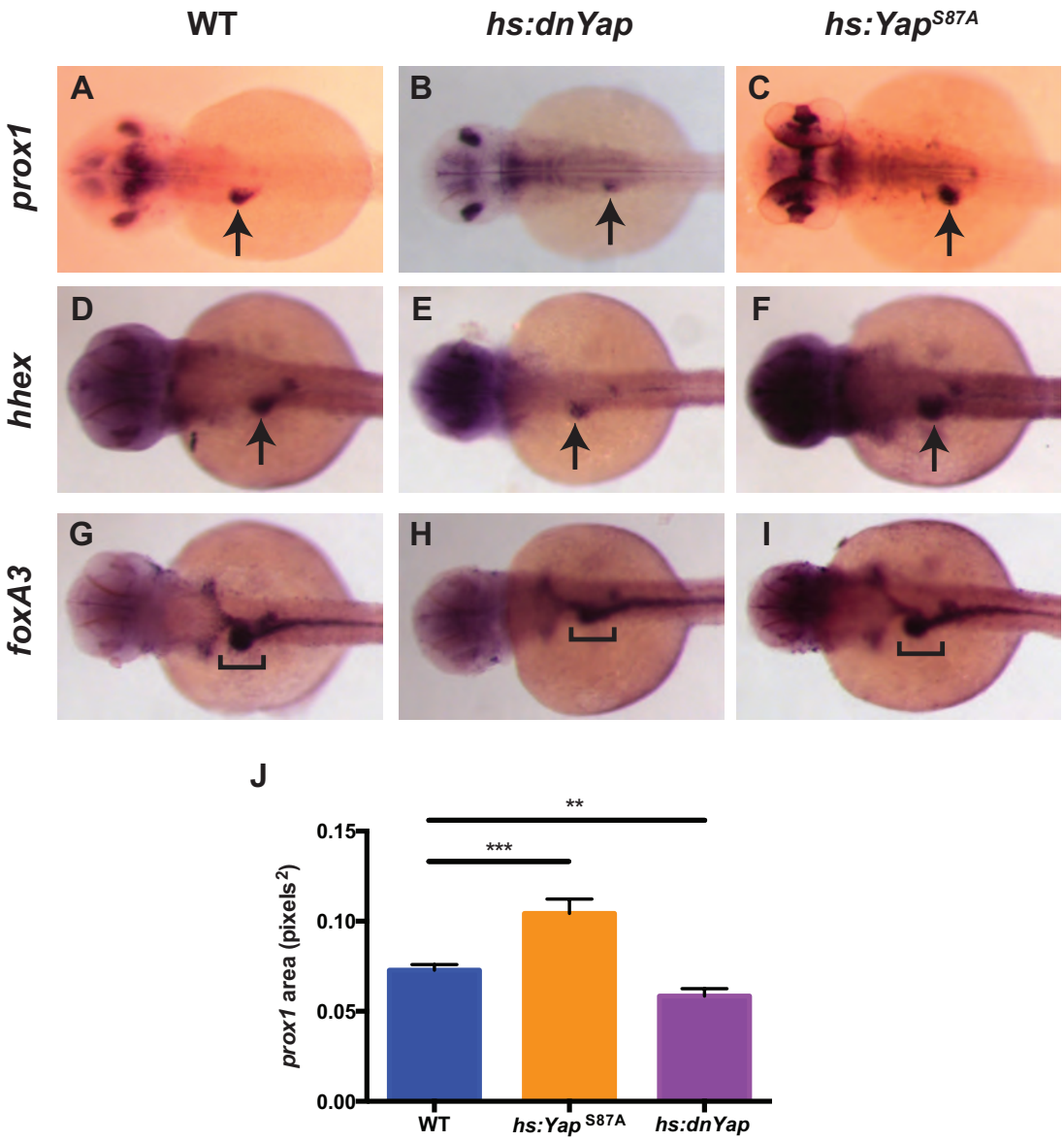

Figure 3.4.9: **Yap is essential for hepatoblast expansion.** Embryos resulting from outcrossing hemizygous *hs:Yap*^{S87A} or *hs:dnYap* were heat shocked at 18 hpf and collected at 36 hpf. *In situ* hybridization for *prox1* (A-C) and *hhex* (D-F) revealed greatly reduced expression of the hepatic progenitor markers (arrows) in *hs:dnYap* hemizygous embryos in comparison to their wild type siblings. *In situ* hybridization for the endoderm marker *foxA3* (G-I) showed frequent decreased leftward gut looping [brackets] in the *hs:dnYap* embryos whereas it appears unaffected in the *hs:Yap*^{S87A} embryos. (J) Measurement of the *prox1* expression area confirmed a significant decrease in hepatoblast expression in hs:dnYap embryos compared to wild type siblings and a increase in hepatoblast expression in *hs:Yap*^{S87A}embryos compared to wild type. Data are represented as the mean ± S.E.M. All images are representative dorsal views, anterior left. n > 30.

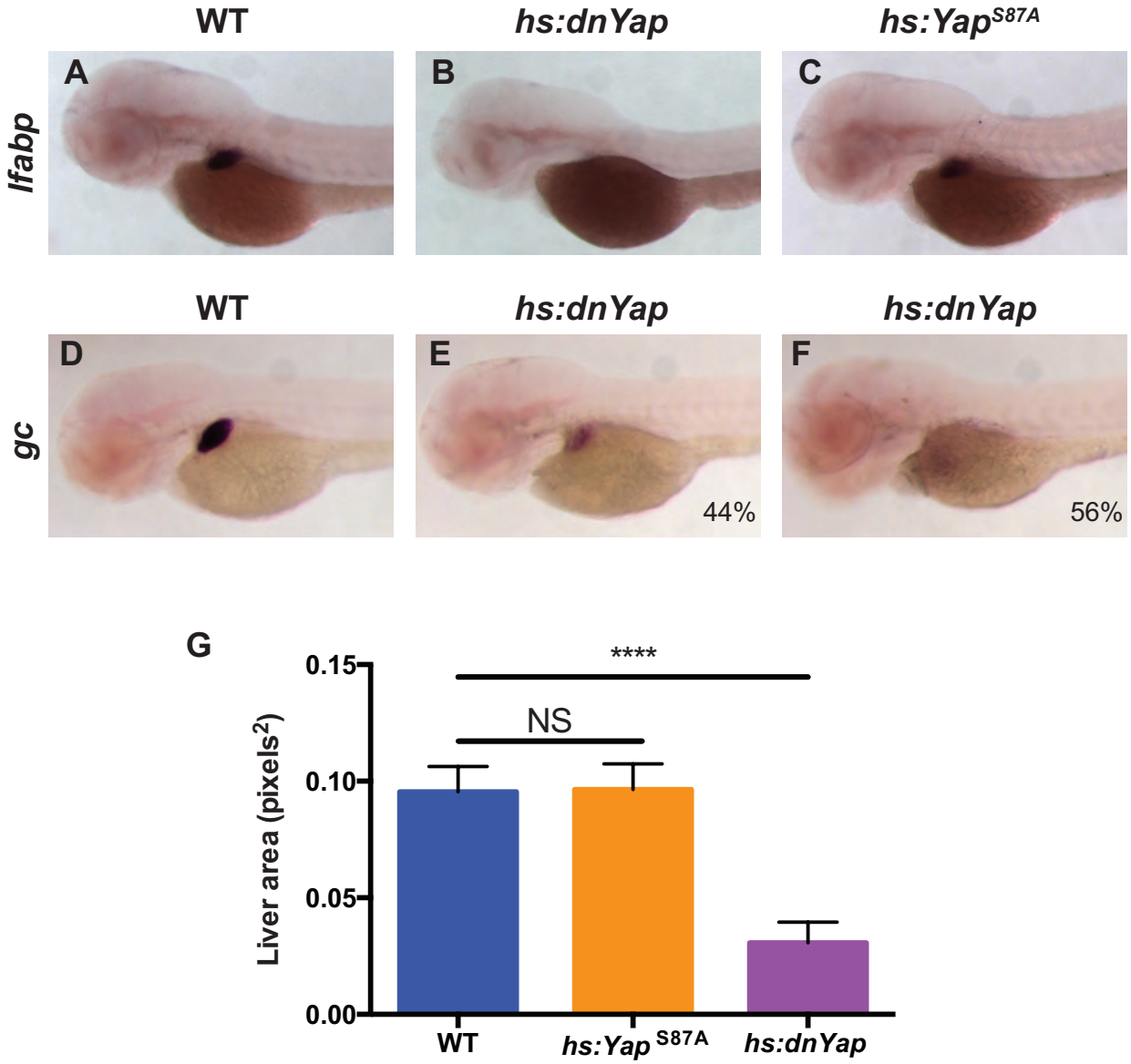

Figure 3.4.10: **Yap transcriptional activity is required for liver formation.** Hemizigous *hs:Yap*^{S87A}, *hs:dnYap*, and their wild type siblings were heat shocked at 18 hpf and harvested at 72 hpf. Expression of hepatocyte marker *lfabp* (A-C) and *gc* (D-F) was analyzed by *in situ* hybridization and demonstrated decreased expression in *hs:dnYap* embryos compared to wild type and *hs:Yap*^{S87A}. Numbers in lower left corner of (E) and (F) denote percentage of *hs:dnYap* displaying either decreased liver size or no detectable liver. (G) Liver size was measured by area of expression of *lfabp* by *in situ* analysis. All images are representative lateral views. NS = not significant; $^{****}p < 0.0001$; $n > 30$.

organ size size. In combination with our data from the Yap knockout fish, this supports a role for Yap in the proliferation and expansion of endoderm progenitor cells and that loss of progenitor proliferation causes a decrease in organ size.

Yap modulates glucose transporters in the developing embryo at the transcriptional level

To gain further insight into the downstream pathways responsible for Yap-driven organ growth, we performed transcriptomic analysis of *yap*$^{-/-}$ embryos in comparison of their phenotypic wild-type siblings at 72 hpf as the and found *yap* knockout embryos had a number of differentially regulated genes (Figure 3.4.11 A). Gene set enrichment analysis (GSEA) confirmed that the known Yap target gene signature was differentially regulated in *yap*$^{-/-}$ embryos (Figure 3.4.11 B,C). Surprisingly, some of the traditional Yap target genes, such as *ctgf* and *amotl2*, were upregulated in *yap*$^{-/-}$ embryos. This suggests that other pathways or transcriptional activators, such as the Yap paralog Taz, could be compensating for loss of Yap activity for some known target genes, which is consistent with our finding of a compensatory increase in *ctgf* and *amotl2b* that we observed following dnYap-induced suppression of these genes.

We next performed gene ontology (GO) analysis to probe which biological processes were most affected by *yap* knockout in the developing embryo. Interestingly, there was a striking representation of metabolic processes, specifically with regards to aerobic respiration (Figure 3.4.12).

Given the possibility that other compensatory mechanisms were affecting the *yap*$^{-/-}$ embryonic transcriptional profile, we decided to compare the downregulated transcripts of *yap*$^{-/-}$ embryos with the downregulated transcripts of *yap*$^{-/-}$*taz*$^{-/-}$ embryos at 72 hpf (Dr. Brian Link and Dr. Yariv Houvras, data not shown) and our previous profile of upregulated transcripts in constitutively active Yap livers. Of these gene sets, there were 191 genes that overlapped (Figure 3.4.13). Of note, the glucose transporter 1(*glut1*, *slc2a1a*), was amongst the most

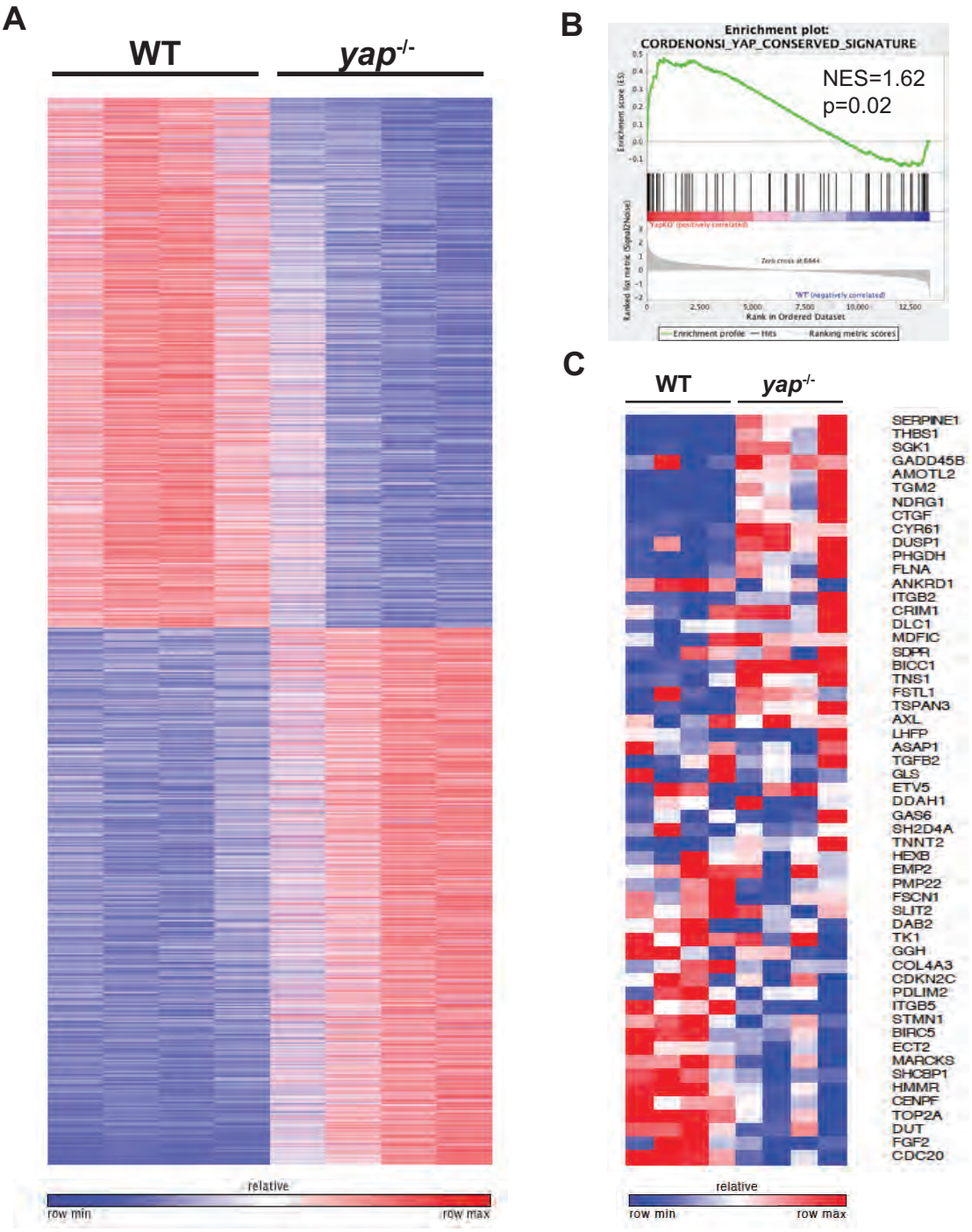

Figure 3.4.11: **Transcriptional changes in *yap*$^{-/-}$ embryos at 72 hpf.** (A) Heat map of RNA-sequencing identified differential gene expression between *yap*$^{-/-}$ embryos and their phenotypic wild type siblings that were generated from incrossing heterozygote Yap$^{+/-}$ zebrafish. There were 3050 genes with decreased expression and 3090 genes with increased expression in Yap knockout embryos ($p<0.05$). Blue signifies lower expression and red signifies higher expression. (B) GSEA graph of the known Yap conserved signature based on *yap*$^{-/-}$ expression vs wild type expression. Normalized enrichment score (NES) and p-value are displayed. (C) Heat map of Yap conserved signature genes based on GSEA plot.

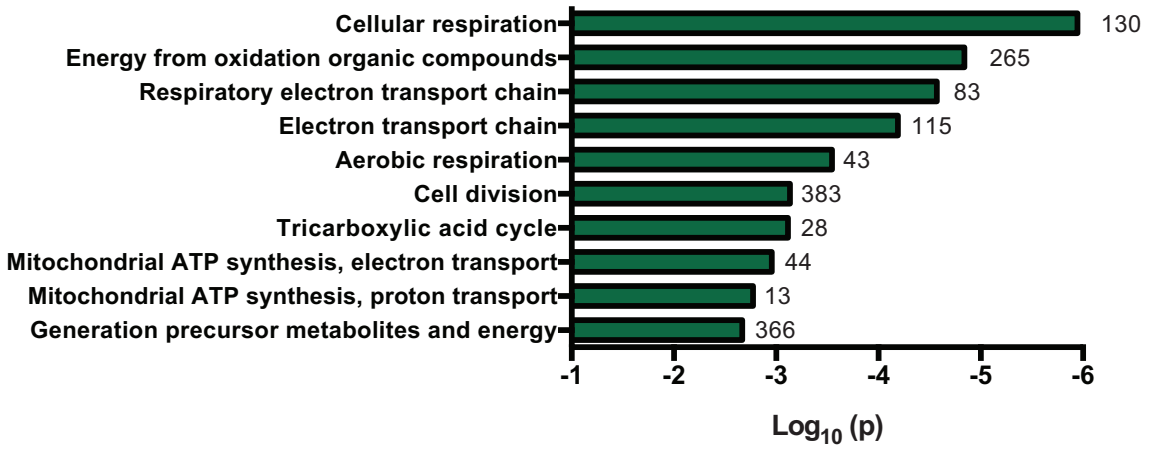

Figure 3.4.12: **Gene ontology analysis of yap knockout embryos**. Selected results of Gene Ontology biological processes downregulated in *yap*$^{-/-}$ embryos. The number of genes represented is indicated and the x-axis is the log (p-value).

differentially downregulated in *yap*$^{-/-}$ and *yap*$^{-/-}$*taz*$^{-/-}$embryos and was also upreguated as a consequence of Yap overexpression and activation in adult zebrafish liver (Figure 3.4.14 A). Further, the glucose transporter 2 (*glut2*, *slc2a2*) was significantly downregulated in both *yap*$^{-/-}$ and *yap*$^{-/-}$*taz*$^{-/-}$embryos (Figure 3.4.14 A). This was of particular interest based on the GO analysis that suggested Yap plays a transcriptional role in the regulation of metabolic processes.

We performed qPCR to validate reduced expression of *glut1* and *glut2* in *yap*$^{-/-}$ embryos at 72 hpf and found that *glut2* was significantly decreased whereas *glut1* expression showed slight decreased expression (Figure 3.4.14 B). The dependence of Yap transcriptional activity on glucose transporter expression further was confirmed by qPCR analysis of heat shocked *hs:Yap*^{S87A} and *hs:dnYap* embryos at 6 hours post heat shock. We found *glut2* expression was significantly enriched and *glut1* showed trends of increased expression with activated Yap expression. *Glut2* was conversely downregulated with expression of the dominant negative Yap (Figure 3.4.14 C).

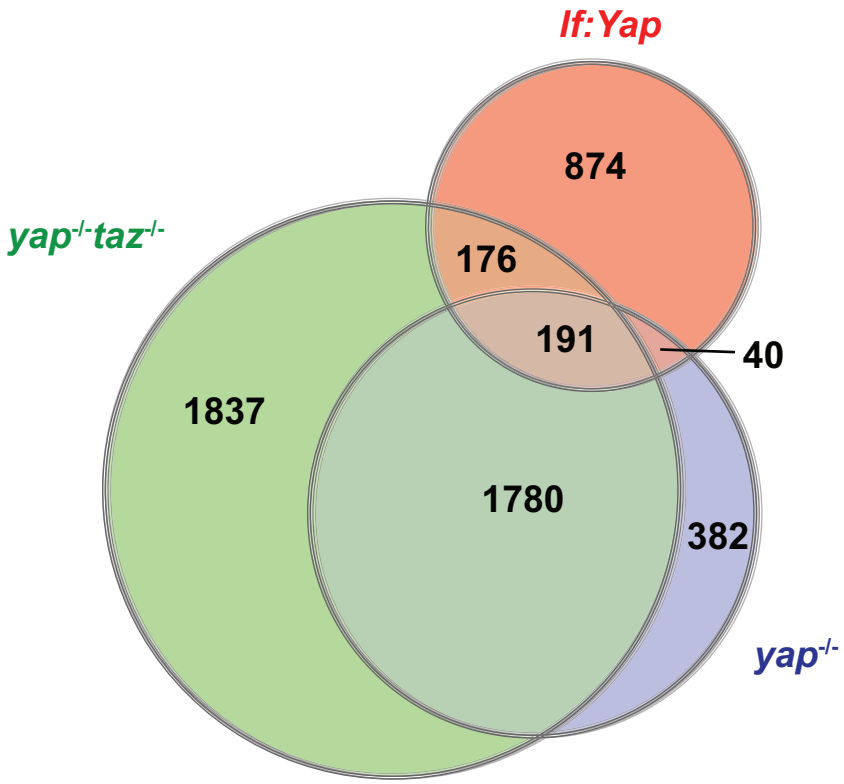

Figure 3.4.13: **Venn diagram comparing differentially regulated genes.** Genes significantly downregulated in *yap*$^{-/-}$ embryos (2393, blue) were compared to genes downregulated in *yap*$^{-/-}$*taz*$^{-/-}$ double knockout embryos (3984, green) and genes upregulated in *lf:Yap*^{S87A} livers (1281, red). The Venn diagram shows the overlap between these groups. Number of genes shared are indicated.

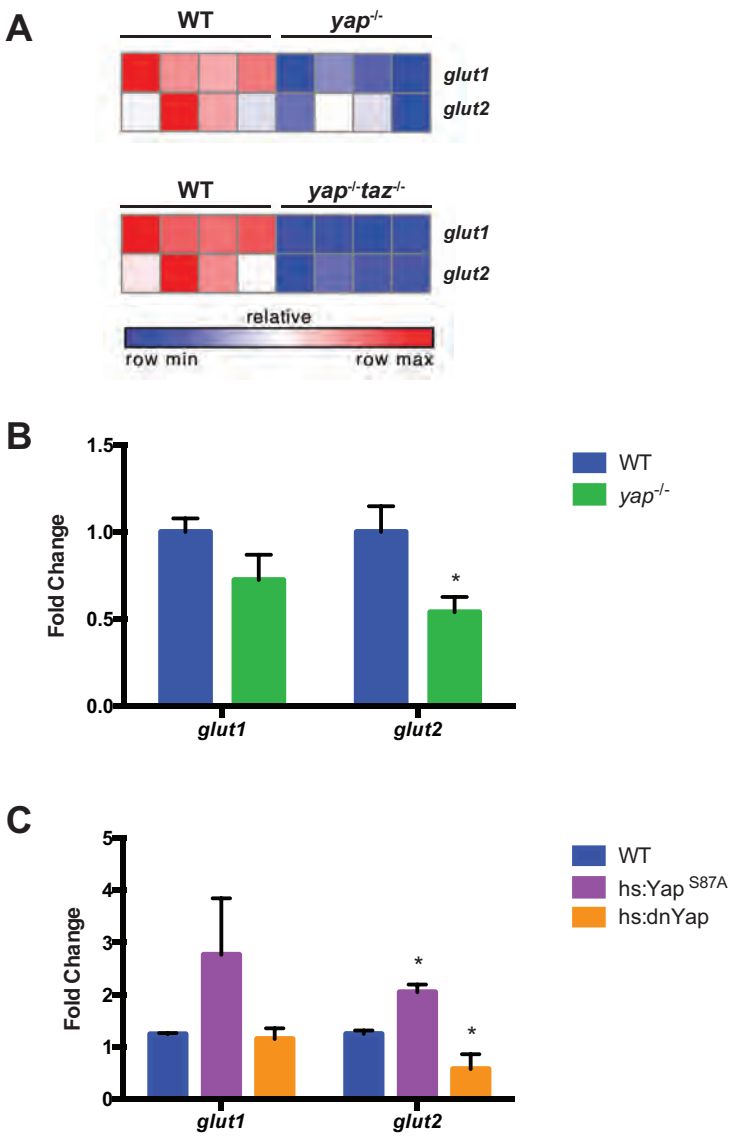

Figure 3.4.14: **Expression of *glut1* and *glut2* is decreased with loss of Yap transcriptional activity and increased with Yap activation.** (A) Heat map analysis of RNA-seq data demonstrates decreased expression of *glut1* and *glut2* in $yap^{-/-}$ embryos with an even greater decrease in $yap^{-/-}taz^{-/-}$ embryos at 72 hpf. (B) Relative fold change of *glut1* and *glut2* in $yap^{-/-}$ embryos at 72 hpf normalized to WT siblings. (B) Relative fold change of *glut1* and *glut2* in $hs{:}Yap^{S87A}$ and *hs:dnYap* embryos compared to their WT sibling controls. Embryos were heat shocked at 26 hpf and collected at 32 hpf. Data are represented as the mean ± S.E.M. All experiments were done in biological triplicate. $^{*}p < 0.05$.

Yap modulates the metabolism of glucose in embryos and nucleotide biosynthesis

Since our transcriptomic analysis identified metabolism as being the most significant cellular process being modulated by loss of Yap, we undertook unbiased polar metabolomic profiling on *yap*$^{-/-}$ embryos and their WT siblings at 72 hpf using liquid choromatography-tandem mass spectrometry (LC-MS) to identify cellular metabolic processes being modulated by loss of Yap. Metabolite clustergram analysis revealed that *yap*$^{-/-}$ embryos had significantly distinct metabolic profiles compared to WT in the steady-state (Figure 3.4.15 A). Most notably, there was a significant decrease of metabolites associated with purine metabolism in *yap*$^{-/-}$ embryos (Figure 3.4.15 B). Examination of nucleotide relative abundances in the steady state showed a dramatic reduction in purine nucleotides in the Yap deficient embryos compared to WT siblings, consistent with defects in purine metabolism (Figure 3.4.16).

Consistent with a decrease in *glut1* and *glut2* expression in *yap*$^{-/-}$ embryos, Yap deficiency also led to significantly lower levels of most glycolytic intermediates, including glucose-6-phosphate (G6P), fructose-6-phosphate (F6P), dihydroxyacetone phosphate (DHAP), and glyceraldehyde-3-phosphate (G3P) with slight decreases in the other metabolites except for fructose-1,6-bisphosphate (FBP) which showed an increase (Figure 3.4.17 A). Additionally, *yap*$^{-/-}$ embryos had decreased lactate, consistent with a decrease in *lactate dehydrogenase a* (*ldha*) expression found by transcriptome analysis (data not shown). Despite having significant changes to glycolysis, we observed that steady-state levels of TCA cycle intermediates were only slightly decreased and for the large part not significantly altered (Figure 3.4.17 B).

We therefore turned our attention to the anabolic pentose phosphate pathway (PPP) as it diverts glucose derivatives from glycolysis into building the ribose ring of nucleotides. In *yap*$^{-/-}$ embryos, we found metabolites of the nonoxidative branch of the PPP to be significantly decreased, namely sedoheptulose-7-bisphosphophosphate (S7P) and erythrose-4-phosphate (E4P), whereas the oxidative arm of the PPP did not show significant changes.

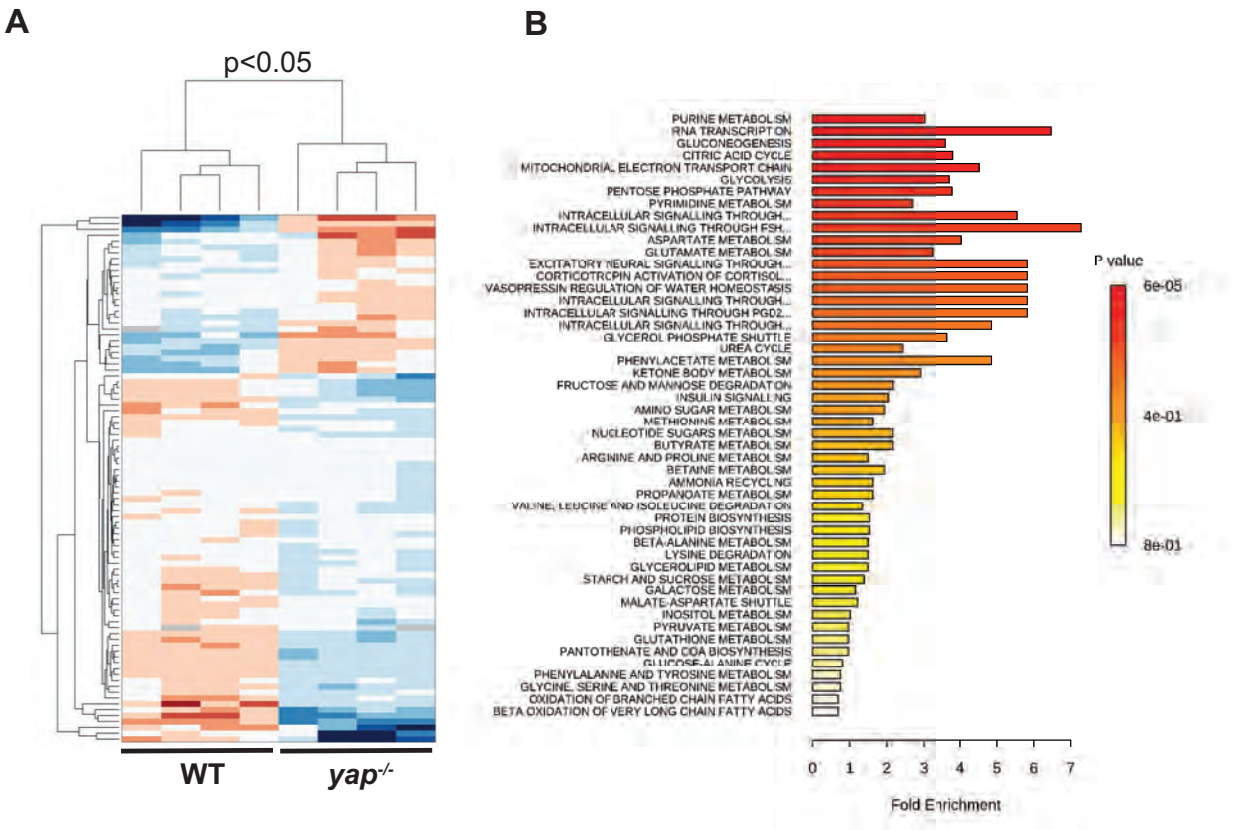

Figure 3.4.15: **Steady state metabolomics reveals Yap modulates the metabolic profile of embryos.** (A) Clustergram analysis of polar metabolites in *yap*$^{-/-}$ and WT embryos at 72 hpf as determined by LC-MS/MS selected reaction monitoring (SRM) analysis, n = 4, p < 0.05. (B) Metabolite Set Enrichment Analysis (MSEA) of overrepresented metabolites as determined by SRM analysis. The color code indicates the calculated p value.

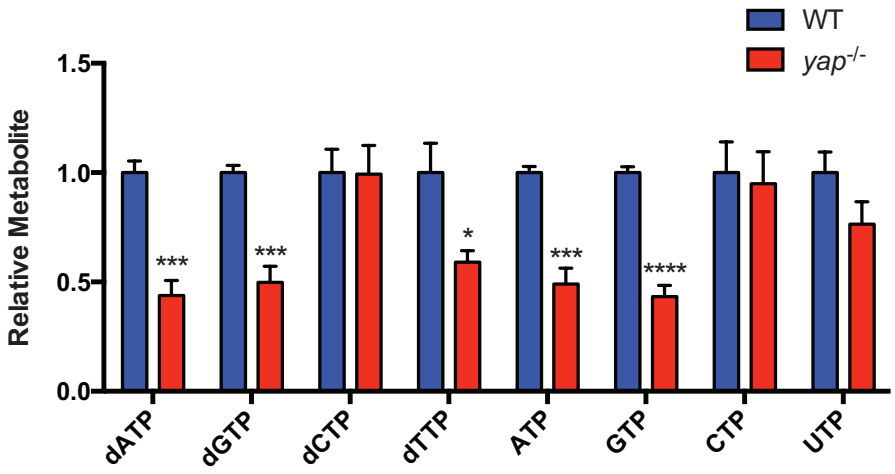

Figure 3.4.16: ***Yap*$^{-/-}$ embryos display dramatic reduction in purine nucleotides.** Relative abundances of deoxyribonucleotides and ribonucleotides as analyzed by LC/MS-selected reaction monitoring (SRM) in WT and *yap*$^{-/-}$embryos at 72 hpf. n = 4 with each sample containing 30 embryos, $^{*}p \leq 0.05$,$^{***}p \leq 0.001$, $^{****}p < 0.0001$.

(Figure 3.4.18). This is in agreement with our found decrease in purines as the PPP is responsible for generating ribose-5-phosphate for *de novo* purine nucleotide synthesis.

To elucidate the the metabolic fate of glucose and the relative pathway activities, we developed a new protocol for whole organism *in vivo* ^{13}C labeling and flux analysis in the zebrafish. We incubated embryos in a 1% solution of U-^{13}C-glucose in E3 (fish) water for 24 hours and then measured incorporation of glucose derived ^{13}C into metabolites by LC-MS. This flux analysis revealed decreased glucose incorporation into the nucleotide precursors deoxyribose-phosphate, carbamoyl-L-aspartate, guanosine, cytosine, and dTDP in the *yap*$^{-/-}$ embryos (Figure 3.4.19). This supports our steady state metabolic findings of decreased purine metabolites in *yap*$^{-/-}$ embryos and suggests decreased *de novo* purine biosynthesis as well as decreased pyrimidine biosynthesis. Further, a concomitant decrease in glycolytic flux was observed (Figure 3.4.20) whereas the TCA cycle showed little change (Figure 3.4.21), consistent with our steady state metabolomics data. Together, these data support an essential role for Yap in nucleotide biosynthesis by reprogramming glucose metabolism into directing its carbon backbone into purine and pyrimidine synthesis.

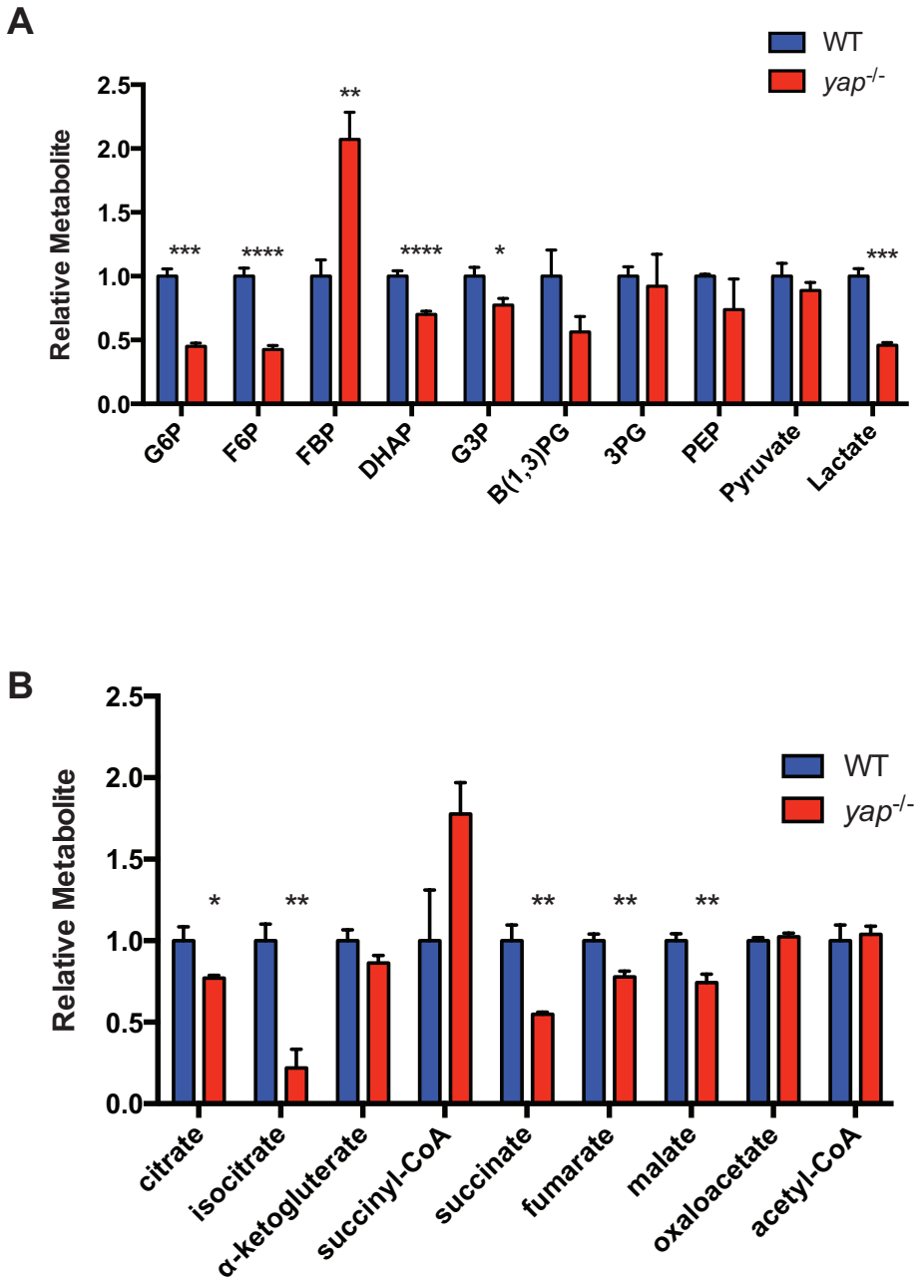

Figure 3.4.17: ***Yap* knockout leads to decreased steady state glycolytic intermediates with little change in TCA cycle intermediates in embryos.** Relative abundance of (A) glycoytic metabolites and (B) TCA cycle metabolites measured by LC-MS-selected reaction monitoring (SRM) analysis in WT and *yap*$^{-/-}$embryos at 72 hpf, relative to WT. Data represented as mean ± S.E.M., n = 4, $^{*}p < 0.05$, $^{**}p < 0.01$. G6P, gluscose-6-phosphate; F6P, fructose-6-phosphate; FBP, fructose-1,6-phosphate; DHAP, dihydroxy-acetone phosphate; G3P, glyceraldehyde-3-phosphate; B(1,3)PG, 1,3-bisphosphoglycerate; 3PG, 3-phosphoglycerate; 2PG, 2-phosphoglycerate; PEP, phopshoenolpyruvate.

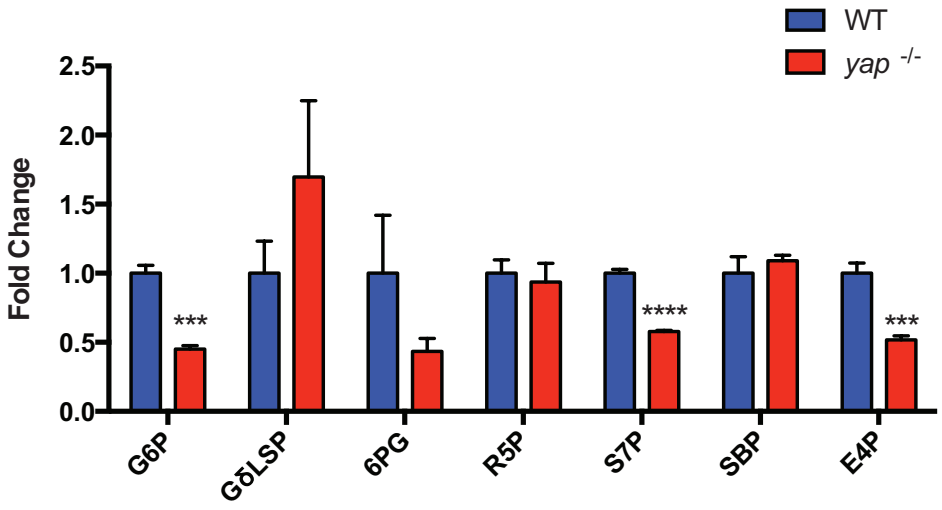

Figure 3.4.18: ***Yap*$^{-/-}$ embryos display decreased nonoxidative Pentose Phosphate Pathway metabolites.** Fold change of steady-state metabolites of the oxidative and nonoxidative branch of the Pentose Phosphate Pathway (PPP) measured by LC-MS/MS-SRM analysis in WT and *yap*$^{-/-}$ embryos at 72 hpf, relative to WT (n = 4). Data represented as mean ± S.E.M. $^{***}p \leq 0.001$, $^{****}p$, 0.0001. G6P, glucose-6-phosphate; GδLSP, 6-phosphoglucono-δ-lactone; 6PG, 6-phosphogluconate; R5P, ribose-5-phosphate; S7P, sedoheptulose-7-bisphosphosphate; E4P, erythrose-4-phosphate.

Glut1 inhibition is able to suppress Yap-induced hepatomegaly

In order to examine whether glucose uptake by Glut1 plays a role in the ability of Yap to promote proliferation and hepatomegaly, we treated our previously described *lf:Yap*^{S87A}*;lf:GFP* zebrafish embryos with the Glut1-specific inhibitor, WZB117 (Liu et al., 2012), during the liver expansion phase of development (72-120 hpf) and measured liver area by fluorescence microscopy (Figure 3.4.22). Strikingly, we found Glut1 inhibition reduced Yap-induced hepatomegaly, in a dose dependent manner, to wild type liver sizes without affecting wild type normal liver growth. These data suggest that Yap-dependent growth requires glucose uptake through Glut glucose transporters and that Yap promotes the usage of glucose into de novo nucleotide biosynthesis.

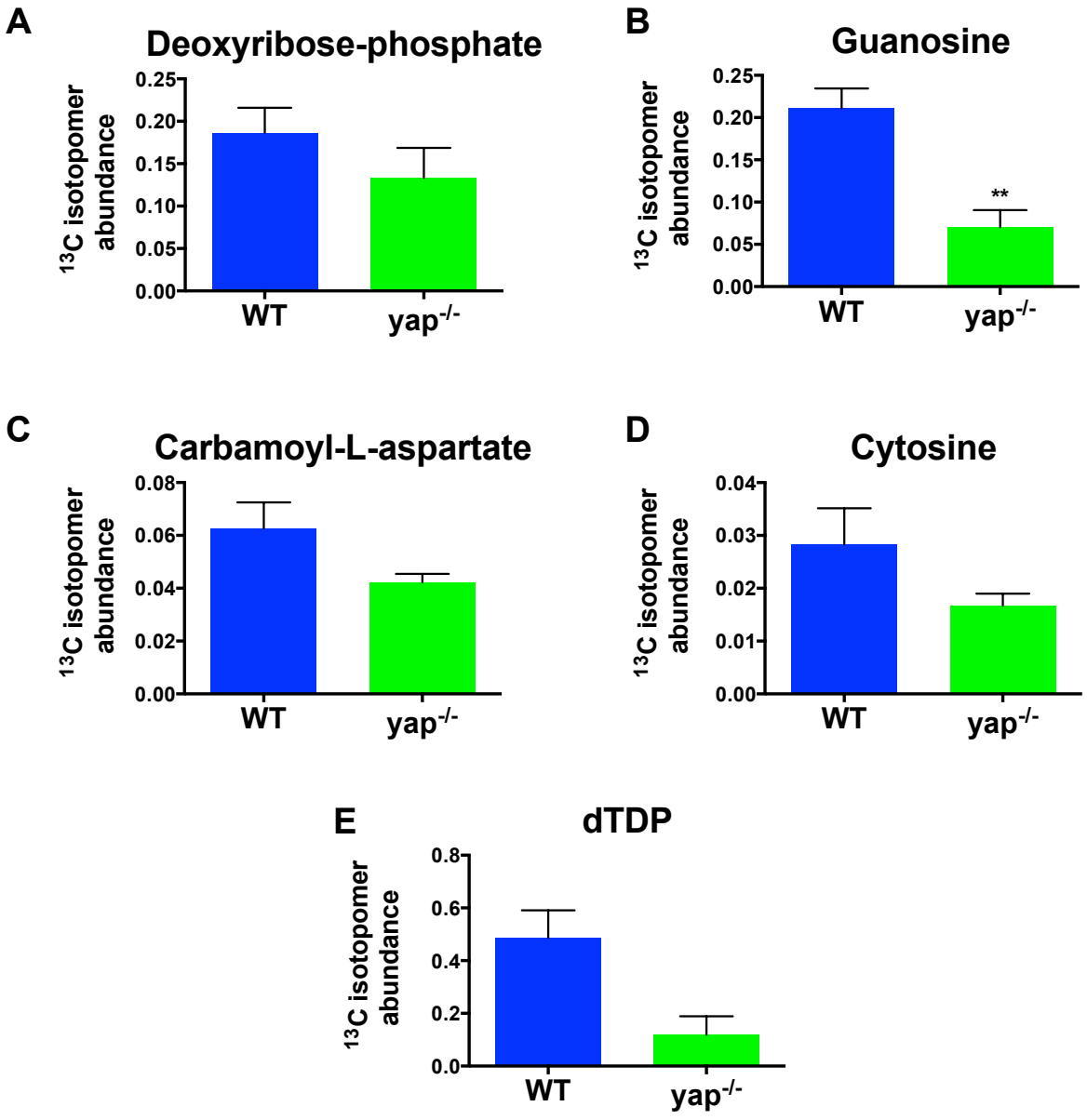

Figure 3.4.19: **Yap deficiency leads to decreased metabolic flux into purine and pyrimidine synthesis.** Metabolic flux analysis of *yap*$^{-/-}$ and WT embryos incubated in a solution of U-^{13}C-glucose showed decreased glucose conversion into (A) deoxyribose-phosphate, (B) guanosine, (C) carbamoyl-L-aspartate, (D) cytosine, and (E) dTDP. y-axis represented as a fraction of ^{13}C isotopomer fraction. n = 3. $^{**}p \leq 0.01$.

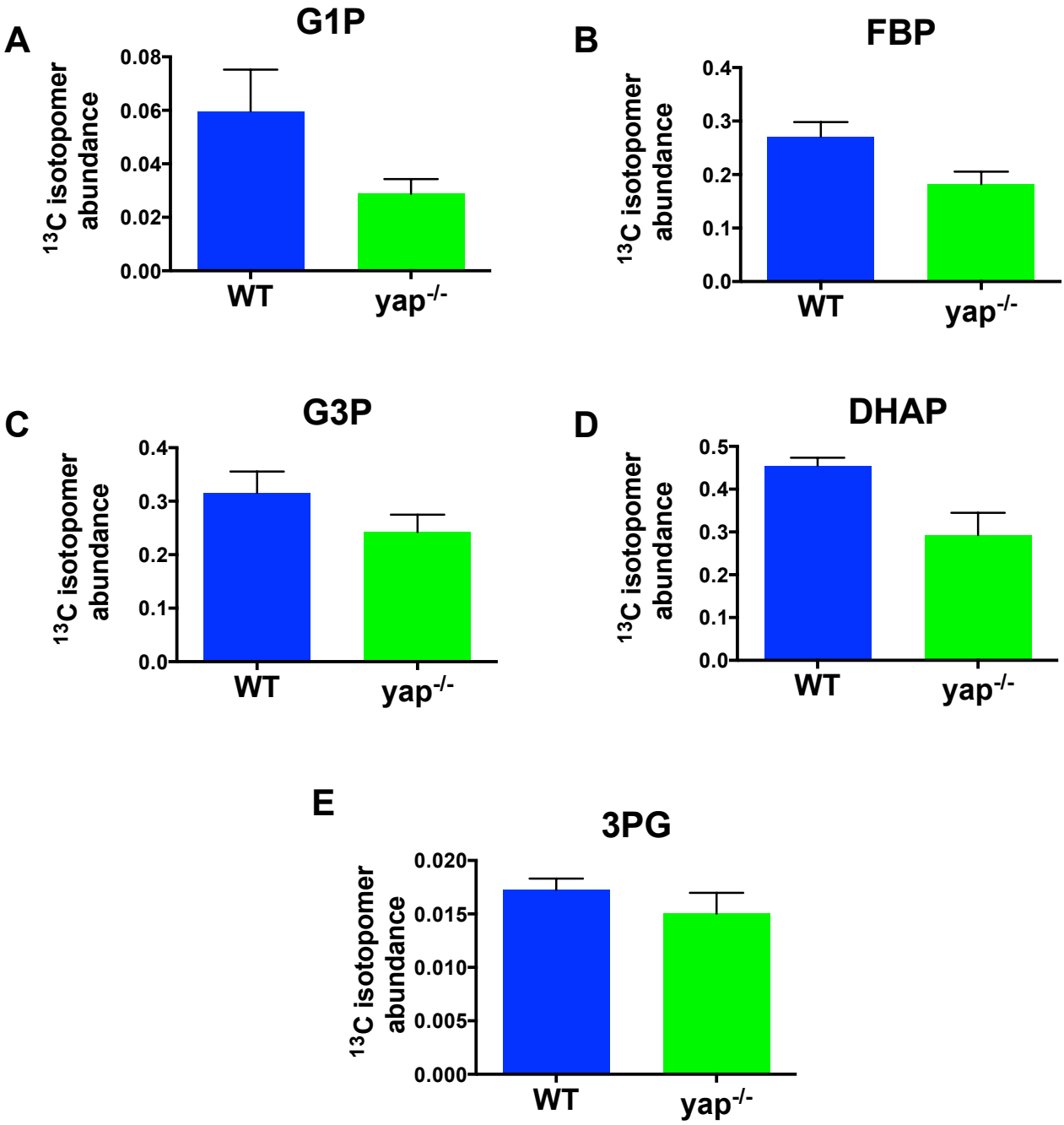

Figure 3.4.20: ***Yap*$^{-/-}$ embryos display decreased flux through glycolysis.** Metabolic flux analysis of U-^{13}C-glucose shows decreased ^{13}C isotopomer abundance in (A) glucose-1-phosphate (G1P), (B) fructose-1,6-bisphosphate (FBP), (C) glyceraldehyde-3-phosphate (G3P), (D) dihydroxyacetone phosphate (DHAP), and (E) 3-phosphoglycerate (3PG). y-axis represented as a fraction of ^{13}C isotopomer fraction. n = 3.

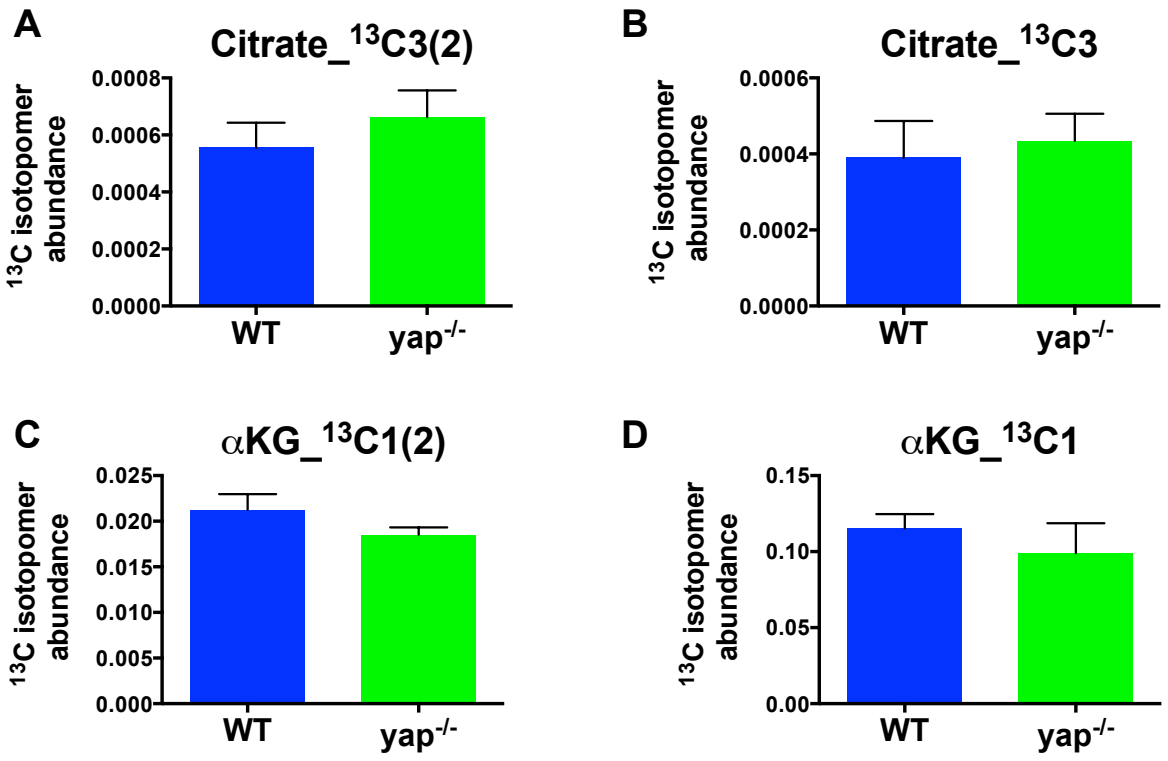

Figure 3.4.21: **TCA cycle flux is not influenced by loss of Yap.** TCA cycle ^{13}C-isotopomers (A,B) citrate and (C,D) a-ketogluterate were not changed in *yap*$^{-/-}$embryos compared to wild type. y-axis represented as a fraction of ^{13}C isotopomer fraction. n = 3.

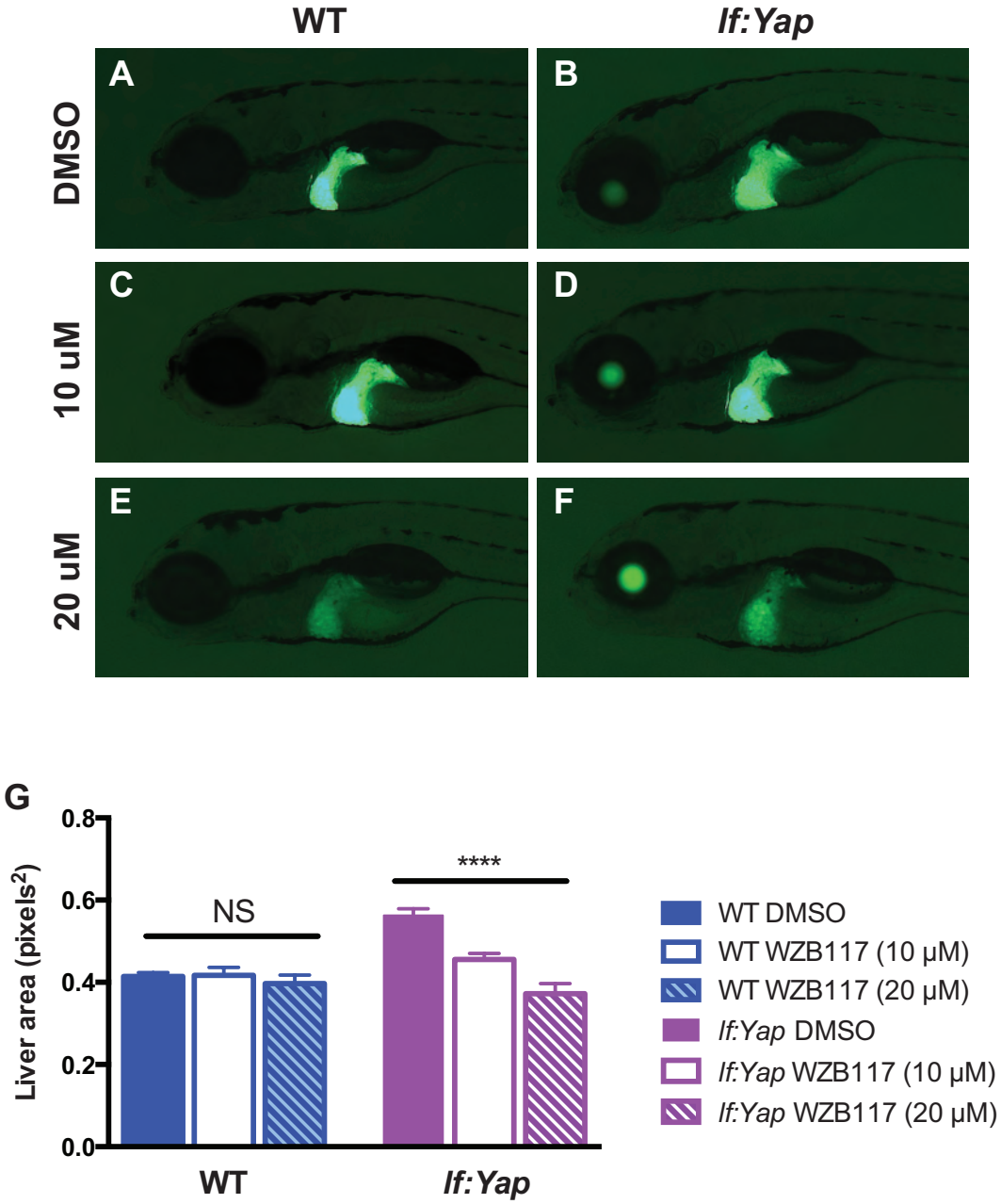

Figure 3.4.22: Inhibition of Glut1 decreases Yap-induced hepatomegaly. (A-F) Fluorescence microscopy of *lf:GFP* and *lf:Yap;lf:GFP* zebrafish embryos treated from 72-120 hpf with either (A,B) DMSO, (C,D) 10 μM of Glut1 inhibitor WZB117, or (E,F) 20 μM WZB117. (G) Quantitative analysis of the effect of WZB117 treatment on liver size as determined by fluorescence microscopy. Data are represented as the mean ± S.E.M. $^{****}p < 0.0001$. $n > 100$.

3.5 Discussion

In this study, we provide evidence that the highly conserved transcriptional co-activator Yap is required for normal growth of hepatic progenitors and liver organ size. Moreover, we find that Yap regulates glucose uptake and promotes usage of the glycolytic carbon backbone into nucleotide biosynthesis. In *yap* knockout zebrafish, which are able to survive past organogenesis and into adulthood, we find that they have reduced endoderm organ size, and specifically greatly reduced liver size as well as defects in hepatoblast growth. We modulated Yap activation during hepatoblast specification using newly developed heat shock transgenic zebrafish, and found that Yap is critical for hepatoblast progenitor bud growth and development into the mature embryonic liver. Deeper investigation into the mechanisms behind the ability of Yap to promote proliferation and growth by transcriptomic and metabolomic analyses revealed glucose transport, by control of expression of *glut1/2,* and glucose utilization to synthesize nucleotides to be greatly decreased in the absence of Yap. Tracer label studies confirmed that Yap plays a role in glucose metabolism and is required for the anabolic usage of glucose into purine and pyrimidine precursors. Targeted chemical inhibition of *glut1* reduced Yap-induced hepatomegaly in embryos to wild type liver sizes. Together, our data identifies a novel role of Yap in glucose uptake and nucleotide biosynthesis in the developing embryo. As glucose transport and its metabolism are frequently deregulated in cancer, this provides new mechanistic insight into potential contributors of this cancerous metabolic phenotype, and as such, reveals additional therapeutic targets.

The Zebrafish as a Model of the Hippo Pathway in Early Development and Liver Development

The Hippo pathway and specifically Yap, the transcriptional co-activator and effector of the pathway, are tremendously conserved throughout the animal kingdom (Hilman and Gat, 2011). Previous investigations in mice have found deletion of Yap to be embryonic lethal in the first half of gestation, resulting from defects in early yolk sac vascular development and

failure of chorioallantoic fusion (Morin-Kensicki et al., 2006). Whereas the Yap$^{-/-}$ mouse is lethal, likely from its defect in the placental system, the *yap*$^{-/-}$ zebrafish is able to survive through embryogenesis and into adulthood. This is likely a result of the zebrafish lacking both yolk sac blood islands and the allantois (Zon and Bahary, 1998), giving it a distinct advantage of survival as it does not require these processes in development and instead develops *ex vivo*. Mice with placental defects, in contrast, tend to always be early embryonic lethal (Drake, 2003). Despite this early embryonic lethality in mice, some similar observations can be made between the *yap*$^{-/-}$ zebrafish embryos and the Yap$^{-/-}$ mouse embryos prior to their death (Morin-Kensicki et al., 2006). We identified *yap*$^{-/-}$ zebrafish to display a range of morphological variability, and Yap$^{-/-}$ mouse embryos also had a range of phenotype from almost normal to severely abnormal. Further, we observed defects in embryo body lengthening and mediolateral defects in endoderm progenitor development which was recapitulated in mice lacking Yap as they had a failure to elongate the body axis and had defects in mediolateral patterning (Morin-Kensicki et al., 2006). Intriguingly, in a recent study examining the *hir* medaka fish mutant, a morphologically flattened body and tissue misalignment was found to be due to a mutation in Yap, which caused a decrease in tissue tension (Porazinski et al., 2015). This suggests that Yap plays not only a role in proliferation and progenitor cell formation but also a central role in organ and body shape.

Our phenotypic findings of smaller endodermal organs and decreased hepatoblast progenitors in *yap*$^{-/-}$ embryos support a role for Yap in proliferation, growth, and organ formation. These properties have similarly been seen in other studies using morpholino knockdown of *yap* in zebrafish, as a decrease in *yap* caused defects in brain development, cardiogenesis, hematopoiesis, renal development, and retina development (Jiang et al., 2009; Skouloudaki et al., 2009; Hu et al., 2013; Fukui et al., 2014; Loh et al., 2014; Porazinski et al., 2015). Consistent with our finding of transcriptional activation of Yap to be essential for progenitor cell population size, Yap has been implicated in the survival of neuroprogenitor cells in the chick (Cao et al., 2008) and maintenance of neuromast progenitor cells in the lateral line

(Loh et al., 2014). Further, Yap was found to regulate Prox1 expression in neuromasts, which supports our finding of decreased *prox1* positive hepatoblasts in *yap*$^{-/-}$ embryos as well as embryos expressing the dominant negative Yap. Interestingly, in lateral line development, *prox1* mRNA expression could rescue the number of differentiated mechanoreceptors in *yap* knockdown embryos, suggesting *prox1* repletion in hepatoblasts deficient for yap could rescue liver formation (Loh et al., 2014).

Our findings that Yap expression is important for hepatoblast progenitor populations are consistent with Hippo activity in the developing endoderm as seen in Hippo reporter transgenic fish, which contains four consensus Tead binding sites upstream of a troponin minimal promoter that drives fluorescent protein expression (Miesfeld and Link, 2014). In these embryos, high fluorescence is seen in undifferentiated endoderm as well as cardiac progenitor cells and muscle of the trunk (Miesfeld and Link, 2014). Furthermore, *yap* morphants showed endodermal widening, and targeted *yap* depletion in endoderm-fated cells demonstrated defects in endoderm formation (Fukui et al., 2014). *Yap* morphants also have shown *yap* is activated in the endoderm by sphingosine 1-phosphate (S1P) and reduced *yap* activity results in defects in the endodermal sheet and cardia bifida (Fukui et al., 2014). These studies in combination with our observation of defects in hepatic bud formation and decreased formation to the left of midline suggest that the Hippo pathway may further facilitate the crosstalk between mesoderm and endoderm development. A number of extremely well defined mesodermal signaling pathways, namely Wnt, FGF and Bmp, have elegantly been shown to play a fundamental role in hepatoblast specification (North and Goessling, 2011). Our findings are reminiscent of defects in Bmp signaling in the zebrafish in which disruption of Bmp during hepatic specification results in decreased hepatoblast formation and laterality defects (Shin et al., 2007). However, it is important to note that our data does not provide information regarding whether Hippo signaling in the mesoderm or endoderm is most critical for liver development and additional studies are needed. Further, our observation of decreased hepatoblast markers *prox1* and *hhex* in hepatoblast budding in *yap*$^{-/-}$

embryos and *hs:dnYap* embryos could be a result of deficiencies in specification, proliferation or increased cellular death. Surprisingly, while heat shock induction of the constitutively active form of Yap increased progenitor cell population size, we did not observe a concomitant increase in liver size. This could be a result of the short temporal response of the heat shock induction. Further, previous gain-of-function zebrafish experiments in which mRNA encoding for *yap* was injected into embryos similarly did not show increases in organ size or overgrowths (Gee et al., 2011; Loh et al., 2014).

Role of Glucose Transporters in Cancer and Development

We find *glucose transporters 1* and *2* (*glut1/2*) are downregulated in $yap^{-/-}$ and $yap^{-/-}taz^{-/-}$embryos and are downregulated with heat shock driven expression of a dominant negative Yap and conversely upregulated by heat shock activation of a transcriptionally active Yap within 6 hours of heat shock. This is of particular interest as glucose availability is a rate limiting step to glycolysis and glucose transporter expression is highly transcriptionally regulated. Additionally, a marked increase in glucose uptake with increased aerobic glycolysis is a characteristic feature of cancer cells, originally described by Otto Warburg almost a century ago (Warburg et al., 1926; Koppenol et al., 2011). This property of increased glucose uptake in cancer has since been harnessed for cancer detection through positron emission tomography (PET) imaging of a radioactive glucose, fluorodeoxyglucose (^{18}F-FDG), that detects high-glucose uptake, and as such, preferentially labels high-glucose consuming tumors.

To date, fourteen family members of the facilitative glucose transporters have been described in mammals (Medina and Owen, 2002). Glut1 is is a rate-limiting facilitative transporter for glucose uptake and is normally ubiquitously expressed at low levels. However, elevated Glut1 expression has been reported in many different cancers, including hepatic, pancreatic, breast, esophageal, brain, renal, lung, cutaneous, colorectal, endometrial, ovarian, and cervical carcinoma (Macheda et al., 2005). Further, it has been correlated with poorer prognosis and more aggressive tumor behavior, especially in hepatocellular carcinoma

and cholangiocarcinoma (Amann et al., 2009). Glut2, on the other hand, is a low-affinity glucose transporter that is primarily expressed in the liver, pancreas, and retina in adult tissues. Glut2 is also overexpressed in some cancers, including gastric, breast, colon and liver carcinoma, and has been found to be highly specific for high-grade precursor lesions in cholangiocarcinoma (Medina and Owen, 2002; Kubo et al., 2014). While Glut2 is the normal glucose transporter in pancreas and Glut2 is associated with high-grade precursor lesions, Glut1 has been the main glucose transporter overexpressed in the progressed tumors (Medina and Owen, 2002). This suggests that glucose transporter expression can be differentially expressed based on the specific cellular background and cancer.

Interestingly, glucose transporters have been found to be regulated by oncogenic pathways. Early experiments identified that transformation of cells with oncogenes such as Src, Ras, or FSV caused early induction of Glut1 expression (Flier et al., 1987; Birnbaum et al., 1987). Oncogenic pathways that have further been implicated in glucose transporter activity are PI3K/Akt signaling (Kohn et al., 1996), Myc (Osthus et al., 2000; Louro et al., 2002; Dang et al., 2008), and p53 (Kawauchi et al., 2008; Zhang et al., 2013). As Yap has been shown to be a potent oncogene, this is in line with our findings of *glut1* and *glut2* expression being decreased in *yap* knockout embryos. While we do not know whether this is a direct effect on transcriptional regulation, intriguingly there is a putative Tead binding consensous motif in the *glut1* enhancer region. Supporting our finding that Yap causes differential expression of glucose transporters, Yap has been shown to upregulate expression of the glucose transporter 3 (Glut3) in human cell lines (Wang et al., 2015). While we did not observe *glut3* specifically to be deregulated by *yap* loss in zebrafish embryos, this could be a result of the differential context of glucose transporters in the developing zebrafish embryo and human cell lines.

Glucose transport is of special interest in the context of development as glucose transporter expression is altered as cells differentiate and glucose metabolism seems to play a critical role in stem cell identity. Indeed, Glut1 and Glut3 are upregulated in blastocyts

requiring highl levels of glycolysis (Pantaleon and Kaye, 1998). Furthermore, muscle progenitor cells, known as satellite cells, express high levels of Glut1 and Glut3 during myogenesis (Guillet-Deniau et al., 1994). As the Hippo signaling pathway has shown marked activity in the muscle and Yap is required for satellite cell activation (Judson et al., 2012), this provides another potential connection between Yap transcriptional activity and glucose transporter expression.

Integration of metabolic signaling in the Hippo Pathway

Our work demonstrates that Yap plays a crucial role in the metabolism of glucose and synthesis of nucleotides as we observed decreased glycolysis and biosynthesis of purine and pyrimidine precursors in *yap* knockout embryos both in steady state metabolite measurements and tracer label flux studies. This influence of Yap on glycolytic flux into nucleotide biosynthesis is a common trademark of cancer cells that direct glucose metabolism into anabolic pathways (Vander Heiden et al., 2009). Furthermore, loss of oncogenic Kras resulting in decreased glycolytic flux into the anabolic PPP pathway (Ying et al., 2012) is reminiscent of our findings in *yap* knockout embryos. Very recently, Yap has been shown to be regulated by the presence of glucose itself. Energy stress on cells in culture either by glucose deprivation or treatment with 2-deoxyglucose, which is unable to undergo further glycolysis, caused Yap activity to be decreased through activation of AMPK which then phosphorylates and activates Lats1/2 for phosphorylation and inhibition of Yap (Mo et al., 2015; Wang et al., 2015; Enzo et al., 2015). When cells were released from energy stress, Yap was found to translocate to the nucleus and interact with Tead to promote transcription of its target genes (Wang et al., 2015). Furthermore, Yap phosphorylation, and hence its cytoplasmic retention, was greater in the liver of fasted mice whereas in the livers of fed mice, Yap was less phosphorylated and was nuclear localized, promoting transcription (Wang et al., 2015). Consistent with a role of metabolic cues as regulators of the Hippo pathway, the mevalonate pathway, which is involved in the biosynthesis of cholesterol, was found to modulate Yap

activity. In combination with our findings that Yap alters glucose uptake and glycolytic flux for anabolic nucleotide biosynthesis, these studies provide the intriguing possibility that the availability of nutrients and the metabolic reprogramming of cells for anabolic growth is integrated by Yap. Finally, our discovery that chemical inhibition of Glut1 *in vivo* causes Yap-driven proliferation to be reduced offers the intriguing possibility that therapeutics targeted towards glucose uptake may be beneficial for cancer patients with high Yap activity tumors.

3.6 Acknowledgements

This work was done in in equal collaboration with Andrew G. Cox. Contributors to this work were also: Joel B. Miesfeld, Allison Tsomides, Keelin O'Connor, Michael Fort, Sagar Chhangawala, Min Yuan, Evan Lien, Brian A. Link, John Asara, Yariv Houvras, and Wolfram Goessling. K.L.H, A.G.C. and W.G. designed experiments, reviewed results and wrote the manuscript. K.L.H. and A.G.C. performed the majority of the experiments. J.B.M. generated the Yap knockout fish and kindly provided the Yap^{S87A} and dnYap plasmids. A.T. and K.O. assisted in zebrafish experiments. K.H., S.C. and Y.H. analyzed RNA-seq datasets. E.L. analyzed metabolomics dataset. B.A.L., J.A., and Y.H. provided intellectual support.

Chapter 4

Conclusions and Future Directions

The Hippo signaling pathway is a powerful regulator of proliferation, growth, and organ size. It requires, like all cellular growth signals, the necessary biosynthesis of the required macromolecular building blocks to support high levels of cellular replication and division. While many studies have investigated the upstream regulators of Hippo signaling, how the Hippo pathway coordinates rapid cellular proliferation with the demands of anabolic synthesis is unknown. Here we study the role of Yap, the evolutionarily conserved transcriptional co-activator and downstream effector of the Hippo pathway, in its role in reprogramming cellular metabolism.

In our first study, we established that the zebrafish is able to faithfully repeat the findings of Yap-induced hepatomegaly with a transgenic model that specifically expresses a constitutively active Yap in hepatocytes. We found Yap induces hepatocyte proliferation and hepatomegaly, both during embryogenesis and in the adult, and that these pre-neoplastic livers are more sensitive to carcinogen-induced cancers. Inquiry into how Yap is able to support this hypercellular proliferation revealed through transcriptomic and metabolomic analyses that Yap directly upregulates glutamine synthetase (Glul) expression and reprograms nitrogen metabolism for *de novo* nucleotide biosynthesis. Interestingly, we found that chemical inhibition and genetic knockdown of Glul reduced Yap-driven hepatomegaly, suggesting that Yap-regulated proliferation is partially dependent on the synthesis of glutamine. As glutamine is a source of nitrogen for nucleotide biosynthesis, we wanted to conduct tracer la-

beling studies to determine the fate of nutritional nitrogen in Yap-driven hepatocyte growth. To accomplish this, we developed a novel protocol with nitrogen tracer labeling for *in vivo* flux analysis in the zebrafish. Excitingly, we found that Yap reprograms nutritional nitrogen flux into nucleotides and that this flux is dependent on glutamine synthetase activity. Together, this data showed that Yap is able to reprogram nitrogen metabolism to provide the necessary nucleotide building blocks for DNA required in cellular proliferation and growth.

We next harnessed the power of the zebrafish as a model for development and investigated the role of Yap in liver progenitor formation. Utilizing a *yap* knockout zebrafish that is viable through adulthood and heat shock inducible transgenic lines that modulate Yap transcriptional activity, we found Yap is required for normal growth of endoderm organs as well as hepatic progenitor cell populations. As the developing embryo has many metabolic demands for cellular proliferation, we wondered whether Yap could be modulating cellular metabolism in the developing embryo for the anabolic synthesis of necessary macromolecules. Transcriptomic, metabolomic, and flux analyses revealed that Yap modulates glucose uptake through expression of glucose transporters *glut1/2* and diverts the carbon glucose backbone into purine and pyrimidine precursors necessary for nucleotide biosynthesis. Inhibition of glucose transporter *glut1* decreased Yap-induced hepatomegaly in embryos to wild type liver sizes. Altogether, these results reveal that Yap is able to reprogram glucose metabolism by regulating glucose uptake and shunting glucose metabolites into nucleotide biosynthesis in the developing embryo.

In total, these complementary gain-of-function and loss-of function studies provide the first evidence that Yap directly modulates cellular metabolism for anabolic growth. We have developed new *in vivo* methods for assessing metabolic fluxes in the zebrafish and using these methods, we have demonstrated that Yap reprograms the cellular metabolism of both glutamine, a nitrogen source, and glucose, a carbon source, into nucleotide biosynthesis to support hyperproliferation and growth.

Our findings open many new avenues of research with regards to the role of Yap in

cellular metabolism as well as how Yap influences these properties in the context of cancer. Currently, we have only examined the pathways feeding into the biosynthesis of nucleotides. However, it is extremely likely that Yap also directs cellular metabolism for the anabolic synthesis of other biomolecular building blocks, such as lipids and amino acids. Our findings of decreased glucose uptake and reduced glycolysis in the absence of Yap is supportive of a role for Yap in fatty acid biosynthesis as most of the carbon for fatty acid synthesis is derived from glucose. As we conducted polar metabolomics analyses, however, changes in lipid metabolism would be largely undetectable in our current studies. Further suggesting a role for Yap in lipid usage and absorption, in our *yap* knockout embryos, we find the yolk, which is composed of lipids and other nutrients, to be improperly reabsorbed. In addition, we observed that *yap* knockout embryos begin to show lethality at 6 dpf, which corresponds to the transition from yolk-dependent nutrition to feeding (Anderson et al., 2011). This suggests that *yap* knockout embryos had defects in nutrient uptake. Further studies are likely to elucidate that Yap is able to coordinate multiple anabolic processes for both detection of the metabolic environment and utilization of these resources for rapid proliferation.

Our findings implicating Yap in regulating glucose uptake and metabolism, in conjunction with the recently published papers regarding glucose availability to regulate Yap activity are intriguing to ponder with regards to the ability of Yap to maintain stem cell populations. Evidence shows that metabolites not only provide energy and support for proliferation, but they also play a role in modulating pluripotency and differentiation (Shyh-Chang et al., 2013). Studies in hematopoietic stem cells have shown that glucose and its transport are key regulators of hematopoietic stem cell fate and proliferation (Miharada et al., 2011; Simsek et al., 2010; Takubo et al., 2010; Harris et al., 2013; Yu et al., 2013; Oburoglu et al., 2014). This is especially interesting in the context of the liver as a gradient glucose concentration is found in mammalian livers dependent on nutritional status (Katz et al., 1977). Intriguingly, though, most of liver glycolysis occurs in the centrilobular region of the hepatocyte lobule

and in this region, it has been hypothesized the liver contains its hepatic adult progenitor cell. It would be interesting to test whether glucose concentration plays a role in the ability of adult stem cells to maintain their stemness in the context of Yap signaling.

With the alterations in metabolism that we see during development and in the pre-neoplastic state, this opens more lines of inquiry as to whether these processes are also modulated in the context of regeneration as many pathways conserved in development and cancer are also found to be activated in the context of regeneration. The liver is the only solid organ capable of regeneration in the human and holds tremendous ability for an appropriate compensatory response to injury. With the liver's unique ability to regenerate as an adult and the causal association of continual injury and repair in the context of cirrhosis, which is a major risk factor for hepatocellular carcinoma, it is tempting to speculate that the Hippo pathway plays a central role to mediating liver regeneration both at the signaling level of cellular division and the metabolic level to provide the necessary energy and building blocks to the expanding hepatocyte pool. Already, the Hippo pathway has been implicated in regeneration in the intestine of mammals as Yap is highly expressed during regeneration in the stem cell crypts and where loss of Yap severely impairs sulfate-induced intestinal regeneration (Cai et al., 2010; Zhao et al., 2011). The zebrafish has the unique ability to regenerate many of its tissues, so using our models, determining the role of Yap in fin, heart, and liver regeneration is feasible. This could provide especially elucidating in the context of liver regeneration as liver injury can be induced in hepatocytes specifically using nitroreductase (NTR) ablation (Curado et al., 2007a,b; Pisharath and Parsons, 2009). Liver injury in these *lf:CFP-NTR* fish has revealed that biliary epithelial cells transdifferentiate to mature hepatocytes during liver regeneration following hepatocyte ablation (Choi et al., 2014; He et al., 2014). Interestingly, Yap has been found to play a critical role in hepatocyte dedifferentiation, and very high overexpression of Yap can change hepatocytes into a biliary-ductal phenotype (Yimlamai et al., 2014). Based on these studies, it is reasonable to hypothesize that Yap signaling might be critical for hepatocyte regeneration and organ

regrowth by promoting plasticity of cell fate as well as pro-proliferative growth signals. Further, based on our studies, it is likely that Yap directs the cellular metabolic program to enhance anabolic pathways to provide for the rapid proliferation necessary for repair.

In the context of cancer, the ability of Yap to act as a central integrator of nutritional biolmolecular availability and metabolic reprogramming for anabolic growth may provide advantageous clonal selection in the context of tumor development. As tumor growth requires survival in non-optimal, challenging growth environments, evolutionary pressures for survival and optimizing nutrient utilization are necessary. For this reason, cells that are able to reprogram cellular metabolism to generate the anabolic building blocks necessary for growth are likely favored. As such, there may be selective pressure in those cells that have increased Yap activity through gene amplification as they could acquire the ability to uptake more glucose, through increased expression of glucose transporters, which will then allow Yap to remain active and continue directing anabolic metabolism for proliferation.

More globally, with our findings of Yap as a regulator of cellular metabolism to aid in the ability to proliferate, these bring about more questions of human physiology and the importance of nutrition in the context of cancer. In studies where mice were injected with aggressive human breast cancer cells, mortality rates were significantly reduced in the group that were calorie restricted to hypoglycemic levels compared to normal fed mice, which had better survival rates than the hyperglycemic group (Santisteban et al., 1985). Interestingly, metformin, which decreases glucose production in the liver, has been shown to be extremely beneficial in reducing the relative risk of liver cancer in epidemiological studies; however, in other cancers this effect was not as great (Zhang et al., 2013). Metformin, recently, has been shown to decrease Yap activity by increasing energy stress on cells (DeRan et al., 2014; Mo et al., 2015). In combination with our findings of yap playing a role in glucose uptake and diversion of its carbon backbone into nucleotides, this suggest that glucose availability could be a potential therapeutic target and regulation of diet could be beneficial. Further, obesity

is a known risk factor for cancer, so modulation of glucose levels could help in the prevention of cancers in obese or hyperglycemic individuals.

Our increased understanding of the metabolic and molecular targets of Yap opens the possibilities of new therapeutic strategies that can be aimed to interfere with Yap mediated metabolic reprogramming. Our studies here include the usage of drugs targeting Glul and Glut1 function, and we have conclusively demonstrated that Yap-mediated hyperproliferation and growth can be reduced with these drugs. Unfortunately, the Glul inhibitor MSO cannot be used in the clinical setting as it inhibits glutamine synthetase in the brain, resulting in seizures. This does raise the need to find more biocompatible compounds that could be targeted to modulate glutamine synthesis and glucose uptake. The zebrafish might provide to be the optimal model as its ability to be used in wide chemical screens has already facilitated the discovery of clinically beneficial treatments (Goessling et al., 2011; Cutler et al., 2013).

In conclusion, we show that Yap in the context of liver development and cancer is able to reprogram normal cellular mechanisms of metabolism to promote the synthesis of macromolecular building blocks. Further, we establish the zebrafish as a powerful model for investigating the mechanisms of signaling pathways to control cellular metabolism *in vivo.* As we have found modulation of Yap-driven cellular reprogramming to reduce Yap-driven growth, these studies offer the promising molecular targets that may beneficial for patients with high Yap activity cancers.

References

Abcouwer, S. F., Bode, B. P. and Souba, W. W. (1995). Glucocorticoids regulate rat glutamine synthetase expression in a tissue-specific manner. J Surg Res *59*, 59–65.

Abcouwer, S. F., Lukaszewicz, G. C. and Souba, W. W. (1996). Glucocorticoids regulate glutamine synthetase expression in lung epithelial cells. Am J Physiol *270*, L141–51.

Adler, J. J., Johnson, D. E., Heller, B. L., Bringman, L. R., Ranahan, W. P., Conwell, M. D., Sun, Y., Hudmon, A. and Wells, C. D. (2013). Serum deprivation inhibits the transcriptional co-activator YAP and cell growth via phosphorylation of the 130-kDa isoform of Angiomotin by the LATS1/2 protein kinases. Proc Natl Acad Sci U S A *110*, 17368–17373.

Alarcon, C., Zaromytidou, A. I., Xi, Q., Gao, S., Yu, J., Fujisawa, S., Barlas, A., Miller, A. N., Manova-Todorova, K., Macias, M. J., Sapkota, G., Pan, D. and Massague, J. (2009). Nuclear CDKs drive Smad transcriptional activation and turnover in BMP and TGF-beta pathways. Cell *139*, 757–769.

Alder, O., Cullum, R., Lee, S., Kan, A. C., Wei, W., Yi, Y., Garside, V. C., Bilenky, M., Griffith, M., Morrissy, A. S., Robertson, G. A., Thiessen, N., Zhao, Y., Chen, Q., Pan, D., Jones, S. J., Marra, M. A. and Hoodless, P. A. (2014). Hippo Signaling Influences HNF4A and FOXA2 Enhancer Switching during Hepatocyte Differentiation. Cell Rep *9*, 261–271.

Amann, T., Maegdefrau, U., Hartmann, A., Agaimy, A., Marienhagen, J., Weiss, T. S., Stoeltzing, O., Warnecke, C., Schölmerich, J., Oefner, P. J., Kreutz, M., Bosserhoff, A. K. and Hellerbrand, C. (2009). GLUT1 expression is increased in hepatocellular carcinoma and promotes tumorigenesis. Am J Pathol *174*, 1544–1552.

Amoyel, M., Simons, B. D. and Bach, E. A. (2014). Neutral competition of stem cells is skewed by proliferative changes downstream of Hh and Hpo. EMBO J *33*, 2295–2313.

Anakk, S., Bhosale, M., Schmidt, V. A., Johnson, R. L., Finegold, M. J. and Moore, D. D. (2013). Bile acids activate YAP to promote liver carcinogenesis. Cell Rep *5*, 1060–1069.

Anderson, J. L., Carten, J. D. and Farber, S. A. (2011). Zebrafish lipid metabolism: from mediating early patterning to the metabolism of dietary fat and cholesterol. Methods Cell Biol *101*, 111–141.

Aragona, M., Panciera, T., Manfrin, A., Giulitti, S., Michielin, F., Elvassore, N., Dupont, S. and Piccolo, S. (2013). A mechanical checkpoint controls multicellular growth through YAP/TAZ regulation by actin-processing factors. Cell *154*, 1047–1059.

Azzolin, L., Zanconato, F., Bresolin, S., Forcato, M., Basso, G., Bicciato, S., Cordenonsi, M. and Piccolo, S. (2012). Role of TAZ as mediator of Wnt signaling. Cell *151*, 1443–1456.

Barry, E. R., Morikawa, T., Butler, B. L., Shrestha, K., de la Rosa, R., Yan, K. S., Fuchs, C. S., Magness, S. T., Smits, R., Ogino, S., Kuo, C. J. and Camargo, F. D. (2013). Restriction of intestinal stem cell expansion and the regenerative response by YAP. Nature *493*, 106–10.

Basu, S., Totty, N. F., Irwin, M. S., Sudol, M. and Downward, J. (2003). Akt phosphorylates the Yes-associated protein, YAP, to induce interaction with 14-3-3 and attenuation of p73-mediated apoptosis. Mol Cell *11*, 11–23.

Ben-Sahra, I., Howell, J. J., Asara, J. M. and Manning, B. D. (2013). Stimulation of de novo pyrimidine synthesis by growth signaling through mTOR and S6K1. Science *339*, 1323–1328.

Benhamouche, S., Curto, M., Saotome, I., Gladden, A. B., Liu, C. H., Giovannini, M. and McClatchey, A. I. (2010). Nf2/Merlin controls progenitor homeostasis and tumorigenesis in the liver. Genes Dev *24*, 1718–1730.

Benhamouche, S., Decaens, T., Godard, C., Chambrey, R., Rickman, D. S., Moinard, C., Vasseur-Cognet, M., Kuo, C. J., Kahn, A., Perret, C. and Colnot, S. (2006). Apc tumor suppressor gene is the "zonation-keeper" of mouse liver. Dev Cell *10*, 759–770.

Beyer, T. A., Weiss, A., Khomchuk, Y., Huang, K., Ogunjimi, A. A., Varelas, X. and Wrana, J. L. (2013). Switch enhancers interpret TGF-β and Hippo signaling to control cell fate in human embryonic stem cells. Cell Rep *5*, 1611–1624.

Birnbaum, M. J., Haspel, H. C. and Rosen, O. M. (1987). Transformation of rat fibroblasts by FSV rapidly increases glucose transporter gene transcription. Science *235*, 1495–1498.

Boggiano, J. C. and Fehon, R. G. (2012). Growth control by committee: intercellular junctions, cell polarity, and the cytoskeleton regulate Hippo signaling. Dev Cell *22*, 695–702.

Boussif, O., Lezoualc'h, F., Zanta, M. A., Mergny, M. D., Scherman, D., Demeneix, B. and Behr, J. P. (1995). A versatile vector for gene and oligonucleotide transfer into cells in culture and in vivo: polyethylenimine. Proc Natl Acad Sci U S A *92*, 7297–7301.

Bucking, C., Lemoine, C. M. and Walsh, P. J. (2013). Waste nitrogen metabolism and excretion in zebrafish embryos: effects of light, ammonia, and nicotinamide. J Exp Zool A Ecol Genet Physiol *319*, 391–403.

Cai, J., Zhang, N., Zheng, Y., de Wilde, R. F., Maitra, A. and Pan, D. (2010). The Hippo signaling pathway restricts the oncogenic potential of an intestinal regeneration program. Genes Dev *24*, 2383–2388.

Cairns, R. A., Harris, I. S. and Mak, T. W. (2011). Regulation of cancer cell metabolism. Nat Rev Cancer *11*, 85–95.

Camargo, F. D., Gokhale, S., Johnnidis, J. B., Fu, D., Bell, G. W., Jaenisch, R. and Brummelkamp, T. R. (2007). YAP1 increases organ size and expands undifferentiated progenitor cells. Curr Biol *17*, 2054–2060.

Cantor, J. R. and Sabatini, D. M. (2012). Cancer cell metabolism: one hallmark, many faces. Cancer Discov *2*, 881–898.

Cao, X., Pfaff, S. L. and Gage, F. H. (2008). YAP regulates neural progenitor cell number via the TEA domain transcription factor. Genes Dev *22*, 3320–3334.

Chandrasekhar, S., Souba, W. W. and Abcouwer, S. F. (1999). Identification of glucocorticoid-responsive elements that control transcription of rat glutamine synthetase. Am J Physiol *276*, L319–31.

Choi, T. Y., Ninov, N., Stainier, D. Y. and Shin, D. (2014). Extensive conversion of hepatic biliary epithelial cells to hepatocytes after near total loss of hepatocytes in zebrafish. Gastroenterology *146*, 776–788.

Christa, L., Simon, M. T., Flinois, J. P., Gebhardt, R., Brechot, C. and Lasserre, C. (1994). Overexpression of glutamine synthetase in human primary liver cancer. Gastroenterology *106*, 1312–1320.

Christofk, H. R., Vander Heiden, M. G., Harris, M. H., Ramanathan, A., Gerszten, R. E., Wei, R., Fleming, M. D., Schreiber, S. L. and Cantley, L. C. (2008). The M2 splice isoform of pyruvate kinase is important for cancer metabolism and tumour growth. Nature *452*, 230–253.

Chu, J. and Sadler, K. C. (2009). New school in liver development: lessons from zebrafish. Hepatology *50*, 1656–1663.

Chung, S., Dzeja, P. P., Faustino, R. S., Perez-Terzic, C., Behfar, A. and Terzic, A. (2007). Mitochondrial oxidative metabolism is required for the cardiac differentiation of stem cells. Nat Clin Pract Cardiovasc Med *4 Suppl 1*, S60–S67.

Collins, J. E., White, S., Searle, S. M. and Stemple, D. L. (2012). Incorporating RNA-seq data into the zebrafish Ensembl genebuild. Genome Res *22*, 2067–2078.

Colnot, S., Decaens, T., Niwa-Kawakita, M., Godard, C., Hamard, G., Kahn, A., Giovannini, M. and Perret, C. (2004). Liver-targeted disruption of Apc in mice activates beta-catenin signaling and leads to hepatocellular carcinomas. Proc Natl Acad Sci U S A *101*, 17216–17221.

Cordenonsi, M., Zanconato, F., Azzolin, L., Forcato, M., Rosato, A., Frasson, C., Inui, M., Montagner, M., Parenti, A. R., Poletti, A., Daidone, M. G., Dupont, S., Basso, G., Bicciato, S. and Piccolo, S. (2011). The Hippo transducer TAZ confers cancer stem cell-related traits on breast cancer cells. Cell *147*, 759–772.

Cunningham, J. T., Moreno, M. V., Lodi, A., Ronen, S. M. and Ruggero, D. (2014). Protein and nucleotide biosynthesis are coupled by a single rate-limiting enzyme, PRPS2, to drive cancer. Cell *157*, 1088–1103.

Curado, S., Anderson, R. M., Jungblut, B., Mumm, J., Schroeter, E. and Stainier, D. Y. (2007a). Conditional targeted cell ablation in zebrafish: a new tool for regeneration studies. Dev Dyn *236*, 1025–1035.

Curado, S., Anderson, R. M., Jungblut, B., Mumm, J., Schroeter, E. and Stainier, D. Y. R. (2007b). Conditional targeted cell ablation in zebrafish: a new tool for regeneration studies. Developmental dynamics : an official publication of the American Association of Anatomists *236*, 1025–35.

Cutler, C., Multani, P., Robbins, D., Kim, H. T., Le, T., Hoggatt, J., Pelus, L. M., Desponts, C., Chen, Y. B., Rezner, B., Armand, P., Koreth, J., Glotzbecker, B., Ho, V. T., Alyea, E., Isom, M., Kao, G., Armant, M., Silberstein, L., Hu, P., Soiffer, R. J., Scadden, D. T., Ritz, J., Goessling, W., North, T. E., Mendlein, J., Ballen, K., Zon, L. I., Antin, J. H. and Shoemaker, D. D. (2013). Prostaglandin-modulated umbilical cord blood hematopoietic stem cell transplantation. Blood *122*, 2074–2081.

Dang, C. V., Kim, J.-w., Gao, P. and Yustein, J. (2008). The interplay between MYC and HIF in cancer. Nat Rev Cancer *8*, 51–56.

Deberardinis, R. J., Sayed, N., Ditsworth, D. and Thompson, C. B. (2008). Brick by brick: metabolism and tumor cell growth. Curr Opin Genet Dev *18*, 54–61.

DeRan, M., Yang, J., Shen, C. H., Peters, E. C., Fitamant, J., Chan, P., Hsieh, M., Zhu, S., Asara, J. M., Zheng, B., Bardeesy, N., Liu, J. and Wu, X. (2014). Energy Stress Regulates Hippo-YAP Signaling Involving AMPK-Mediated Regulation of Angiomotin-like 1 Protein. Cell Rep *9*, 495–503.

Deuel, T. F., Louie, M. and Lerner, A. (1978). Glutamine synthetase from rat liver. Purification, properties, and preparation of specific antisera. J Biol Chem *253*, 6111–6118.

Dibble, C. C. and Manning, B. D. (2013). Signal integration by mTORC1 coordinates nutrient input with biosynthetic output. Nat Cell Biol *15*, 555–564.

Dong, J., Feldmann, G., Huang, J., Wu, S., Zhang, N., Comerford, S. A., Gayyed, M. F., Anders, R. A., Maitra, A. and Pan, D. (2007). Elucidation of a universal size-control mechanism in Drosophila and mammals. Cell *130*, 1120–1133.

Dovey, M., White, R. M. and Zon, L. I. (2009). Oncogenic NRAS cooperates with p53 loss to generate melanoma in zebrafish. Zebrafish *6*, 397–404.

Drake, C. J. (2003). Embryonic and adult vasculogenesis. Birth Defects Res C Embryo Today *69*, 73–82.

Dupont, S., Morsut, L., Aragona, M., Enzo, E., Giulitti, S., Cordenonsi, M., Zanconato, F., Le Digabel, J., Forcato, M., Bicciato, S., Elvassore, N. and Piccolo, S. (2011). Role of YAP/TAZ in mechanotransduction. Nature *474*, 179–183.

Duvel, K., Yecies, J. L., Menon, S., Raman, P., Lipovsky, A. I., Souza, A. L., Triantafellow, E., Ma, Q., Gorski, R., Cleaver, S., Vander Heiden, M. G., MacKeigan, J. P., Finan, P. M., Clish, C. B., Murphy, L. O. and Manning, B. D. (2010). Activation of a metabolic gene regulatory network downstream of mTOR complex 1. Mol Cell *39*, 171–183.

Ehmer, U., Zmoos, A. F., Auerbach, R. K., Vaka, D., Butte, A. J., Kay, M. A. and Sage, J. (2014). Organ size control is dominant over Rb family inactivation to restrict proliferation in vivo. Cell Rep *8*, 371–381.

Enzo, E., Santinon, G., Pocaterra, A., Aragona, M., Bresolin, S., Forcato, M., Grifoni, D., Pession, A., Zanconato, F., Guzzo, G., Bicciato, S. and Dupont, S. (2015). Aerobic glycolysis tunes YAP/TAZ transcriptional activity. EMBO J *DOI*, 10.15252/embj.201490379.

Fang, M., Shen, Z., Huang, S., Zhao, L., Chen, S., Mak, T. W. and Wang, X. (2010). The ER UDPase ENTPD5 promotes protein N-glycosylation, the Warburg effect, and proliferation in the PTEN pathway. Cell *143*, 711–724.

Fernandez, L. A., Northcott, P. A., Dalton, J., Fraga, C., Ellison, D., Angers, S., Taylor, M. D. and Kenney, A. M. (2009). YAP1 is amplified and up-regulated in hedgehog-associated medulloblastomas and mediates Sonic hedgehog-driven neural precursor proliferation. Genes Dev *23*, 2729–2741.

Ferreira, L. M. R., Hebrant, A. and Dumont, J. E. (2012). Metabolic reprogramming of the tumor. Oncogene *31*, 3999–4011.

Field, H. A., Dong, P. D., Beis, D. and Stainier, D. Y. (2003). Formation of the digestive system in zebrafish. II. Pancreas morphogenesis. Dev Biol *261*, 197–208.

Filosa, S., Fico, A., Paglialunga, F., Balestrieri, M., Crooke, A., Verde, P., Abrescia, P., Bautista, J. M. and Martini, G. (2003). Failure to increase glucose consumption through the pentose-phosphate pathway results in the death of glucose-6-phosphate dehydrogenase gene-deleted mouse embryonic stem cells subjected to oxidative stress. Biochem J *370*, 935–943.

Fitamant, J., Kottakis, F., Benhamouche, S., Tian, H. S., Chuvin, N., Parachoniak, C. A., Nagle, J. M., Perera, R. M., Lapouge, M., Deshpande, V., Zhu, A. X., Lai, A., Min, B., Hoshida, Y., Avruch, J., Sia, D., Campreciós, G., McClatchey, A. I., Llovet, J. M., Morrissey, D., Raj, L. and Bardeesy, N. (2015). YAP Inhibition Restores Hepatocyte Differentiation in Advanced HCC, Leading to Tumor Regression. Cell Rep *DOI*, 10.1016/j.celrep.2015.02.027.

Flier, J. S., Mueckler, M. M., Usher, P. and Lodish, H. F. (1987). Elevated levels of glucose transport and transporter messenger RNA are induced by ras or src oncogenes. Science *235*, 1492–1495.

Folmes, C. D., Nelson, T. J., Martinez-Fernandez, A., Arrell, D. K., Lindor, J. Z., Dzeja, P. P., Ikeda, Y., Perez-Terzic, C. and Terzic, A. (2011). Somatic Oxidative Bioenergetics Transitions into Pluripotency-Dependent Glycolysis to Facilitate Nuclear Reprogramming. Cell Metab *14*, 264–271.

Fujii, M., Toyoda, T., Nakanishi, H., Yatabe, Y., Sato, A., Matsudaira, Y., Ito, H., Murakami, H., Kondo, Y., Kondo, E., Hida, T., Tsujimura, T., Osada, H. and Sekido, Y. (2012). TGF-beta synergizes with defects in the Hippo pathway to stimulate human malignant mesothelioma growth. J Exp Med *209*, 479–494.

Fukui, H., Terai, K., Nakajima, H., Chiba, A., Fukuhara, S. and Mochizuki, N. (2014). S1P-Yap1 signaling regulates endoderm formation required for cardiac precursor cell migration in zebrafish. Dev Cell *31*, 128–136.

Galli, G. G., Honnens de Lichtenberg, K., Carrara, M., Hans, W., Wuelling, M., Mentz, B., Multhaupt, H. A., Fog, C. K., Jensen, K. T., Rappsilber, J., Vortkamp, A., Coulton, L., Fuchs, H., Gailus-Durner, V., Hrabe de Angelis, M., Calogero, R. A., Couchman, J. R. and Lund, A. H. (2012). Prdm5 regulates collagen gene transcription by association with RNA polymerase II in developing bone. PLoS Genet *8*, e1002711.

Gee, S. T., Milgram, S. L., Kramer, K. L., Conlon, F. L. and Moody, S. a. (2011). Yes-associated protein 65 (YAP) expands neural progenitors and regulates Pax3 expression in the neural plate border zone. PloS one *6*, e20309.

Goessling, W., Allen, R. S., Guan, X., Jin, P., Uchida, N., Dovey, M., Harris, J. M., Metzger, M. E., Bonifacino, A. C., Stroncek, D., Stegner, J., Armant, M., Schlaeger, T., Tisdale, J. F., Zon, L. I., Donahue, R. E. and North, T. E. (2011). Prostaglandin E2 enhances human cord blood stem cell xenotransplants and shows long-term safety in preclinical nonhuman primate transplant models. Cell Stem Cell *8*, 445–458.

Goessling, W., North, T. E., Lord, A. M., Ceol, C., Lee, S., Weidinger, G., Bourque, C., Strijbosch, R., Haramis, A.-P., Puder, M., Clevers, H., Moon, R. T. and Zon, L. I. (2008). APC mutant zebrafish uncover a changing temporal requirement for wnt signaling in liver development. Dev Biol *320*, 161–174.

Goulev, Y., Fauny, J. D., Gonzalez-Marti, B., Flagiello, D., Silber, J. and Zider, A. (2008). SCALLOPED interacts with YORKIE, the nuclear effector of the hippo tumor-suppressor pathway in Drosophila. Curr Biol *18*, 435–441.

Guertin, D. A. and Sabatini, D. M. (2007). Defining the role of mTOR in cancer. Cancer Cell *12*, 9–22.

Guichard, C., Amaddeo, G., Imbeaud, S., Ladeiro, Y., Pelletier, L., Maad, I. B., Calderaro, J., Bioulac-Sage, P., Letexier, M., Degos, F., Clement, B., Balabaud, C., Chevet, E.,

Laurent, A., Couchy, G., Letouze, E., Calvo, F. and Zucman-Rossi, J. (2012). Integrated analysis of somatic mutations and focal copy-number changes identifies key genes and pathways in hepatocellular carcinoma. Nat Genet *44*, 694–698.

Guillet-Deniau, I., Leturque, A. and Girard, J. (1994). Expression and cellular localization of glucose transporters (GLUT1, GLUT3, GLUT4) during differentiation of myogenic cells isolated from rat foetuses. J Cell Sci *107*, 487–496.

Hamilton, F. (1822). An Account of the Fishes Found in the River Ganges and Its Branches. Arhibald Constable and Company, Edinburgh.

Hanahan, D. and Weinberg, R. A. (2000). The hallmarks of cancer. Cell *100*, 57–70.

Hanahan, D. and Weinberg, R. A. (2011). Hallmarks of cancer: the next generation. Cell *144*, 646–674.

Harris, J. M., Esain, V., Frechette, G. M., Harris, L. J., Cox, A. G., Cortes, M., Garnaas, M. K., Carroll, K. J., Cutting, C. C., Khan, T., Elks, P. M., Renshaw, S. A., Dickinson, B. C., Chang, C. J., Murphy, M. P., Paw, B. H., Vander Heiden, M. G., Goessling, W. and North, T. E. (2013). Glucose metabolism impacts the spatiotemporal onset and magnitude of HSC induction in vivo. Blood *121*, 2483–93.

Harvey, K. F., Pfleger, C. M. and Hariharan, I. K. (2003). The Drosophila Mst ortholog, hippo, restricts growth and cell proliferation and promotes apoptosis. Cell *114*, 457–467.

Harvey, K. F., Zhang, X. and Thomas, D. M. (2013). The Hippo pathway and human cancer. Nature reviews. Cancer *13*, 246–57.

He, J., Lu, H., Zou, Q. and Luo, L. (2014). Regeneration of liver after extreme hepatocyte loss occurs mainly via biliary transdifferentiation in zebrafish. Gastroenterology *146*, 789–800 e8.

Heallen, T., Zhang, M., Wang, J., Bonilla-Claudio, M., Klysik, E., Johnson, R. L. and Martin, J. F. (2011). Hippo pathway inhibits Wnt signaling to restrain cardiomyocyte proliferation and heart size. Science (New York, N.Y.) *332*, 458–61.

Hensley, C. T., Wasti, A. T. and DeBerardinis, R. J. (2013). Glutamine and cancer: cell biology, physiology, and clinical opportunities. The Journal of clinical investigation *123*, 3678–84.

Her, G. M., Chiang, C. C., Chen, W. Y. and Wu, J. L. (2003a). In vivo studies of liver-type fatty acid binding protein (L-FABP) gene expression in liver of transgenic zebrafish (Danio rerio). FEBS Lett *538*, 125–133.

Her, G. M., Yeh, Y. H. and Wu, J. L. (2003b). 435-bp liver regulatory sequence in the liver fatty acid binding protein (L-FABP) gene is sufficient to modulate liver regional expression in transgenic zebrafish. Dev Dyn *227*, 347–356.

Hilman, D. and Gat, U. (2011). The evolutionary history of YAP and the hippo/YAP pathway. Mol Biol Evol *28*, 2403–2417.

Hossain, Z., Ali, S. M., Ko, H. L., Xu, J., Ng, C. P., Guo, K., Qi, Z., Ponniah, S., Hong, W. and Hunziker, W. (2007). Glomerulocystic kidney disease in mice with a targeted inactivation of Wwtr1. Proc Natl Acad Sci U S A *104*, 1631–6.

Howe, K., Clark, M. D., Torroja, C. F., Torrance, J., Berthelot, C., Muffato, M., Collins, J. E., Humphray, S., McLaren, K., Matthews, L., McLaren, S., Sealy, I., Caccamo, M., Churcher, C., Scott, C., Barrett, J. C., Koch, R., Rauch, G.-J., White, S., Chow, W., Kilian, B., Quintais, L. T., Guerra-Assunção, J. A., Zhou, Y., Gu, Y., Yen, J., Vogel, J.-H., Eyre, T., Redmond, S., Banerjee, R., Chi, J., Fu, B., Langley, E., Maguire, S. F., Laird, G. K., Lloyd, D., Kenyon, E., Donaldson, S., Sehra, H., Almeida-King, J., Loveland, J., Trevanion, S., Jones, M., Quail, M., Willey, D., Hunt, A., Burton, J., Sims, S., McLay, K., Plumb, B., Davis, J., Clee, C., Oliver, K., Clark, R., Riddle, C., Elliot, D., Eliott, D., Threadgold, G., Harden, G., Ware, D., Begum, S., Mortimore, B., Mortimer, B., Kerry, G., Heath, P., Phillimore, B., Tracey, A., Corby, N., Dunn, M., Johnson, C., Wood, J., Clark, S., Pelan, S., Griffiths, G., Smith, M., Glithero, R., Howden, P., Barker, N., Lloyd, C., Stevens, C., Harley, J., Holt, K., Panagiotidis, G., Lovell, J., Beasley, H., Henderson, C., Gordon, D., Auger, K., Wright, D., Collins, J., Raisen, C., Dyer, L., Leung, K., Robertson, L., Ambridge, K., Leongamornlert, D., McGuire, S., Gilderthorp, R., Griffiths, C., Manthravadi, D., Nichol, S., Barker, G., Whitehead, S., Kay, M., Brown, J., Murnane, C., Gray, E., Humphries, M., Sycamore, N., Barker, D., Saunders, D., Wallis, J., Babbage, A., Hammond, S., Mashreghi-Mohammadi, M., Barr, L., Martin, S., Wray, P., Ellington, A., Matthews, N., Ellwood, M., Woodmansey, R., Clark, G., Cooper, J. D., Cooper, J., Tromans, A., Grafham, D., Skuce, C., Pandian, R., Andrews, R., Harrison, E., Kimberley, A., Garnett, J., Fosker, N., Hall, R., Garner, P., Kelly, D., Bird, C., Palmer, S., Gehring, I., Berger, A., Dooley, C. M., Ersan-Ürün, Z., Eser, C., Geiger, H., Geisler, M., Karotki, L., Kirn, A., Konantz, J., Konantz, M., Oberländer, M., Rudolph-Geiger, S., Teucke, M., Lanz, C., Raddatz, G., Osoegawa, K., Zhu, B., Rapp, A., Widaa, S., Langford, C., Yang, F., Schuster, S. C., Carter, N. P., Harrow, J., Ning, Z., Herrero, J., Searle, S. M. J., Enright, A., Geisler, R., Plasterk, R. H. A., Lee, C., Westerfield, M., de Jong, P. J., Zon, L. I., Postlethwait, J. H., Nüsslein-Volhard, C., Hubbard, T. J. P., Roest Crollius, H., Rogers, J. and Stemple, D. L. (2013). The zebrafish reference genome sequence and its relationship to the human genome. Nature *496*, 498–503.

Howell, J. J., Ricoult, S. J., Ben-Sahra, I. and Manning, B. D. (2013). A growing role for mTOR in promoting anabolic metabolism. Biochem Soc Trans *41*, 906–912.

Hu, J., Sun, S., Jiang, Q., Sun, S., Wang, W., Gui, Y. and Song, H. (2013). Yes-associated protein (yap) is required for early embryonic development in zebrafish (danio rerio). Int J Biol Sci *9*, 267–278.

Huang, J. and Kalderon, D. (2014). Coupling of Hedgehog and Hippo pathways promotes stem cell maintenance by stimulating proliferation. J Cell Biol *205*, 325–338.

Huang, J., Wu, S., Barrera, J., Matthews, K. and Pan, D. (2005). The Hippo signaling pathway coordinately regulates cell proliferation and apoptosis by inactivating Yorkie, the Drosophila Homolog of YAP. Cell *122*, 421–434.

Imajo, M., Miyatake, K., Iimura, A., Miyamoto, A. and Nishida, E. (2012). A molecular mechanism that links Hippo signalling to the inhibition of Wnt/beta-catenin signalling. EMBO J *31*, 1109–1122.

Jain, M., Nilsson, R., Sharma, S., Madhusudhan, N., Kitami, T., Souza, A. L., Kafri, R., Kirschner, M. W., Clish, C. B. and Mootha, V. K. (2012). Metabolite profiling identifies a key role for glycine in rapid cancer cell proliferation. Science *336*, 1040–1044.

Jemal, A., Bray, F., Center, M. M., Ferlay, J., Ward, E. and Forman, D. (2011). Global cancer statistics. Technical Report 2.

Jia, J., Zhang, W., Wang, B., Trinko, R. and Jiang, J. (2003). The Drosophila Ste20 family kinase dMST functions as a tumor suppressor by restricting cell proliferation and promoting apoptosis. Genes Dev *17*, 2514–2519.

Jiang, Q., Liu, D., Gong, Y., Wang, Y., Sun, S., Gui, Y. and Song, H. (2009). Yap Is Required for the Development of Brain, Eyes, and Neural Crest in Zebrafish. Biochem Biophys Res Commun *384*, 114–9.

Judson, R. N., Tremblay, A. M., Knopp, P., White, R. B., Urcia, R., De Bari, C., Zammit, P. S., Camargo, F. D. and Wackerhage, H. (2012). The Hippo pathway member Yap plays a key role in influencing fate decisions in muscle satellite cells. J Cell Sci *125*, 6009–6019.

Jung, J., Zheng, M., Goldfarb, M. and Zaret, K. S. (1999). Initiation of mammalian liver development from endoderm by fibroblast growth factors. Science *284*, 1998–2003.

Justice, R. W., Zilian, O., Woods, D. F., Noll, M. and Bryant, P. J. (1995). The Drosophila tumor suppressor gene warts encodes a homolog of human myotonic dystrophy kinase and is required for the control of cell shape and proliferation. Genes Dev *9*, 534–546.

Kapoor, A., Yao, W., Ying, H., Hua, S., Liewen, A., Wang, Q., Zhong, Y., Wu, C. J., Sadanandam, A., Hu, B., Chang, Q., Chu, G. C., Al-Khalil, R., Jiang, S., Xia, H., Fletcher-Sananikone, E., Lim, C., Horwitz, G. I., Viale, A., Pettazzoni, P., Sanchez, N., Wang, H., Protopopov, A., Zhang, J., Heffernan, T., Johnson, R. L., Chin, L., Wang, Y. A., Draetta, G. and DePinho, R. A. (2014). Yap1 activation enables bypass of oncogenic Kras addiction in pancreatic cancer. Cell *158*, 185–197.

Katz, N., Teutsch, H. F., Jungermann, K. and Sasse, D. (1977). Heterogeneous reciprocal localization of fructose-1,6-bisphosphatase and of glucokinase in microdissected periportal and perivenous rat liver tissue. FEBS letters *83*, 272–6.

Kawauchi, K., Araki, K., Tobiume, K. and Tanaka, N. (2008). p53 regulates glucose metabolism through an IKK-NF-kappaB pathway and inhibits cell transformation. Nat Cell Biol *10*, 611–618.

Keng, V. W., Yagi, H., Ikawa, M., Nagano, T., Myint, Z., Yamada, K., Tanaka, T., Sato, A., Muramatsu, I., Okabe, M., Sato, M. and Noguchi, T. (2000). Homeobox gene Hex is essential for onset of mouse embryonic liver development and differentiation of the monocyte lineage. Biochem Biophys Res Commun *276*, 1155–1161.

Kim, G. J., Kim, H. and Park, Y. N. (2013). Increased expression of Yes-associated protein 1 in hepatocellular carcinoma with stemness and combined hepatocellular-cholangiocarcinoma. PloS one *8*, e75449.

Kohn, A. D., Summers, S. A., Birnbaum, M. J. and Roth, R. A. (1996). Expression of a constitutively active Akt Ser/Thr kinase in 3T3-L1 adipocytes stimulates glucose uptake and glucose transporter 4 translocation. J Biol Chem *271*, 31372–31378.

Kondoh, H., Lleonart, M. E., Nakashima, Y., Yokode, M., Tanaka, M., Bernard, D., Gil, J. and Beach, D. (2007). A high glycolytic flux supports the proliferative potential of murine embryonic stem cells. Antioxid Redox Signal *9*, 293–9.

Konsavage Jr., W. M., Kyler, S. L., Rennoll, S. A., Jin, G. and Yochum, G. S. (2012). Wnt/beta-catenin signaling regulates Yes-associated protein (YAP) gene expression in colorectal carcinoma cells. J Biol Chem *287*, 11730–11739.

Koppenol, W. H., Bounds, P. L. and Dang, C. V. (2011). Otto Warburg's contributions to current concepts of cancer metabolism. Nat Rev Cancer *11*, 325–337.

Kubo, Y., Aishima, S., Tanaka, Y., Shindo, K., Mizuuchi, Y., Abe, K., Shirabe, K., Maehara, Y., Honda, H. and Oda, Y. (2014). Different expression of glucose transporters in the progression of intrahepatic cholangiocarcinoma. Hum Pathol *45*, 1610–1617.

Kung, H. N., Marks, J. R. and Chi, J. T. (2011). Glutamine synthetase is a genetic determinant of cell type-specific glutamine independence in breast epithelia. PLoS Genet *7*, e1002229.

Kwan, K. M., Fujimoto, E., Grabher, C., Mangum, B. D., Hardy, M. E., Campbell, D. S., Parant, J. M., Yost, H. J., Kanki, J. P. and Chien, C.-B. (2007). The Tol2kit: a multisite gateway-based construction kit for Tol2 transposon transgenesis constructs. Developmental dynamics : an official publication of the American Association of Anatomists *236*, 3088–99.

Labow, B. I., Souba, W. W. and Abcouwer, S. F. (2001). Mechanisms governing the expression of the enzymes of glutamine metabolism–glutaminase and glutamine synthetase. J Nutr *131*, 2467S–74S; discussion 2486S–7S.

Lachenmayer, A., Alsinet, C., Savic, R., Cabellos, L., Toffanin, S., Hoshida, Y., Villanueva, A., Minguez, B., Newell, P., Tsai, H. W., Barretina, J., Thung, S., Ward, S. C., Bruix, J., Mazzaferro, V., Schwartz, M., Friedman, S. L. and Llovet, J. M. (2012). Wnt-pathway activation in two molecular classes of hepatocellular carcinoma and experimental modulation by sorafenib. Clin Cancer Res *18*, 4997–5007.

Lai, Z.-C., Wei, X., Shimizu, T., Ramos, E., Rohrbaugh, M., Nikolaidis, N., Ho, L.-L. and Li, Y. (2005). Control of cell proliferation and apoptosis by mob as tumor suppressor, mats. Cell *120*, 675–685.

Langenau, D. M., Traver, D., Ferrando, A. A., Kutok, J. L., Aster, J. C., Kanki, J. P., Lin, S., Prochownik, E., Trede, N. S., Zon, L. I. and Look, A. T. (2003). Myc-induced T cell leukemia in transgenic zebrafish. Science *299*, 887–890.

Laplante, M. and Sabatini, D. M. (2012). mTOR signaling in growth control and disease. Cell *149*, 274–293.

Lee, K.-P., Lee, J.-H., Kim, T.-S., Kim, T.-H., Park, H.-D., Byun, J.-S., Kim, M.-C., Jeong, W.-I., Calvisi, D. F., Kim, J.-M. and Lim, D.-S. (2010). The Hippo-Salvador pathway restrains hepatic oval cell proliferation, liver size, and liver tumorigenesis. Proc Natl Acad Sci U S A *107*, 8248–8253.

Li, S., Brown, M. S. and Goldstein, J. L. (2010). Bifurcation of insulin signaling pathway in rat liver: mTORC1 required for stimulation of lipogenesis, but not inhibition of gluconeogenesis. Proc Natl Acad Sci U S A *107*, 3441–3446.

Li, Z., Zheng, W., Wang, Z., Zeng, Z., Zhan, H., Li, C., Zhou, L., Yan, C., Spitsbergen, J. M. and Gong, Z. (2013). A transgenic zebrafish liver tumor model with inducible Myc expression reveals conserved Myc signatures with mammalian liver tumors. Dis Model Mech *6*, 414–423.

Lian, I., Kim, J., Okazawa, H., Zhao, J., Zhao, B., Yu, J., Chinnaiyan, A., Israel, M. A., Goldstein, L. S., Abujarour, R., Ding, S. and Guan, K. L. (2010). The role of YAP transcription coactivator in regulating stem cell self-renewal and differentiation. Genes Dev *24*, 1106–1118.

Liang, N., Zhang, C., Dill, P., Panasyuk, G., Pion, D., Koka, V., Gallazzini, M., Olson, E. N., Lam, H., Henske, E. P., Dong, Z., Apte, U., Pallet, N., Johnson, R. L., Terzi, F., Kwiatkowski, D. J., Scoazec, J. Y., Martignoni, G. and Pende, M. (2014). Regulation of YAP by mTOR and autophagy reveals a therapeutic target of tuberous sclerosis complex. J Exp Med *211*, 2249–2263.

Lieschke, G. J. and Currie, P. D. (2007). Animal models of human disease: zebrafish swim into view. Nat Rev Genet *8*, 353–367.

Liu, S. and Leach, S. D. (2011). Screening pancreatic oncogenes in zebrafish using the Gal4/UAS system. Methods Cell Biol *105*, 367–381.

Liu, Y., Cao, Y., Zhang, W., Bergmeier, S., Qian, Y., Akbar, H., Colvin, R., Ding, J., Tong, L., Wu, S., Hines, J. and Chen, X. (2012). A small-molecule inhibitor of glucose transporter 1 downregulates glycolysis, induces cell-cycle arrest, and inhibits cancer cell growth in vitro and in vivo. Mol Cancer Ther *11*, 1672–1682.

Loh, S.-L., Teh, C., Muller, J., Guccione, E., Hong, W. and Korzh, V. (2014). Zebrafish yap1 plays a role in differentiation of hair cells in posterior lateral line. Scientific reports *4*, 4289.

Louro, I. D., Bailey, E. C., Li, X., South, L. S., McKie-Bell, P. R., Yoder, B. K., Huang, C. C., Johnson, M. R., Hill, A. E., Johnson, R. L. and Ruppert, J. M. (2002). Comparative gene expression profile analysis of GLI and c-MYC in an epithelial model of malignant transformation. Cancer Res *62*, 5867–5873.

Lu, L., Li, Y., Kim, S. M., Bossuyt, W., Liu, P., Qiu, Q., Wang, Y., Halder, G., Finegold, M. J., Lee, J.-S. and Johnson, R. L. (2010). Hippo signaling is a potent in vivo growth and tumor suppressor pathway in the mammalian liver. Proc Natl Acad Sci U S A *107*, 1437–1442.

Macheda, M. L., Rogers, S. and Best, J. D. (2005). Molecular and cellular regulation of glucose transporter (GLUT) proteins in cancer. J Cell Physiol *202*, 654–662.

Makita, R., Uchijima, Y., Nishiyama, K., Amano, T., Chen, Q., Takeuchi, T., Mitani, A., Nagase, T., Yatomi, Y., Aburatani, H., Nakagawa, O., Small, E. V., Cobo-Stark, P., Igarashi, P., Murakami, M., Tominaga, J., Sato, T., Asano, T., Kurihara, Y. and Kurihara, H. (2008). Multiple renal cysts, urinary concentration defects, and pulmonary emphysematous changes in mice lacking TAZ. Am J Physiol Renal Physiol *294*, F542–F553.

Manganelli, G., Fico, A., Masullo, U., Pizzolongo, F., Cimmino, A. and Filosa, S. (2012). Modulation of the pentose phosphate pathway induces endodermal differentiation in embryonic stem cells. PloS one *7*, e29321.

Martinez Barbera, J. P., Clements, M., Thomas, P., Rodriguez, T., Meloy, D., Kioussis, D. and Beddington, R. S. (2000). The homeobox gene Hex is required in definitive endodermal tissues for normal forebrain, liver and thyroid formation. Development *127*, 2433–45.

Mayers, J. R. and Vander Heiden, M. G. (2015). Famine versus feast: understanding the metabolism of tumors in vivo. Trends Biochem Sci *40*, 130–140.

Mayers, J. R., Wu, C., Clish, C. B., Kraft, P., Torrence, M. E., Fiske, B. P., Yuan, C., Bao, Y., Townsend, M. K., Tworoger, S. S., Davidson, S. M., Papagiannakopoulos, T., Yang, A., Dayton, T. L., Ogino, S., Stampfer, M. J., Giovannucci, E. L., Qian, Z. R., Rubinson, D. A., Ma, J., Sesso, H. D., Gaziano, J. M., Cochrane, B. B., Liu, S., Wactawski-Wende, J., Manson, J. E., Pollak, M. N., Kimmelman, A. C., Souza, A., Pierce, K., Wang, T. J., Gerszten, R. E., Fuchs, C. S., Vander Heiden, M. G. and Wolpin, B. M. (2014). Elevation of circulating branched-chain amino acids is an early event in human pancreatic adenocarcinoma development. Nat Med *20*, 1193–1198.

Mazurek, S., Boschek, C. B., Hugo, F. and Eigenbrodt, E. (2005). Pyruvate kinase type M2 and its role in tumor growth and spreading. Semin Cancer Biol *15*, 300–308.

Medina, R. A. and Owen, G. I. (2002). Glucose transporters: expression, regulation and cancer. Biological Research *35*, 9–26.

Menke, A. L., Spitsbergen, J. M., Wolterbeek, A. P. and Woutersen, R. A. (2011). Normal anatomy and histology of the adult zebrafish. Toxicol Pathol *39*, 759–775.

Miesfeld, J. B. and Link, B. a. (2014). Establishment of transgenic lines to monitor and manipulate Yap/Taz-Tead activity in zebrafish reveals both evolutionarily conserved and divergent functions of the Hippo pathway. Mech Dev *133*, 177–188.

Miharada, K., Karlsson, G., Rehn, M., Rörby, E., Siva, K., Cammenga, J. and Karlsson, S. (2011). Cripto regulates hematopoietic stem cells as a hypoxic-niche-related factor through cell surface receptor GRP78. Cell Stem Cell *9*, 330–344.

Miller, E., Yang, J., DeRan, M., Wu, C., Su, A. I., Bonamy, G. M., Liu, J., Peters, E. C. and Wu, X. (2012). Identification of serum-derived sphingosine-1-phosphate as a small molecule regulator of YAP. Chem Biol *19*, 955–962.

Mo, J.-S., Meng, Z., Kim, Y. C., Park, H. W., Hansen, C. G., Kim, S., Lim, D.-S. and Guan, K.-L. (2015). Cellular energy stress induces AMPK-mediated regulation of YAP and the Hippo pathway. Nat Cell Biol *17*, 500–510.

Mohseni, M., Sun, J., Lau, A., Curtis, S., Goldsmith, J., Fox, V. L., Wei, C., Frazier, M., Samson, O., Wong, K. K., Kim, C. and Camargo, F. D. (2014). A genetic screen identifies an LKB1-MARK signalling axis controlling the Hippo-YAP pathway. Nat Cell Biol *16*, 108–117.

Monks, A., Chisena, C. A. and Cysyk, R. L. (1985). Influence of ammonium ions on hepatic de novo pyrimidine biosynthesis. Arch Biochem Biophys *236*, 1–10.

Morin, N., Vallaeys, T., Hendrickx, L., Natalie, L. and Wilmotte, A. (2010). An efficient DNA isolation protocol for filamentous cyanobacteria of the genus Arthrospira. Journal of microbiological methods *80*, 148–54.

Morin-Kensicki, E. M., Boone, B. N., Howell, M., Stonebraker, J. R., Teed, J., Alb, J. G., Magnuson, T. R., O'Neal, W. and Milgram, S. L. (2006). Defects in yolk sac vasculogenesis, chorioallantoic fusion, and embryonic axis elongation in mice with targeted disruption of Yap65. Mol Cell Biol *26*, 77–87.

Mukherjee, S. (2010). The Emperor of All Maladies. 1st edition, Scribner, New York.

Nault, J. C., Calderaro, J., Di Tommaso, L., Balabaud, C., Zafrani, E. S., Bioulac-Sage, P., Roncalli, M. and Zucman-Rossi, J. (2014). Telomerase reverse transcriptase promoter mutation is an early somatic genetic alteration in the transformation of premalignant nodules in hepatocellular carcinoma on cirrhosis. Hepatology *60*, 1983–1992.

Nguyen, A. T., Emelyanov, A., Koh, C. H., Spitsbergen, J. M., Parinov, S. and Gong, Z. (2012). An inducible kras(V12) transgenic zebrafish model for liver tumorigenesis and chemical drug screening. Dis Model Mech *5*, 63–72.

Nguyen, H. B., Babcock, J. T., Wells, C. D. and Quilliam, L. A. (2013). LKB1 tumor suppressor regulates AMP kinase/mTOR-independent cell growth and proliferation via the phosphorylation of Yap. Oncogene *32*, 4100–4109.

Nicolay, B. N., Bayarmagnai, B., Moon, N. S., Benevolenskaya, E. V. and Frolov, M. V. (2010). Combined inactivation of pRB and hippo pathways induces dedifferentiation in the Drosophila retina. PLoS Genet *6*, e1000918.

Nishioka, N., Inoue, K.-i., Adachi, K., Kiyonari, H., Ota, M., Ralston, A., Yabuta, N., Hirahara, S., Stephenson, R. O., Ogonuki, N., Makita, R., Kurihara, H., Morin-Kensicki, E. M., Nojima, H., Rossant, J., Nakao, K., Niwa, H. and Sasaki, H. (2009). The Hippo signaling pathway components Lats and Yap pattern Tead4 activity to distinguish mouse trophectoderm from inner cell mass. Dev Cell *16*, 398–410.

Noël, E. S., Reis, M. D., Arain, Z. and Ober, E. A. (2010). Analysis of the Albumin/alpha-Fetoprotein/Afamin/Group specific component gene family in the context of zebrafish liver differentiation. Gene Expr Patterns *10*, 237–43.

North, T. E. and Goessling, W. (2011). Endoderm specification, liver development, and regeneration. Methods Cell Biol *101*, 205–223.

Ober, E. A., Verkade, H., Field, H. A. and Stainier, D. Y. R. (2006). Mesodermal Wnt2b signalling positively regulates liver specification. Nature *442*, 688–691.

Oburoglu, L., Tardito, S., Fritz, V., de Barros, S. C., Merida, P., Craveiro, M., Mamede, J., Cretenet, G., Mongellaz, C., An, X., Klysz, D., Touhami, J., Boyer-Clavel, M., Battini, J. L., Dardalhon, V., Zimmermann, V. S., Mohandas, N., Gottlieb, E., Sitbon, M., Kinet, S. and Taylor, N. (2014). Glucose and glutamine metabolism regulate human hematopoietic stem cell lineage specification. Cell Stem Cell *15*, 169–184.

Oh, H. and Irvine, K. D. (2008). In vivo regulation of Yorkie phosphorylation and localization. Development *135*, 1081–1088.

Oka, T. and Sudol, M. (2009). Nuclear localization and pro-apoptotic signaling of YAP2 require intact PDZ-binding motif. Genes Cells *14*, 607–615.

Osthus, R. C., Shim, H., Kim, S., Li, Q., Reddy, R., Mukherjee, M., Xu, Y., Wonsey, D., Lee, L. A. and Dang, C. V. (2000). Deregulation of glucose transporter 1 and glycolytic gene expression by c-Myc. J Biol Chem *275*, 21797–21800.

Pan, D. (2010). The hippo signaling pathway in development and cancer. Developmental cell *19*, 491–505.

Pantalacci, S., Tapon, N. and Léopold, P. (2003). The Salvador partner Hippo promotes apoptosis and cell-cycle exit in Drosophila. Nat Cell Biol *5*, 921–927.

Pantaleon, M. and Kaye, P. L. (1998). Glucose transporters in preimplantation development. Rev Reprod *3*, 77–81.

Patton, E. E., Widlund, H. R., Kutok, J. L., Kopani, K. R., Amatruda, J. F., Murphey, R. D., Berghmans, S., Mayhall, E. A., Traver, D., Fletcher, C. D., Aster, J. C., Granter, S. R., Look, A. T., Lee, C., Fisher, D. E. and Zon, L. I. (2005). BRAF mutations are sufficient to promote nevi formation and cooperate with p53 in the genesis of melanoma. Curr Biol *15*, 249–254.

Piccolo, S., Dupont, S. and Cordenonsi, M. (2014). The Biology of YAP/TAZ: Hippo Signaling and Beyond. Physiol Rev *94*, 1287–1312.

Pisharath, H. and Parsons, M. J. (2009). Nitroreductase-mediated cell ablation in transgenic zebrafish embryos. Methods Mol Biol *546*, 133–143.

Porazinski, S., Wang, H., Asaoka, Y., Behrndt, M., Miyamoto, T., Morita, H., Hata, S., Sasaki, T., Krens, S. F. G., Osada, Y., Asaka, S., Momoi, A., Linton, S., Miesfeld, J. B., Link, B. A., Senga, T., Castillo-Morales, A., Urrutia, A. O., Shimizu, N., Nagase, H., Matsuura, S., Bagby, S., Kondoh, H., Nishina, H., Heisenberg, C.-P. and Furutani-Seiki, M. (2015). YAP is essential for tissue tension to ensure vertebrate 3D body shape. Nature *DOI*, 10.1038/nature14215.

Prigione, A., Fauler, B., Lurz, R., Lehrach, H. and Adjaye, J. (2010). The senescence-related mitochondrial/oxidative stress pathway is repressed in human induced pluripotent stem cells. Stem Cells *28*, 721–733.

Ramos, A. and Camargo, F. D. (2012). The Hippo signaling pathway and stem cell biology. Trends Cell Biol *22*, 339–346.

Robitaille, A. M., Christen, S., Shimobayashi, M., Cornu, M., Fava, L. L., Moes, S., Prescianotto-Baschong, C., Sauer, U., Jenoe, P. and Hall, M. N. (2013). Quantitative phosphoproteomics reveal mTORC1 activates de novo pyrimidine synthesis. Science *339*, 1320–1323.

Rosenbluh, J., Nijhawan, D., Cox, A. G., Li, X., Neal, J. T., Schafer, E. J., Zack, T. I., Wang, X., Tsherniak, A., Schinzel, A. C., Shao, D. D., Schumacher, S. E., Weir, B. A., Vazquez, F., Cowley, G. S., Root, D. E., Mesirov, J. P., Beroukhim, R., Kuo, C. J., Goessling, W. and Hahn, W. C. (2012). beta-Catenin-Driven Cancers Require a YAP1 Transcriptional Complex for Survival and Tumorigenesis. Cell *151*, 1457–1473.

Roskams, T. and Kojiro, M. (2010). Pathology of early hepatocellular carcinoma: conventional and molecular diagnosis. Semin Liver Dis *30*, 17–25.

Rossi, J. M., Dunn, N. R., Hogan, B. L. and Zaret, K. S. (2001). Distinct mesodermal signals, including BMPs from the septum transversum mesenchyme, are required in combination for hepatogenesis from the endoderm. Genes Dev *15*, 1998–2009.

Sabaawy, H. E., Azuma, M., Embree, L. J., Tsai, H.-J., Starost, M. F. and Hickstein, D. D. (2006). TEL-AML1 transgenic zebrafish model of precursor B cell acute lymphoblastic leukemia. Proc Natl Acad Sci U S A *103*, 15166–15171.

Santisteban, G. A., Ely, J. T., Hamel, E. E., Read, D. H. and Kozawa, S. M. (1985). Glycemic modulation of tumor tolerance in a mouse model of breast cancer. Biochem Biophys Res Commun *132*, 1174–9.

Santoriello, C., Gennaro, E., Anelli, V., Distel, M., Kelly, A., Köster, R. W., Hurlstone, A. and Mione, M. (2010). Kita driven expression of oncogenic HRAS leads to early onset and highly penetrant melanoma in zebrafish. PloS one *5*, e15170.

Santoriello, C. and Zon, L. I. (2012). Hooked! Modeling human disease in zebrafish. J Clin Invest *122*, 2337–2343.

Schindelin, J., Arganda-Carreras, I., Frise, E., Kaynig, V., Longair, M., Pietzsch, T., Preibisch, S., Rueden, C., Saalfeld, S., Schmid, B., Tinevez, J. Y., White, D. J., Hartenstein, V., Eliceiri, K., Tomancak, P. and Cardona, A. (2012). Fiji: an open-source platform for biological-image analysis. Nat Methods *9*, 676–682.

Schlegelmilch, K., Mohseni, M., Kirak, O., Pruszak, J., Rodriguez, J. R., Zhou, D., Kreger, B. T., Vasioukhin, V., Avruch, J., Brummelkamp, T. R. and Camargo, F. D. (2011). Yap1 acts downstream of α-catenin to control epidermal proliferation. Cell *144*, 782–795.

Schmidt, A., Braeuning, A., Ruck, P., Seitz, G., Armeanu-Ebinger, S., Fuchs, J., Warmann, S. W. and Schwarz, M. (2011). Differential expression of glutamine synthetase and cytochrome P450 isoforms in human hepatoblastoma. Toxicology *281*, 7–14.

Septer, S., Edwards, G., Gunewardena, S., Wolfe, A., Li, H., Daniel, J. and Apte, U. (2012). Yes-associated protein is involved in proliferation and differentiation during postnatal liver development. Am J Physiol Gastrointest Liver Physiol *302*, G493–503.

Shao, D. D., Xue, W., Krall, E. B., Bhutkar, A., Piccioni, F., Wang, X., Schinzel, A. C., Sood, S., Rosenbluh, J., Kim, J. W., Zwang, Y., Roberts, T. M., Root, D. E., Jacks, T. and Hahn, W. C. (2014). KRAS and YAP1 converge to regulate EMT and tumor survival. Cell *158*, 171–184.

Shin, D., Lee, Y., Poss, K. D. and Stainier, D. Y. R. (2011). Restriction of hepatic competence by Fgf signaling. Development (Cambridge, England) *138*, 1339–48.

Shin, D., Shin, C. H., Tucker, J., Ober, E. a., Rentzsch, F., Poss, K. D., Hammerschmidt, M., Mullins, M. C. and Stainier, D. Y. R. (2007). Bmp and Fgf signaling are essential for liver specification in zebrafish. Development (Cambridge, England) *134*, 2041–50.

Shyh-Chang, N., Daley, G. Q. and Cantley, L. C. (2013a). Stem cell metabolism in tissue development and aging. Development *140*, 2535–2547.

Shyh-Chang, N., Zhu, H., Yvanka de Soysa, T., Shinoda, G., Seligson, M. T., Tsanov, K. M., Nguyen, L., Asara, J. M., Cantley, L. C. and Daley, G. Q. (2013b). Lin28 enhances tissue repair by reprogramming cellular metabolism. Cell *155*, 778–792.

Si-Tayeb, K., Lemaigre, F. P. and Duncan, S. A. (2010). Organogenesis and development of the liver. Dev Cell *18*, 175–189.

Simsek, T., Kocabas, F., Zheng, J., Deberardinis, R. J., Mahmoud, A. I., Olson, E. N., Schneider, J. W., Zhang, C. C. and Sadek, H. A. (2010). The distinct metabolic profile of hematopoietic stem cells reflects their location in a hypoxic niche. Cell Stem Cell *7*, 380–390.

Skaper, S. D., O'Brien, W. E. and Schafer, I. A. (1978). The influence of ammonia on purine and pyrimidine nucleotide biosynthesis in rat liver and brain in vitro. Biochem J *172*, 457–464.

Skouloudaki, K., Puetz, M., Simons, M., Courbard, J.-R., Boehlke, C., Hartleben, B., Engel, C., Moeller, M. J., Englert, C., Bollig, F., Schafer, T., Ramachandran, H., Mlodzik, M., Huber, T. B., Kuehn, E. W., Kim, E., Kramer-Zucker, A. and Walz, G. (2009). Scribble participates in Hippo signaling and is required for normal zebrafish pronephros development. Proc Natl Acad Sci U S A *106*, 8579–8584.

Society, A. C. (2015). Cancer Facts & Figures 2015. Technical report American Cancer Society Atlanta.

Sorrentino, G., Ruggeri, N., Specchia, V., Cordenonsi, M., Mano, M., Dupont, S., Manfrin, A., Ingallina, E., Sommaggio, R., Piazza, S., Rosato, A., Piccolo, S. and Del Sal, G. (2014). Metabolic control of YAP and TAZ by the mevalonate pathway. Nat Cell Biol *16*, 357–366.

Sosa-Pineda, B., Wigle, J. T. and Oliver, G. (2000). Hepatocyte migration during liver development requires Prox1. Nat Genet *25*, 254–255.

Steinhardt, A. A., Gayyed, M. F., Klein, A. P., Dong, J., Maitra, A., Pan, D., Montgomery, E. A. and Anders, R. A. (2008). Expression of Yes-associated protein in common solid tumors. Hum Pathol *39*, 1582–1589.

Streisinger, G., Walker, C., Dower, N., Knauber, D. and Singer, F. (1981). Production of clones of homozygous diploid zebra fish (Brachydanio rerio). Nature *291*, 293–296.

Sudol, M. (1994). Yes-associated protein (YAP65) is a proline-rich phosphoprotein that binds to the SH3 domain of the Yes proto-oncogene product. Oncogene *9*, 2145–2152.

Sudol, M., Bork, P., Einbond, A., Kastury, K., Druck, T., Negrini, M., Huebner, K. and Lehman, D. (1995). Characterization of the mammalian YAP (Yes-associated protein) gene and its role in defining a novel protein module, the WW domain. J Biol Chem *270*, 14733–14741.

Sudol, M. and Harvey, K. F. (2010). Modularity in the Hippo signaling pathway. Trends in biochemical sciences *35*, 627–33.

Sudol, M., Shields, D. C. and Farooq, A. (2012). Structures of YAP protein domains reveal promising targets for development of new cancer drugs. Semin Cell Dev Biol *23*, 827–833.

Taguchi, Y., Takizawa, T., Ishibashi, H., Sagawa, T., Arai, R., Inoue, S., Yamaguchi, H. and Abe, S. (2010). Therapeutic effects on murine oral candidiasis by oral administration of cassia (Cinnamomum cassia) preparation. Nihon Ishinkin Gakkai Zasshi *51*, 13–21.

Takahashi, K. and Yamanaka, S. (2006). Induction of pluripotent stem cells from mouse embryonic and adult fibroblast cultures by defined factors. Cell *126*, 663–676.

Takubo, K., Goda, N., Yamada, W., Iriuchishima, H., Ikeda, E., Kubota, Y., Shima, H., Johnson, R. S., Hirao, A., Suematsu, M. and Suda, T. (2010). Regulation of the HIF-1alpha level is essential for hematopoietic stem cell. Cell Stem Cell *7*, 391–402.

Tao, J., Calvisi, D. F., Ranganathan, S., Cigliano, A., Zhou, L., Singh, S., Jiang, L., Fan, B., Terracciano, L., Armeanu-Ebinger, S., Ribback, S., Dombrowski, F., Evert, M., Chen, X. and Monga, S. P. (2014). Activation of beta-catenin and Yap1 in human hepatoblastoma and induction of hepatocarcinogenesis in mice. Gastroenterology *147*, 690–701.

Tapon, N., Harvey, K. F., Bell, D. W., Wahrer, D. C. R., Schiripo, T. A., Haber, D. A. and Hariharan, I. K. (2002). salvador Promotes both cell cycle exit and apoptosis in Drosophila and is mutated in human cancer cell lines. Cell *110*, 467–478.

Tian, Y., Kolb, R., Hong, J.-H., Carroll, J., Li, D., You, J., Bronson, R., Yaffe, M. B., Zhou, J. and Benjamin, T. (2007). TAZ promotes PC2 degradation through a SCFbeta-Trcp E3 ligase complex. Mol Cell Biol *27*, 6383–6395.

Tremblay, K. D. and Zaret, K. S. (2005). Distinct populations of endoderm cells converge to generate the embryonic liver bud and ventral foregut tissues. Dev Biol *280*, 87–99.

Tschop, K., Conery, A. R., Litovchick, L., Decaprio, J. A., Settleman, J., Harlow, E. and Dyson, N. (2011). A kinase shRNA screen links LATS2 and the pRB tumor suppressor. Genes Dev *25*, 814–830.

Tumaneng, K., Russell, R. C. and Guan, K.-L. (2012a). Organ size control by Hippo and TOR pathways. Current biology : CB *22*, R368–79.

Tumaneng, K., Russell, R. C. and Guan, K. L. (2012b). Organ size control by Hippo and TOR pathways. Curr Biol *22*, R368–R379.

Udan, R. S., Kango-Singh, M., Nolo, R., Tao, C. and Halder, G. (2003). Hippo promotes proliferation arrest and apoptosis in the Salvador/Warts pathway. Nat Cell Biol *5*, 914–920.

van der Vos, K. E., Eliasson, P., Proikas-Cezanne, T., Vervoort, S. J., van Boxtel, R., Putker, M., van Zutphen, I. J., Mauthe, M., Zellmer, S., Pals, C., Verhagen, L. P., Groot Koerkamp, M. J. A., Braat, A. K., Dansen, T. B., Holstege, F. C., Gebhardt, R., Burgering, B. M. and Coffer, P. J. (2012). Modulation of glutamine metabolism by the PI(3)K-PKB-FOXO network regulates autophagy. Nat Cell Biol *14*, 829–837.

Vander Heiden, M. G., Cantley, L. C. and Thompson, C. B. (2009). Understanding the Warburg effect: the metabolic requirements of cell proliferation. Science *324*, 1029–1033.

Varelas, X., Miller, B. W., Sopko, R., Song, S., Gregorieff, A., Fellouse, F. A., Sakuma, R., Pawson, T., Hunziker, W., McNeill, H., Wrana, J. L. and Attisano, L. (2010a). The Hippo pathway regulates Wnt/beta-catenin signaling. Dev Cell *18*, 579–591.

Varelas, X., Samavarchi-Tehrani, P., Narimatsu, M., Weiss, A., Cockburn, K., Larsen, B. G., Rossant, J. and Wrana, J. L. (2010b). The Crumbs complex couples cell density sensing to Hippo-dependent control of the TGF-beta-SMAD pathway. Dev Cell *19*, 831–844.

Varelas, X. and Wrana, J. L. (2012). Coordinating developmental signaling: novel roles for the Hippo pathway. Trends Cell Biol *22*, 88–96.

Varum, S., Rodrigues, A. S., Moura, M. B., Momcilovic, O., Easley, C. A., Ramalho-Santos, J. a., Van Houten, B. and Schatten, G. (2011). Energy metabolism in human pluripotent stem cells and their differentiated counterparts. PloS one *6*, e20914.

Vassilev, A., Kaneko, K. J., Shu, H., Zhao, Y. and DePamphilis, M. L. (2001). TEAD/TEF transcription factors utilize the activation domain of YAP65, a Src/Yes-associated protein localized in the cytoplasm. Genes Dev *15*, 1229–1241.

von Gise, A., Lin, Z., Schlegelmilch, K., Honor, L. B., Pan, G. M., Buck, J. N., Ma, Q., Ishiwata, T., Zhou, B., Camargo, F. D. and Pu, W. T. (2012). YAP1, the nuclear target of Hippo signaling, stimulates heart growth through cardiomyocyte proliferation but not hypertrophy. Proc Natl Acad Sci U S A *109*, 2394–2399.

Wang, W., Xiao, Z.-D., Li, X., Aziz, K. E., Gan, B., Johnson, R. L. and Chen, J. (2015). AMPK modulates Hippo pathway activity to regulate energy homeostasis. Nat Cell Biol *17*, 490–499.

Wang, Y., Dong, Q., Zhang, Q., Li, Z., Wang, E. and Qiu, X. (2010). Overexpression of yes-associated protein contributes to progression and poor prognosis of non-small-cell lung cancer. Cancer Sci *101*, 1279–1285.

Warburg, O. (1956). On the origin of cancer cells. Science *123*, 309–14.

Warburg, O., Wind, F. and Negelein, E. (1926). Über den Stoffwechsel von Tumoren im Körper. Klinische Wochenschrift *5*, 829–832.

Weber, M., Mickoleit, M. and Huisken, J. (2014). Light sheet microscopy. Methods Cell Biol *123*, 193–215.

White, R., Rose, K. and Zon, L. (2013). Zebrafish cancer: the state of the art and the path forward. Nat Rev Cancer *13*, 624–636.

Wu, S., Huang, J., Dong, J. and Pan, D. (2003). Hippo encodes a Ste-20 family protein kinase that restricts cell proliferation and promotes apoptosis in conjunction with salvador and warts. Cell *114*, 445–456.

Xin, M., Kim, Y., Sutherland, L. B., Qi, X., McAnally, J., Schwartz, R. J., Richardson, J. A., Bassel-Duby, R. and Olson, E. N. (2011). Regulation of insulin-like growth factor signaling by Yap governs cardiomyocyte proliferation and embryonic heart size. Sci Signal *4*, ra70.

Xu, M. Z., Yao, T.-J., Lee, N. P. Y., Ng, I. O. L., Chan, Y.-T., Zender, L., Lowe, S. W., Poon, R. T. P. and Luk, J. M. (2009). Yes-associated protein is an independent prognostic marker in hepatocellular carcinoma. Cancer *115*, 4576–85.

Xu, T., Wang, W., Zhang, S., Stewart, R. A. and Yu, W. (1995). Identifying tumor suppressors in genetic mosaics: the Drosophila lats gene encodes a putative protein kinase. Development *121*, 1053–1063.

Yagi, R., Chen, L. F., Shigesada, K., Murakami, Y. and Ito, Y. (1999). A WW domain-containing yes-associated protein (YAP) is a novel transcriptional co-activator. EMBO J *18*, 2551–2562.

Yao, Y., Lin, J., Yang, P., Chen, Q., Chu, X., Gao, C. and Hu, J. (2012). Fine structure, enzyme histochemistry, and immunohistochemistry of liver in zebrafish. Anat Rec (Hoboken) *295*, 567–576.

Yimlamai, D., Christodoulou, C., Galli, G. G., Yanger, K., Pepe-Mooney, B., Gurung, B., Shrestha, K., Cahan, P., Stanger, B. Z. and Camargo, F. D. (2014). Hippo pathway activity influences liver cell fate. Cell *157*, 1324–1338.

Ying, H., Kimmelman, A. C., Lyssiotis, C. A., Hua, S., Chu, G. C., Fletcher-Sananikone, E., Locasale, J. W., Son, J., Zhang, H., Coloff, J. L., Yan, H., Wang, W., Chen, S., Viale, A., Zheng, H., Paik, J. H., Lim, C., Guimaraes, A. R., Martin, E. S., Chang, J., Hezel, A. F., Perry, S. R., Hu, J., Gan, B., Xiao, Y., Asara, J. M., Weissleder, R., Wang, Y. A., Chin, L., Cantley, L. C. and DePinho, R. A. (2012). Oncogenic Kras maintains pancreatic tumors through regulation of anabolic glucose metabolism. Cell *149*, 656–670.

Yoshida, Y., Takahashi, K., Okita, K., Ichisaka, T. and Yamanaka, S. (2009). Hypoxia enhances the generation of induced pluripotent stem cells. Cell Stem Cell *5*, 237–241.

Yu, F. X. and Guan, K. L. (2013). The Hippo pathway: regulators and regulations. Genes Dev *27*, 355–371.

Yu, F.-X., Meng, Z., Plouffe, S. W. and Guan, K.-L. (2015). Hippo pathway regulation of gastrointestinal tissues. Annu Rev Physiol *77*, 201–27.

Yu, F.-X., Zhao, B., Panupinthu, N., Jewell, J. L., Lian, I., Wang, L. H., Zhao, J., Yuan, H., Tumaneng, K., Li, H., Fu, X.-D., Mills, G. B. and Guan, K.-L. (2012). Regulation of the Hippo-YAP pathway by G-protein-coupled receptor signaling. Cell *150*, 780–791.

Yu, W.-M., Liu, X., Shen, J., Jovanovic, O., Pohl, E. E., Gerson, S. L., Finkel, T., Broxmeyer, H. E. and Qu, C.-K. (2013). Metabolic regulation by the mitochondrial phosphatase PTPMT1 is required for hematopoietic stem cell differentiation. Cell Stem Cell *12*, 62–74.

Yuan, M., Breitkopf, S. B., Yang, X. and Asara, J. M. (2012). A positive/negative ion-switching, targeted mass spectrometry-based metabolomics platform for bodily fluids, cells, and fresh and fixed tissue. Nat Protoc *7*, 872–881.

Yuneva, M. O., Fan, T. W. M., Allen, T. D., Higashi, R. M., Ferraris, D. V., Tsukamoto, T., Matés, J. M., Alonso, F. J., Wang, C., Seo, Y., Chen, X. and Bishop, J. M. (2012). The metabolic profile of tumors depends on both the responsible genetic lesion and tissue type. Cell Metab *15*, 157–70.

Zender, L., Spector, M. S., Xue, W., Flemming, P., Cordon-Cardo, C., Silke, J., Fan, S.-T., Luk, J. M., Wigler, M., Hannon, G. J., Mu, D., Lucito, R., Powers, S. and Lowe, S. W. (2006). Identification and validation of oncogenes in liver cancer using an integrative oncogenomic approach. Cell *125*, 1253–1267.

Zhang, C., Liu, J., Liang, Y., Wu, R., Zhao, Y., Hong, X., Lin, M., Yu, H., Liu, L., Levine, A. J., Hu, W. and Feng, Z. (2013). Tumour-associated mutant p53 drives the Warburg effect. Nat Commun *4*, 2935.

Zhang, H., Pasolli, H. A. and Fuchs, E. (2011a). Yes-associated protein (YAP) transcriptional coactivator functions in balancing growth and differentiation in skin. Proc Natl Acad Sci U S A *108*, 2270–2275.

Zhang, J., Khvorostov, I., Hong, J. S., Oktay, Y., Vergnes, L., Nuebel, E., Wahjudi, P. N., Setoguchi, K., Wang, G., Do, A., Jung, H.-J., McCaffery, J. M., Kurland, I. J., Reue, K., Lee, W.-N. P., Koehler, C. M. and Teitell, M. A. (2011b). UCP2 regulates energy metabolism and differentiation potential of human pluripotent stem cells. EMBO J *30*, 4860–4873.

Zhang, L., Ren, F., Zhang, Q., Chen, Y., Wang, B. and Jiang, J. (2008). The TEAD/TEF family of transcription factor Scalloped mediates Hippo signaling in organ size control. Dev Cell *14*, 377–387.

Zhang, N., Bai, H., David, K. K., Dong, J., Zheng, Y., Cai, J., Giovannini, M., Liu, P., Anders, R. a. and Pan, D. (2010). The Merlin/NF2 tumor suppressor functions through the YAP oncoprotein to regulate tissue homeostasis in mammals. Developmental cell *19*, 27–38.

Zhang, P., Li, H., Tan, X., Chen, L. and Wang, S. (2013). Association of metformin use with cancer incidence and mortality: a meta-analysis. Cancer Epidemiol *37*, 207–18.

Zhang, W., Nandakumar, N., Shi, Y., Manzano, M., Smith, A., Graham, G., Gupta, S., Vietsch, E. E., Laughlin, S. Z., Wadhwa, M., Chetram, M., Joshi, M., Wang, F., Kallakury, B., Toretsky, J., Wellstein, A. and Yi, C. (2014). Downstream of mutant KRAS, the transcription regulator YAP is essential for neoplastic progression to pancreatic ductal adenocarcinoma. Sci Signal *7*, ra42.

Zhang, X., George, J., Deb, S., Degoutin, J. L., Takano, E. A., Fox, S. B., Bowtell, D. D. L. and Harvey, K. F. (2011). The Hippo pathway transcriptional co-activator, YAP, is an ovarian cancer oncogene. Oncogene *30*, 2810–2822.

Zhao, B., Li, L., Tumaneng, K., Wang, C.-Y. and Guan, K.-L. (2010). A coordinated phosphorylation by Lats and CK1 regulates YAP stability through SCF(beta-TRCP). Genes Dev *24*, 72–85.

Zhao, B., Tumaneng, K. and Guan, K. L. (2011). The Hippo pathway in organ size control, tissue regeneration and stem cell self-renewal. Nat Cell Biol *13*, 877–883.

Zhao, B., Wei, X., Li, W., Udan, R. S., Yang, Q., Kim, J., Xie, J., Ikenoue, T., Yu, J., Li, L., Zheng, P., Ye, K., Chinnaiyan, A., Halder, G., Lai, Z.-C. and Guan, K.-L. (2007). Inactivation of YAP oncoprotein by the Hippo pathway is involved in cell contact inhibition and tissue growth control. Genes Dev *21*, 2747–61.

Zhao, B., Ye, X., Yu, J., Li, L., Li, W., Li, S., Lin, J. D., Wang, C. Y., Chinnaiyan, A. M., Lai, Z. C. and Guan, K. L. (2008). TEAD mediates YAP-dependent gene induction and growth control. Genes Dev *22*, 1962–1971.

Zhou, D., Conrad, C., Xia, F., Park, J.-s., Payer, B., Yin, Y., Lauwers, G. Y., Thasler, W., Lee, J. T., Avruch, J. and Bardeesy, N. (2009). Article Mst1 and Mst2 Maintain Hepatocyte Quiescence and Suppress Hepatocellular Carcinoma Development through Inactivation of the Yap1 Oncogene. Cancer Cell *16*, 425–438.

Zhou, D., Zhang, Y., Wu, H., Barry, E., Yin, Y., Lawrence, E., Dawson, D., Willis, J. E., Markowitz, S. D., Camargo, F. D. and Avruch, J. (2011). Mst1 and Mst2 protein kinases restrain intestinal stem cell proliferation and colonic tumorigenesis by inhibition of Yes-associated protein (Yap) overabundance. Proc Natl Acad Sci U S A *108*, E1312–E1320.

Zhu, S., Lee, J.-S., Guo, F., Shin, J., Perez-Atayde, A. R., Kutok, J. L., Rodig, S. J., Neuberg, D. S., Helman, D., Feng, H., Stewart, R. A., Wang, W., George, R. E., Kanki, J. P. and Look, A. T. (2012). Activated ALK collaborates with MYCN in neuroblastoma pathogenesis. Cancer Cell *21*, 362–73.

Zon, L. I. and Bahary, N. (1998). Use of the zebrafish (danio rerio) to define hematopoiesis. Stem Cells *16*, 67–78.